



**HAL**  
open science

# Modeling, control and optimization of energy flows : implementation on the charging of electric vehicles

Ghimar Merhy

► **To cite this version:**

Ghimar Merhy. Modeling, control and optimization of energy flows : implementation on the charging of electric vehicles. Other. Université de Picardie Jules Verne, 2020. English. NNT : 2020AMIE0042 . tel-03624714

**HAL Id: tel-03624714**

**<https://theses.hal.science/tel-03624714v1>**

Submitted on 30 Mar 2022

**HAL** is a multi-disciplinary open access archive for the deposit and dissemination of scientific research documents, whether they are published or not. The documents may come from teaching and research institutions in France or abroad, or from public or private research centers.

L'archive ouverte pluridisciplinaire **HAL**, est destinée au dépôt et à la diffusion de documents scientifiques de niveau recherche, publiés ou non, émanant des établissements d'enseignement et de recherche français ou étrangers, des laboratoires publics ou privés.



# Thèse de Doctorat

*Mention Sciences de l'Ingénieur  
Spécialité Automatique*

présentée à *l'Ecole Doctorale en Sciences, Technologie et Santé (ED 585)*

**de l'Université de Picardie Jules Verne**

par

**Ghimar MERHY**

pour obtenir le grade de Docteur de l'Université de Picardie Jules Verne

***Contribution à la modélisation, la commande et l'optimisation  
des flux énergétiques : application à la gestion de recharge  
des véhicules électriques***

Soutenue le 14 décembre 2020, après avis des rapporteurs, devant le jury d'examen :

<b>M. D. Lefebvre, Professeur, Université le Havre Normandie</b>	<b>Président du jury</b>
<b>M. L. Idoumghar, Professeur, Université de Haute Alsace</b>	<b>Rapporteur</b>
<b>M. R. Roche, MCF-HDR, Univ. de technologie de Belfort-Montbéliard</b>	<b>Rapporteur</b>
<b>M. M. Chadli, Professeur, Université Paris-Saclay</b>	<b>Examineur</b>
<b>M. I. Kacem, Professeur, Université de Lorraine</b>	<b>Examineur</b>
<b>M. A. Yasar, Professeur, Université de Hasselt</b>	<b>Examineur</b>
<b>M. A. Nait-Sidi-Moh, MCF-HDR, Univ. de Picardie Jules Verne</b>	<b>Directeur de thèse</b>
<b>M. N. Moubayed, Professeur, Univ. Libanaise</b>	<b>Co-directeur de thèse</b>



## **Doctoral Thesis**

*Department of Engineering Science  
Specialization: Automation Systems*

submitted to the *Doctoral School of Science, Technology and Health*

**Picardie Jules Verne University**

by

**Ghimar MERHY**

Submitted in fulfillment of the requirements for the Degree of Doctor of  
Philosophy of the Picardie Jules Verne University

***Modeling, control and optimization of energy flows:  
Implementation on the charging of electric vehicles***

Oral defence approved and held on December 14<sup>th</sup>, in front of the jury:

<b>Mr. D. Lefebvre, Professor, Le Havre Normandie University</b>	<b>President</b>
<b>Mr. L. Idoumghar, Professor, Haute Alsace University</b>	<b>Reviewer</b>
<b>Mr. R. Roche, Asso. Professor, Univ. of tech. of Belfort-Montbéliard</b>	<b>Reviewer</b>
<b>Mr. M. Chadli, Professor, Paris-Saclay University</b>	<b>Examiner</b>
<b>Mr. I. Kacem, Professor, Lorraine University</b>	<b>Examiner</b>
<b>Mr. A. Yasar, Professor, Hasselt University</b>	<b>Examiner</b>
<b>Mr. A. Nait-Sidi-Moh, Asso. Professor, Picardie Jules Verne University</b>	<b>Supervisor</b>
<b>Mr. N. Moubayed, Professor, Lebanese University</b>	<b>Co-supervisor</b>



## **Résumé**

Cette étude se focalise sur les systèmes énergétiques impliquant des véhicules électriques utilisés comme moyens de stockage et de restitution d'énergie et sur l'optimisation des flux énergétiques réversibles entre les véhicules électriques, le réseau et les habitations. Une approche de modélisation et d'optimisation a été développée pour une gestion optimale des flux entre les VE et les infrastructures.

Le contrôle des flux énergétiques du véhicule a été élaboré à travers la proposition d'un algorithme d'optimisation multi-objectifs et multi-critères dépendant de l'offre et la demande de l'électricité. L'algorithme génétique est utilisé pour calculer les solutions optimisées du problème d'optimisation relatif à la recharge et la décharge des VE. Les fonctions objectifs sont ensuite normalisées et la méthode de la somme pondérée est utilisée avec des poids aléatoires définis selon l'ordre de priorité du décideur dans différents scénarios afin d'aboutir à une solution optimisée finale. Les calculs sont vérifiés et l'optimisation validée grâce au solveur gamultiobj du logiciel Matlab.

Afin de contrôler les flux d'énergie, et visant à atteindre un système équilibré, un algorithme de contrôle et de régulation a été développé. Une amélioration de cet algorithme a été proposée de sorte que le nombre de véhicules retenus par la recharge ou la décharge soit minimisé, dans le but d'obtenir un système équilibré sans détériorer les batteries des véhicules. Ainsi a été développée une stratégie de gestion énergétique permettant de contrôler les flux énergétiques établissant une loi de commande bidirectionnelle qui serait une solution d'adaptation de l'offre à la demande d'électricité.

### **Mots-clés:**

Energies renouvelables, Véhicules électriques, Recharge/décharge, Régulation, Optimisation, Flux énergétiques bidirectionnels, Production et Consommation d'électricité.

## **Abstract**

Our research work mostly proposes an energetic strategy based on a multi-objective and multi-criteria optimization algorithm related to the control of the bidirectional energy flows X2V/V2X between the electric vehicles and X (where X represents the grid, home or building) depending on the available supply or demand of electric energy. The study proposes a control and regulation algorithm aiming to reach a balanced production/consumption system. The balance is mostly acquired through the bidirectional control of the energy flows related to a domestic residence (supplied with renewable sources), electric vehicles (adopted as means of storage and retrieval) and the grid. Then, the defined system's modeling is formulated and a multi-objective optimization of electric vehicles' charging and discharging modes defined by the regulation algorithm is assessed in order to attain an optimal fulfillment of the system's energetic needs. The vehicles' batteries are adopted as means of energy storage and retrieval depending on the electricity supply and demand.

The storage and retrieval's optimization is performed using the genetic algorithm method. Consecutively, the study's objective functions are normalized and the weighted sum approach is implemented with the use of several case studies. And then, the optimized values resulting from the calculation are computed and verified by simulation using Matlab software. Finally, once the regulation algorithm has been set, and the corresponding optimizations implemented, the algorithm's simulation has been performed. Thus, a convenient control of the reversible energy flows, as well as the energy production and consumption has been confirmed.

### **Keywords:**

Renewable energy, Electric Vehicles, Charging/discharging, Regulation, Optimization, Bidirectional Energy flows, Electricity Production and Consumption.

## Table of Contents

Résumé .....	4
Abstract.....	5
Table of Contents.....	6
List of Personal Publications .....	9
List of figures.....	11
List of tables.....	12
Résumé Substantiel de la thèse en Français.....	16
General Introduction.....	22
Chapter 1 - Literature Review.....	26
1. 1    Introduction.....	28
1. 2    Energy systems and demand side management .....	30
1. 3    EV Charging/discharging through V2X/X2V technologies.....	31
1. 4    Energy systems modeling .....	36
1.4.1    Electric Vehicles, batteries, battery chargers and converters.....	36
1.4.2    Wind turbines .....	45
1.4.3    PV panels .....	46
1. 5    Multi-Objective Optimization.....	49
1. 6    Energy management strategies.....	52
1. 7    Conclusion .....	58
Chapter 2 - Energy System's modeling and sizing .....	59
2.1    Introduction.....	61
2.2    Energy System's definition.....	61
2.2.1 Energy System's global architecture.....	61
2.2.2. Energy System's topology .....	64
2.3 Modeling and sizing of the system's components .....	65
2.3.1    Energetic model of EV's propulsion.....	66
2.3.2    Sizing of the vehicle's batteries .....	69
2.3.3    Sizing of the photovoltaic panels .....	72
2.3.4    Sizing of the wind turbine.....	75
2.3.5    Sizing of power converters .....	77
2.4 System's energetic modeling .....	79

2.5	Conclusion .....	83
Chapter 3 - Energy Storage multi-objective optimization .....		84
3.1	Introduction.....	86
3.2	Multi-Objective Optimization for charging.....	87
3.2.1	Objectives definition and modeling .....	87
3.2.2	Multi-objective optimization – Genetic Algorithm.....	91
3.3	Optimization Scenarios .....	104
3.4	Weighted Sum Approach .....	107
3.5	Computation and Verification.....	110
3.6	Conclusion .....	115
Chapter 4 - Energy retrieval multi-objective optimization .....		117
4.1	Introduction.....	119
4.2	Multi-Objective Optimization for discharging.....	119
4.2.1	Objectives definition and modeling .....	120
4.2.2	Multi-objective optimization – Genetic Algorithm.....	123
4.3	Optimization Scenarios .....	134
4.4	Weighted Sum Approach .....	136
4.5	Computation and Verification.....	138
4.6	Conclusion .....	140
Chapter 5 - Control and regulation of energy flows based on electricity supply and demand .....		142
5.1	Introduction.....	144
5.2	Control and regulation algorithm.....	144
5.2.1	Energy Storage – Production exceeding consumption.....	148
5.2.2	Energy retrieval – Consumption exceeding production.....	150
5.2.3	Equilibrium state of the system.....	151
5.3	Validation and Simulation of the control algorithm .....	152
5.3.1	Assigned input data.....	152
5.3.2	Output and Results .....	153
5.3.3	Discussion .....	156
5.4	Improved regulation through the optimization of number of vehicles.....	156
5.4.1	Assigned input data.....	157
5.4.2	Output and Results .....	159
5.4.3	Discussion .....	161



5.5 Conclusion .....	165
General Conclusion.....	166
References.....	169
Appendices.....	179

## **List of Personal Publications**

### **International Journals:**

- 1- G. Merhy, A. Nait-Sidi-Moh, N. Moubayed, “Control, Regulation, and Optimization of Electric Vehicles’ Reversible Energy Flows through an Energy Management Strategy”, *Sustainable Cities and Society (SCS - IF = 4.624)*, Volume 57, June 2020, pp. 102-159.
- 2- G. Merhy, A. Nait-Sidi-Moh, N. Moubayed, “A Multi-Objective Optimization of Electric Vehicles Energy Flows: The charging process”, *Annals of Operations Research (ANOR – IF = 2.284)*, 2020, DOI 10.1007/s10479-020-03529-4.
- 3- G. Merhy, N. Moubayed, A. Nait-Sidi-Moh, “Energy Flows Management: Notes on implementation of the charging and discharging of Electric Vehicles technologies”, *International Journal of E-Learning and Educational Technologies in the Digital Media (IJEETDM)*, Volume 4 Issue 2, pp. 53-60.

### **International Conferences:**

- 1- G. Merhy, A. Nait-Sidi-Moh, N. Moubayed, “Control of Electric Vehicles Energy Flows through a Multi-Objective and Multi-Criteria Optimization Algorithm”, *The International Conference on Multiple Objective Programming and Goal Programming (MOPGP 2017)* – October 30-31, 2017, Metz, France.
- 2- G. Merhy, N. Moubayed, A. Nait-Sidi-Moh, “Energy Flows Management: Notes on implementation of the charging and discharging of Electric Vehicles technologies”, *The Third International Conference on Electrical and Electronic Engineering, Telecommunication Engineering and Mechatronics (EEETEM 2017)* – April 26-28, 2017, Beirut, Lebanon.

### **National Conferences:**

- 1- G. Merhy, A. Nait-Sidi-Moh, N. Moubayed, “Energy Management Strategy for Electric Vehicles Energy Flows: Control and Regulation”, *20ème congrès annuel de la société Française de Recherche Opérationnelle et d’Aide à la décision (ROADEF 2019)* – February 19-21, 2019, Le Havre, France.

**Communications without published proceedings or peer review:**

- 1- Journée Régionale des Doctorants en Automatique (JRDA), July 3<sup>rd</sup> 2018, Amiens, France.**

## List of figures

Figure 1.1: Evolution of the global electric car stock according to the IEA [8] .....	30
Figure 1.2: DC/DC boost chopper wiring diagram .....	41
Figure 1.3: Phase 1: $0 < t < \alpha T$ .....	42
Figure 1.4: Phase 2: $\alpha T < t < T$ .....	42
Figure 1.5: DC/DC bidirectional converter wiring diagram .....	43
Figure 1.6: Phase 1: $0 < t < \alpha T$ .....	44
Figure 1.7: Phase 2: $\alpha T < t < T$ .....	44
Figure 1.8: Summary on the different types of PV modules .....	48
Figure 2.1: Energy System's global architecture .....	63
Figure 2.2: Energy flow block diagram .....	63
Figure 2.3: The studied energy system's topology .....	64
Figure 2.4: Electric vehicle's configuration .....	65
Figure 2.5: Ni/MH Battery Panasonic BK1100FHU [87] .....	71
Figure 2.6: Lead-acid batteries Motoma MS48V3000 [88] .....	72
Figure 2.7: Monocrystalline PV module DualSun 280 Wp [90] .....	75
Figure 2.8: ETNEO AN3000 wind turbine [91] .....	76
Figure 2.9: AC/DC inverter SolarEdge SE9KUS 9kW [92] .....	79
Figure 3.1: gamultiobj solver settings .....	110
Figure 4.1: gamultiobj solver discharging setting .....	138
Figure 5.1: Control and Regulation Algorithm's Organizational Chart .....	145
Figure 5.2: Input and Output Production and Consumption curves .....	155
Figure 5.3: Input and Output SoC bar graphs .....	155
Figure 5.4: Number of vehicles charged/discharged before and after classification .....	161
Figure 5.5: Day 13 - Input & Output SoC - without & with classification .....	162
Figure 5.6: Day 15 - Input & Output SoC - without & with classification .....	162
Figure 5.7: Day 22 - Input & Output SoC - without & with classification .....	163
Figure 5.8: Day 30 - Input & Output SoC - without & with classification .....	164

## List of tables

Table 1.1: Comparison between Gasoline powered vehicles and electric vehicles [4].....	37
Table 1.2: Comparison between batteries types [33].....	39
Table 1.3: Comparison between different battery technologies based on depth of discharge and performance [34] .....	39
Table 1.4: Comparison between Horizontal Axis and Vertical Axis wind turbines .....	45
Table 1.5: PV modules efficiency .....	48
Table 1.6: Multi-Objective optimization methods and procedures .....	50
Table 1.7: Types of Energy Management Strategies .....	57
Table 2.1: Daily home appliances energy consumption .....	72
Table 3.1: The optimization's initial population of 12 chromosomes with their solution and ranking.....	92
Table 3.2: Second generation of 6 chromosomes with their solution and ranking.....	94
Table 3.3: Surviving population of 4 chromosomes .....	95
Table 3.4: fittest 2 chromosomes of the population .....	95
Table 3.5: Initial population of 12 chromosomes .....	97
Table 3.6: Matings and offsprings generation .....	97
Table 3.7: Six new generated offsprings as a result of the matings .....	97
Table 3.8: the generation of 4 offsprings through the surviving population.....	98
Table 3.9: New surviving population of 4 chromosomes .....	98
Table 3.10: The fittest two chromosomes of the population .....	98
Table 3.11: Initial population of 12 chromosomes .....	99
Table 3.12: Matings and offsprings generation .....	99
Table 3.13: Six new generated offsprings as a result of the matings .....	100
Table 3.14: The generation of 4 offsprings through the surviving population.....	100
Table 3.15: New surviving population of 4 chromosomes .....	100
Table 3.16: The fittest 2 chromosomes of the population .....	101
Table 3.17: Initial population of 12 chromosomes .....	102
Table 3.18: Matings and offsprings generation .....	103
Table 3.19: Generated offsprings as a result of the matings.....	103
Table 3.20: Generation of four offsprings through the surviving population .....	103
Table 3.21: Surviving population of four chromosomes.....	104
Table 3.22: The fittest two chromosomes of the population .....	104
Table 3.23: Optimized solution for Charging Scenario 1 .....	105
Table 3.24: Optimized solution for Charging Scenario 2 .....	105
Table 3.25: Optimized solution for Charging Scenario 3 .....	105
Table 3.26: Optimized solution for Charging Scenario 4 .....	106
Table 3.27: Optimized solution for Charging Scenario 5 .....	106
Table 3.28: Optimized solution for Charging Scenario 6 .....	106
Table 3.29: Optimized solution for Charging Scenario 7 .....	107
Table 3.30: Weighted Sum Approach results for all 7 charging scenarios .....	109
Table 3.31: MOGA/Weighted sum approach calculation results .....	109

Table 3.32: Weighted Sum Approach results for all 7 charging scenarios .....	111
Table 3.33: Optimized solution with an initial population of 12 chromosomes and a fraction of 1/12 ..	111
Table 3.34: Pareto-front computed with an initial population of 50 chromosomes.....	111
Table 3.35: Pareto-front computed with an initial population of 25 chromosomes.....	113
Table 3.36: Pareto-front with the ranks where $P_{ch} < P_p + P_{aux}$ deleted .....	114
Table 3.37: Optimized solution with an initial population of 50 chromosomes and a fraction of 1/50 .	114
Table 3.38: Optimized solution with an initial population of 250 chromosomes and a fraction of 1/250 .....	115
Table 4.1: Batteries' charging and discharging efficiency.....	124
Table 4.2: Initial population of 12 chromosomes .....	125
Table 4.3: Matings and offsprings generation .....	125
Table 4.4: Six new generated offsprings as a result of chromosomes matings.....	126
Table 4.5: Generation of 4 offsprings through the surviving population .....	126
Table 4.6: New surviving population of 4 chromosomes .....	126
Table 4.7: The fittest two chromosomes of the population .....	126
Table 4.8: Initial population of 12 chromosomes .....	128
Table 4.9: Matings and offsprings generation .....	128
Table 4.10: Six new generated offsprings as a result of the matings .....	128
Table 4.11: Generation of four offsprings through the surviving population .....	129
Table 4.12: New surviving population of 4 chromosomes .....	129
Table 4.13: The fittest two chromosomes of the population .....	129
Table 4.14: Initial population of 12 chromosomes .....	130
Table 4.15: Matings and offsprings generation .....	131
Table 4.16: Six generated offsprings as a result of chromosomes matings.....	131
Table 4.17: Generation of four offsprings through the surviving population .....	131
Table 4.18: New surviving population of four chromosomes.....	131
Table 4.19: The fittest two chromosomes of the population .....	132
Table 4.20: Initial population of 12 chromosomes .....	132
Table 4.21: Matings and offsprings generation .....	133
Table 4.22: Six generated offsprings as a result of chromosomes matings.....	133
Table 4.23: Generation of four offsprings through the surviving population .....	133
Table 4.24: New surviving population of four chromosomes.....	134
Table 4.25: The fittest two chromosomes of the population .....	134
Table 4.26: Optimized solution for Discharging Scenario 1.....	135
Table 4.27: Optimized solution for Discharging Scenario 2.....	135
Table 4.28: Optimized solution for Discharging Scenario 3.....	136
Table 4.29: Optimized Solution - initial population of 12 chromosomes .....	137
Table 4.30: MOGA/Weighted sum approach calculation results .....	138
Table 4.31: Multi-objective optimization Pareto-front computation result.....	139
Table 4.32: Optimized Solution - initial population of 12 chromosomes .....	139
Table 4.33: Optimized Solution - initial population with 200 chromosomes .....	140
Table 5.1: Control and Regulation Algorithm's Input Data.....	153

Table 5.2: Control and Regulation Algorithm's Output Data .....	154
Table 5.3: Vehicles' batteries number of cycles and SoC percentage to be kept in the vehicle .....	158
Table 5.4: Input and Output SoC values before and after vehicles' classification.....	159
Table 5.5: Number of vehicles charged/discharged before and after classification .....	160





## Résumé Substantiel de la thèse en Français

Pendant que la population mondiale croît continuellement, les besoins énergétiques de l'homme ne cessent de s'amplifier également, ce qui donne lieu non seulement à l'épuisement des réserves disponibles mais aussi à des émissions énormes de gaz à effet de serre dans l'atmosphère. Par suite, en raison du changement climatique et de la pollution causée par les émissions de gaz carbonique, la santé publique semble être menacée et l'espérance de vie humaine réduite. Par conséquent, vu que le secteur du transport constitue l'une des industries les plus grandes et les plus polluantes, l'électrification des véhicules semble être une solution efficace pour les problèmes liés à la pollution, notamment que le nombre de véhicules électriques adoptés mondialement prouve un intérêt vif et croissant pour ce domaine. En fait, avec l'utilisation de véhicules électriques, les menaces humanitaires destructrices associées à la pollution de l'air, au changement climatique, à la hausse des prix de l'essence et à la rareté du pétrole sont minimisées.

Face à l'impossibilité de stockage d'électricité en grandes quantités, et en vue d'ajuster en permanence l'offre d'électricité à la demande, il faudrait développer des solutions alternatives. Parmi ces solutions, nous proposons d'adapter les batteries des véhicules électriques (VE) afin de prendre en charge le stockage et la restitution de l'énergie en plus de leurs fonctions habituelles comme moyens de propulsion des VEs.

Ce travail de recherche se focalise sur les systèmes énergétiques impliquant des véhicules électriques utilisés comme moyens de stockage et de restitution d'énergie et sur l'optimisation des flux énergétiques relatifs à ces systèmes. D'abord, l'étude se concentre sur une revue de littérature permettant de cerner le sujet et d'étudier les différentes approches développées pour ce problème. Le chapitre 1 sera donc consacré à cet état de l'art. En effet, les véhicules électriques, ainsi que les systèmes énergétiques ont été étudiés sur la base des travaux disponibles dans la littérature. Les composantes des systèmes énergétiques de véhicules électriques ont également été envisagées ; entre autres les différents types de batteries de véhicules, leurs chargeurs et convertisseurs ainsi que les sources renouvelables de production d'énergie. Aussi ont été discutées les opérations de recharge et de décharge des véhicules électriques à partir des technologies V2X/X2V représentant le flux énergétique du véhicule vers le réseau électrique et

vice versa (V2G/G2V), le flux énergétique du véhicule vers la maison et vice versa (V2H/H2V) ainsi que le flux énergétique du véhicule vers le bâtiment et vice versa (V2B/B2V). En outre, l'optimisation multi-objectifs et ses nombreuses approches ont été discutées. Certaines stratégies de gestion d'énergie liées aux horaires de recharge et de décharge des véhicules électriques ont également été abordées.

Après avoir pris connaissance des études développées dans la littérature en relation avec le sujet, une approche de modélisation et d'optimisation a été développée afin d'apporter une contribution permettant la gestion optimale et efficace des flux énergétiques entre les VE et les infrastructures.

Pour ce fait, un système énergétique incluant une maison, un véhicule électrique et la grille est bien défini dans le chapitre 2. La maison est alimentée à partir de sources d'énergie renouvelables et le véhicule sera utilisé comme moyen de stockage ou de restitution d'énergie en fonction, d'une part, de l'offre et de la demande d'électricité, et d'autre part des besoins en énergie du VE lui-même. Eventuellement, l'objectif de cette étude serait de minimiser la dépendance du réseau électrique, et de maintenir un certain équilibre entre l'offre et la demande d'électricité, et ceci en utilisant les batteries des véhicules électriques entre autres.

Ainsi, la production d'électricité est collectée grâce à l'énergie solaire et éolienne résultant de la saisie des données de la station météorologique. La consommation d'énergie est définie par les appareils électroménagers fonctionnels dans l'habitat. La recharge et la décharge des véhicules électriques disponibles seraient donc définies par la marge de différence entre la production et la consommation d'électricité et le manque ou l'excès des besoins énergétiques.

Pour ce faire, et suite à l'établissement d'un cahier de charge relatif au système élaboré dans ce travail de thèse, nous avons entamé la modélisation énergétique du système, ainsi que le dimensionnement et la modélisation de ses différentes composantes dont les batteries embarquées, les batteries stationnaires, les convertisseurs de puissance, l'éolienne et les panneaux photovoltaïques à installer au toit de la maison au cas de l'installation V2H/H2V proposée.

En particulier, la modélisation et le dimensionnement du système énergétique mis en relief dans cette étude et de ses composantes seront détaillés dans le chapitre 2. La modélisation énergétique globale de l'ensemble du système en fonction de la production et la consommation d'énergie sera également représentée.

Le système étudié implique un véhicule électrique doté d'une batterie embarquée de type NiMH d'une capacité de 75 Ah et d'une profondeur de décharge de 80%. L'habitat effectue une consommation journalière de 31.1 kWh partiellement ou complètement compensée par la production d'énergie de 33 modules photovoltaïques monocristallins d'une puissance nominale de 280Wp dans des conditions standard, ainsi que la production d'une éolienne à axe horizontal d'une puissance de 2.8kW. La consommation journalière calculée pour l'habitat comprend l'énergie consommée pour le chauffage et la ventilation, le chauffage de l'eau, l'éclairage, les appareils audiovisuels, la cuisine, le lavage, le séchage, le réfrigérateur, ainsi que l'utilisation des appareils électroniques et la prise électrique du véhicule.

Outre que les véhicules électriques ont énormément participé à la réduction de la pollution dans le monde entier, leurs batteries embarquées peuvent être utilisées comme moyen de stockage et de restitution d'énergie électrique qui ne semble pas être facilement stockée en grandes quantités. En fait, la recharge des véhicules peut être programmée en fonction de l'offre et la demande d'électricité et des besoins énergétiques. Ainsi, tant que l'offre en électricité dépasse la demande, les batteries de véhicules seraient utilisées comme moyen de stockage afin de récupérer l'énergie excédentaire et d'en profiter lorsque la tendance est inversée. Les véhicules chargeraient alors leurs batteries où l'énergie serait stockée. Le contrôle des flux énergétiques du véhicule a été élaboré à travers la proposition d'un algorithme d'optimisation multi-objectifs et multi-critères dépendant de l'offre et la demande de l'électricité. Donc, le stockage d'énergie est proposé dans le chapitre 3 via un algorithme d'optimisation multi-objectifs des flux d'énergie pénétrant les véhicules électriques à partir de ressources renouvelables liées à la maison ou au bâtiment au cours du processus de recharge.

Ainsi, la modélisation des objectifs qu'il faudra atteindre pour une recharge optimale et les contraintes qui y sont associées a été établie.

L'objectif de l'optimisation serait d'acquies les solutions Pareto-optimales pour le système développé visant à trouver l'état de charge maximal, l'énergie de vallée, l'énergie de propulsion et les pertes minimales pouvant être atteintes par les véhicules électriques pendant leur phase de charge. Pour ce faire, le chapitre 3 détaille cette optimisation tout en décrivant d'abord les fonctions-objectifs liées à l'optimisation de la recharge de véhicules. L'algorithme génétique multi objectifs a été adopté comme approche d'optimisation pour calculer les solutions optimisées des fonctions-objectifs.

Par ailleurs, vu que certaines fonctions-objectifs ne semblaient pas atteindre leurs valeurs optimisées simultanément, leur optimisation imposera l'interférence de la priorisation d'un objectif par rapport à l'autre ; et afin de combiner les solutions obtenues en une solution optimisée globale du système, les fonction-objectifs ont été normalisées. Une fois le Pareto-front des fonctions-objectifs défini, la méthode de la somme pondérée a été appliquée via différents scénarios d'optimisation où des poids aléatoires sont attribués aux fonctions dépendamment des objectifs fixés et de l'ordre de préférence du décideur.

Enfin, les valeurs optimisées obtenues ont été vérifiées et validées par simulation à l'aide du solveur gamultiobj du logiciel Matlab, prouvant ainsi la pertinence de l'algorithme proposé. Le Pareto-front obtenu par simulation vérifie bien le calcul de l'algorithme génétique en montrant une convergence vers les valeurs de référence et optimums théoriques définis.

A chaque fois qu'un déficit de production survient par rapport à la demande d'électricité, la décharge des véhicules électriques s'effectue, et l'énergie excédentaire stockée dans les batteries pourrait être récupérée, en outre de l'usage personnel du véhicule, pour alimenter le réseau électrique ou les habitats. La restitution d'énergie prend en compte la quantité d'énergie qui devrait être conservée dans la batterie des véhicules pour leurs besoins personnels et les trajets prévus. Le chapitre 4 détaillera cette restitution d'énergie à travers une optimisation multi-objectifs des flux d'énergie sortant du véhicule durant sa décharge. Par suite, en suivant la même procédure optée dans le chapitre 3, cette optimisation ainsi que les objectifs qui y sont associés seront modélisés. Ce processus de récupération d'énergie a été réalisé au moyen d'une optimisation à objectifs multiples visant à minimiser l'état de charge de la batterie, le temps de décharge des véhicules et les pertes, et à maximiser la durée de vie de la batterie. Pareillement au

cas du stockage et de la recharge des véhicules, l'algorithme génétique est utilisé pour calculer les solutions optimisées du problème d'optimisation relatif à la décharge. Les fonctions objectifs sont ensuite normalisées et la méthode de la somme pondérée est utilisée avec des poids aléatoires définis selon l'ordre de priorité du décideur dans différents scénarios afin d'aboutir à une solution optimisée finale. Les calculs sont également vérifiés et l'optimisation validée par simulation grâce au solveur gamultiobj du logiciel Matlab.

En conséquence, l'optimisation proposée a contribué à la création d'une solution optimisée efficace pour les quatre fonctions de fitness qui convergerait vers l'optimum théorique calculé, tout en tenant compte des besoins énergétiques du véhicule qui devrait être conservés dans la batterie pour son usage personnel.

Malgré les différences entre les objectifs définis pour la recharge et ceux pour la décharge, l'optimisation appliquée a prouvé, par calculs et par simulation, que les solutions optimisées convergent vers leurs références théoriques.

Cependant, suite à l'application de la méthode des algorithmes génétiques, les fonctions dépendant des mêmes variables pourraient affecter les solutions optimisées les unes des autres. D'où la nécessité de créer un compromis et un ordre de priorités des objectifs pour la combinaison finale des optimums.

La marge de différence entre la production et la consommation d'énergie cède souvent la place à un énorme gaspillage. En effet, la production excessive d'énergie serait rejetée, tandis que la production déficiente se traduirait par des compensations coûteuses de l'énergie consommée; d'où la nécessité d'une régulation de l'énergie. Afin de contrôler les flux d'énergie circulant entre une résidence domestique alimentée par des sources d'énergie renouvelable, les véhicules électriques et le réseau, et visant à atteindre un système équilibré, un algorithme de contrôle et de régulation a été développé dans le chapitre 5. Cet algorithme prend en charge les processus de recharge et de décharge des véhicules en fonction de la production et de la consommation d'énergie, en d'autres termes de l'offre et la demande d'électricité. L'algorithme a été testé avec un échantillon de 31 jours avec différentes valeurs d'entrées pour la production et la consommation ainsi que des états de charge des flottes automobiles renfermant 3 à 6 véhicules électriques chacune.

En outre, comme l'algorithme permettait d'intégrer un nombre infini de véhicules, une amélioration a été proposée de sorte que le nombre de véhicules retenus par la recharge ou la décharge soit minimisé. Ainsi, le transfert d'énergie serait pratique et la consommation de batteries serait réduite. Subséquemment, dans la version améliorée de l'algorithme, les véhicules disponibles subissent une classification selon leur état de charge et la longévité de leur batterie avant d'injecter ou de récupérer leur énergie, dans le but d'obtenir un système équilibré sans détériorer les batteries des véhicules. Par conséquent, les processus de stockage et de restitution d'énergie ont été optimisés grâce à la minimisation du nombre de véhicules chargés ou déchargés. Ainsi a été développée une stratégie de gestion énergétique permettant de contrôler les flux énergétiques dans les deux sens V2X et X2V établissant une loi de commande bidirectionnelle qui serait une solution d'adaptation de l'offre à la demande d'électricité.

## General Introduction

Along with the continuous growth of the world's population, the energetic needs keep getting amplified, which leads to the exhaustion of all the available reserves as well as huge emissions of greenhouse gases. Thus human life expectancy keeps decreasing and public health seems to be consistently threatened by the climate change and disastrous pollution of toxic carbon dioxide gases emitted. Hence, noting that the transportation sector consists of one of the largest and most polluting industries, the vehicles electrification is increasingly adopted as an efficient solution to the pollution crisis.

As the worldwide storage capacity of electric energy is still limited, the adaptation and regulation of electricity supply and demand have become crucial. One way to realize this regulation is through energy storage and retrieval within the electric vehicles' batteries.

This study seeks the control and regulation of the reversible energy flows between the electric grid, houses and electric vehicles and their optimization in a way to reach a balanced system while reducing the difference margin between electricity production and consumption; thus charging or discharging the electric vehicles according to the available excess or lack of energy. It focuses on energy systems involving electric vehicles' charging and discharging as well as the optimization of energy flows linked to these systems. Thus, the chapter 1 of the study exhibits the state of the art where the available literature discusses the problem and its different approaches. Hence, electric vehicles and energy systems are first treated. The components of electric vehicle energy systems are then considered; among others, the different types of vehicles' batteries, their chargers and converters, in addition to renewable energy sources. Besides, electric vehicles' charging and discharging operations and the bidirectional energy flows between the vehicles, the electric grid, the home and the buildings are debated as energy consumers. Additionally, multi-objective optimization of energy systems and many of its approaches are exposed. Some energy management strategies and charging/discharging scheduling are also considered.

Subsequently, an energy system including a residential household, an electric vehicle and the grid is defined in chapter 2. The house is powered by renewable energy sources and the vehicle's batteries are used as means of storage and retrieval of energy. Eventually, the study

seeks to omit the grid's supply in a way to maintain the balance between the electricity demand and supply. The electricity supply is collected through solar and wind energy resulting from meteorological station data. As for the electricity demand, it is defined by the functional household appliances. The vehicles' charging and discharging would then be defined by the margin of difference between the electricity production and its consumption, and the lack or excess of the energetic needs.

Consequently, the technical specifications related to the energy system developed in this research work have been established. Then, the energetic modeling of the system, as well as the sizing and modeling of all its components, including the vehicle's on-board batteries, the house's stationary batteries, as well as the power converters, wind turbine and photovoltaic panels to be installed on the roof of the proposed system's house have been studied. Particularly, the modeling and sizing of the energy system highlighted in this study is detailed in Chapter 2, and the global model of the entire system is presented with regards to the energy production and consumption.

In order to manipulate the circulating reversible flows and manage the vehicles' charging and discharging based on the excess or lack of energy, the energy production and consumption are first assessed and compared. Accordingly, the charging or discharging of vehicles is launched and either process is optimized to avoid any energy waste.

As electric vehicles' batteries can be used for energy storage and retrieval, their charging and discharging can be scheduled according to the supply and demand of electricity. Thus as long as the electricity supply exceeds its demand, vehicles batteries would be used as means of storage to recover the excess of energy and benefit from its usage. The vehicles would then charge their batteries where energy would be stored.

Successively, the control of vehicle energy flows is developed through a multi-objective optimization algorithm that depends on the electricity supply and demand. The vehicles' charging and energy storage is proposed in chapter 3, via a multi-objective optimization of the energy flows penetrating the vehicles from the renewable sources supplying the house or the building. Hence, the modeling of the objectives to be sought for an optimized charging and its associated constraints are conferred. The objective aimed by the optimization is to acquire the



Pareto-optimal solutions for the developed system aiming to find the maximal state of charge, the valley energy and the propulsive energy along with the minimal losses attained by the vehicles during their charging process. Thus, chapter 3 describes this optimization in details. The multi-objective genetic algorithm is adopted as an optimization approach to compute the optimized solutions of all the defined objective functions. Moreover, as some objective functions seem to be conflicting, their optimization imposes the prioritization of some objectives with respect to others. In order to combine the solutions obtained into a global optimized one, the objectives have been normalized and the weighted sum approach has been applied through different optimization scenarios where random weights are assigned to the function depending on the decision maker's order of preference. The final optimized solutions are validated by simulation using the gamultiobj solver of Matlab software, proving the relevance of the proposed algorithm. The resulting Pareto-front verifies the genetic algorithm calculations by showing a convergence towards the defined reference values and theoretical optima.

However, when there's a lack of production with regards to the electricity demand, the vehicles discharge and the excess of energy stored in the batteries would be restituted to feed the grid or habitats. This energy restitution takes into account the energy that must be kept in the vehicles' batteries for their personal needs and planned journeys. Chapter 4 highlights this energy restitution through a multi-objective optimization of the energy flows leaving the vehicle during its discharge. Consequently, following the same procedure as in chapter 3, the optimization aims to minimize the state of charge, the discharging time and the losses and to maximize the battery life of the vehicles. Likewise, the genetic algorithm is adopted to calculate the optimized solutions of the discharging optimization problem. The objective functions are then normalized and the weighted sum approach is used with random weights according to the decision maker's priorities, to end up with a global optimized solution. The calculations are also verified and validated using the gamultiobj solver of Matlab. Despite the differences between the objectives defined for the charging and discharging phases, the optimizations' computation proved that the optimized solutions converge towards their theoretical references. However, following the application of the method of the genetic algorithm, the functions depending on the same variables could affect the optimized solutions of each other, hence the need to create a compromise and prioritization of goals for the final combination of optima.

In order to avoid energy waste and tighten the difference margin between energy production and consumption, energy regulation would help control the flows of energy circulating in the study's energy system. Therefore, a control and regulation algorithm aiming for a balanced system has been developed in chapter 5. This algorithm is responsible for the management of charging and discharging scheduling based on the electricity production and consumption variations. It is first tested with a sample of 31 days where different input values for production and consumption and different state of charge values for fleets of 3 to 6 vehicles each are implemented. Then, the algorithm has been improved through the minimization of the number of charging and discharging vehicles. In this case, the transfer of energy would be more practical and the battery lives exhaustion would be reduced. Thus, in the improved version of the algorithm, the available vehicles are classified according to their state of charge and the longevity of their battery, in order to obtain a balanced system without damaging the batteries. Therefore, an energy management strategy has been developed to control the bidirectional energy flows with respect to the electricity supply and demand, as well as the eventual needs of the vehicles.

## **Chapter 1 - Literature Review**

1. 1	Introduction.....	28
1. 2	Energy systems and demand side management .....	30
1. 3	EV Charging/discharging through V2X/X2V technologies.....	31
1. 4	Energy systems modeling .....	36
1.4.1	Electric Vehicles, batteries, battery chargers and converters.....	36
1.4.2	Wind turbines.....	45
1.4.3	PV panels .....	46
1. 5	Multi-Objective Optimization.....	49
1. 6	Energy management strategies.....	52
1. 7	Conclusion .....	58

## 1.1 Introduction

As the world's population keeps growing, the human needs in energy keep increasing beyond the extraction and burning of fossil fuels (coal, gas, oil). In fact, humanity has been consuming 20 % more energy than the Earth's production of energy in a given period. Besides exhausting the available reserves, the energy produced from fossil fuels pours huge quantities of greenhouse gases GHG in the atmosphere. The CO<sub>2</sub> emissions resulting from fuel combustion have reached approximately 29 billion tons in the year 2009 [1]. Noting that the global demand for fossil primary energy keeps increasing, the emissions resulting from oil, gas and coal keep increasing as well. As a result of the climate change and the pollution caused by the emission of carbon gases, public health seems to be threatened and the human life expectancy reduced. Noting that, on average, more than 90 % of humans' time is spent in the building and the vehicle, the energy consumption keeps increasing since the 80s in the residential-tertiary and the transportation sectors. With the new generation of combustion engines using direct injection and electromagnetic valve control, the vehicles currently burn less fuel and throw away less CO<sub>2</sub> than thirty years ago [1].

Besides, some of the main problems that have been occupying humanity in the last decades are those of water and air pollution, the emission of greenhouse gases as well as fossil fuels and the limited nonrenewable resources. All industries worldwide seek the reduction of pollution and greenhouse gases emissions. In addition, the internal combustion engines' (diesel and gasoline) efficiency, where more than 60 % of the fuel is lost into heat, remains low compared with the efficiency of electric engines. Hence, the electrification of vehicles recently emerged as a silent and non-polluting alternative to conventional vehicles; its development and commercialization recently seem to be expanding [1], [2], [3].

Noting that the transportation sector is responsible for huge greenhouse gases emissions (approximately 22 % of the total emissions) severely affecting the atmosphere. Consequently, several studies have shown the interest in reduction of the pollution related to transportation [4]. In addition, as the industry of transportation is one of the biggest and most polluting, the electrification of vehicles seems to be a significant solution for the problem of pollution to be

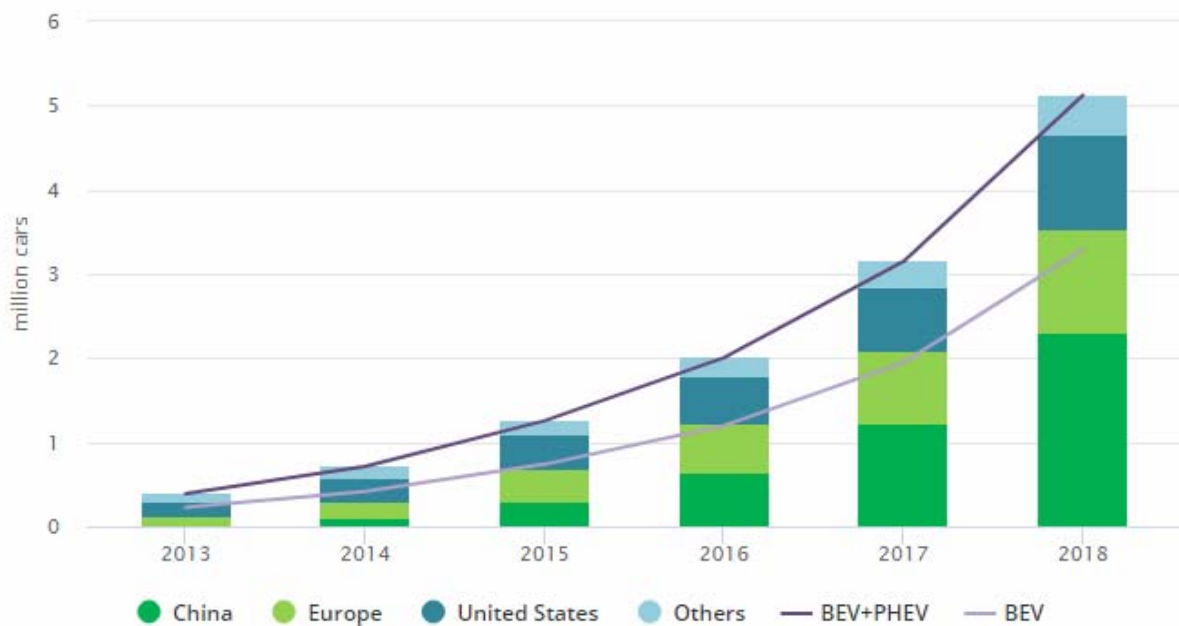
taken into consideration. The number of Electric Vehicles (EV), Battery Electric Vehicles (BEV) and Plug-in Hybrid Electric Vehicles (PHEV) has gradually increased to reach 5.1 million vehicles in 2018 as this number keeps increasing considerably showing the increase of interest in the electric transportation's technology [1], [2], [3].

However, despite all its advantages, the electric vehicles' biggest problem resides in their low battery autonomy, limiting the vehicles' scope to a travel distance of a hundred kilometers in average [1]. Electrified vehicles play a major role in the challenging optimization of the returns of the transportation energy consumption. Actually, with the use of electric vehicles, the destructive humanitarian threats associated with air pollution, climate change, rising gas prices and oil scarcity, are minimized [5].

The increase in the number of electric vehicles requires heavy arrangements of transmission and electricity distribution systems to transport a larger electricity flow and to set up sufficient charging sites [1].

In the year 2014, EV constituted around 3 % of the total sale of new vehicles [6]. Yet, they are expected to reach around 25 % of global sales of cars by the year 2025. For instance, in France, the introduction of EVs is underway, and many charging stations have already been implemented in private and open areas. The Committee of the Regional Council of Ile-de-France has awarded, on the 18<sup>th</sup> of June 2014, a grant of nearly one million euros for the installation of 130 new EV charging stations. By 2020, 16000 charging stations will be installed in this area [7].

According to the International Energy Agency (IEA) and the Electric Power Research Institute (EPRI) the number of electric vehicles will keep increasing in the future [7]. This growth seems possible as major automobile companies are investing in electrified vehicles technology. Moreover, the energy storage demand keeps increasing as well. The energy storage market in the United States is expected to grow 7 times bigger than the market in 2015 [6]. Consequently, Fig. 1.1 shows the evolution of the global electric car stock between 2013 and 2018 based on the IEA studies.



IEA. All rights reserved.

Note: BEV = battery electric vehicle, PHEV = plug-in hybrid electric vehicle.

**Figure 1.1: Evolution of the global electric car stock according to the IEA [8]**

## 1.2 Energy systems and demand side management

In the coming years, it is expected that a strong EV development would highly affect the electrical network. In fact, it would change its voltage plane and its load profile with an increase in peak consumptions. It would also contribute to higher losses as well as an injection of harmonics into the network, and a risk of congestion on the grid. Hence, it would amplify the voltage imbalance between phases, and create an accelerated aging of the distribution transformers. Uncontrolled EV charging causes an increase of 50% to the peak consumption in a residential section where there's a low EV penetration rate, and 2.4 to 3.3 times for sections where there is a medium to high EV penetration rate. Particularly, establishing energy management strategies and adopting a controlled charging of vehicles would avoid a huge energy waste and significantly reduce the peak consumption. Moreover, a simultaneous charging of all vehicles, for instance in the evening around 7 p.m., would lead to a consumption peak which is more likely to disturb the quality of the electric grid service. Therefore, maintaining the

balance between the demand for electricity and its supply requires a smart management charging strategy [7].

Implementing demand response where demand directly interacts with the generation supply in modern power systems contributes to an efficient balance in the demand-supply relationship [9]. Eventually, it is because of the successful energy management systems that a big number of electric vehicles can be handled by the distribution networks. In fact, on the country scale, the electricity demands of the networks might vary based on the large number of electric vehicles and their needs. [3].

### **1.3 EV Charging/discharging through V2X/X2V technologies**

The process of charging the EV from the grid is called Grid to Vehicle (G2V), while the discharging process of transmitting electricity from the EV to the grid is called Vehicle to Grid (V2G). Similarly, electric vehicles can also discharge the surplus of their batteries' energy back into residential houses or buildings. These processes are respectively referred to as Vehicle to Home (V2H) or Vehicle to Building (V2B) [9].

The initial design of electric vehicles aimed the carbon emission reduction and energy saving, and their distributed storage system potential has been recognized. Eventually, the excess of energy generated by the renewable energy sources can be stored within the electric vehicle's battery, and then transmitted either to smart homes (V2H) or buildings (V2B) or back to the power grid (V2G) [9].

In fact, noting that the power electronics domain keeps getting more and more developed, electric vehicles do not only help in the pollution reduction and increase the renewable energy sources dependency, but also assist the power grid in the production of electricity as they perform as storage elements for the energy sources. Moreover, the bi-directional exchange created between electric vehicles and the grid would allow the charging of the vehicles' batteries as well as the power injection back to the grid. So the power grid gets stabilized in terms of frequency and voltage regulation and power demands would be fulfilled particularly during peak hours [2].



In [1], EV (Electric Vehicles) technology has been investigated through the three discharging operations: Vehicle to Home V2H, Vehicle to Grid V2G and Vehicle to Building V2B generally highlighting the possibility of discharging and sending the EV battery's surplus energy back to residential homes or buildings, or to the power grid.

It is to be mentioned that the power grid transmission V2G is the least efficient mode of all three modes as it has the largest transmission power losses. EV owners need to be motivated with rewards to perform in the greatest interests of the global power systems as they schedule the charging, V2H and V2G according to the market sell-back and real-time prices [9], [10], [11].

The V2G, V2H and V2B concepts might contribute to better efficiency, stability and reliability with regards to the grid's performance. However, without setting a rational scheduling, serious problems might occur due to deregulated charging or discharging, especially for a fleet of electric vehicles [9], [12], [13].

The simulation results for an optimization scheduling of EV with V2G and V2H have shown that EV functions as V2H (or V2B) at peak real-time price or G2V at valley real-time price or V2G whenever the sell-back market price is considerably higher than real-time price [9]. Comparing the V2G, V2H and V2B modes, the V2H infrastructure achievement is the less complicated. V2H and V2B structures are close, yet V2B needs more technology support. In urban areas, where the infrastructure upgrade would be complicated and expensive, the setup of V2H or V2B would be easy [9], [14]. As for V2G, it involves expensive installations for long power lines and aggregators supporting a bi-directional transmission between the vehicles and the grid [15]. As estimated, 2200 MWh to 4400 MWh power from EV will be basically consumed in 2020 [16].

The modeling of frequency regulation through a large scaled V2G system has been investigated in [6]. Based on the experiments and the operation data of electric vehicles' fleet within a municipality, the operations strategies and the performance of several biddings are characterized through a simulation model (using Simio Simulation Software) including random events, fleet and frequency regulation parameters [6], [17]. Fleet vehicle data was collected from three fleet of EVs that are city-owned, providing the information related to trip scenarios over a

four months span as well as the battery usage and the trips' length [6]. Referring to the grid signal, fleet operators have the possibility to make a decision concerning the bid amounts and whether the available resources can meet the grid demands. It is to be noted that the revenue increases and the fleet would less probably meet the grid demand with the increase of the bid amount. Thus the decision maker should weigh the opportunity costs resulting from successful bids against the failing bids that cannot fulfill the grid requests [6], [18].

In [2], an EV battery's bi-directional charger consisting of an AC/DC VSI (Voltage Source Inverter) converter and a DC/DC DAB (Dual Active Bridge) converter is designed. It performs as a shunt active power filter. This charger is controlled within a vehicle's operation whereas the home is powered by the grid. The energy injection into the power grid with the proper control can occur as the charger is completely bi-directional [19]. In order to ensure an appropriate functioning of the bi-directional charger, it would be recommended to exploit a control algorithm that takes in charge the management of the transition between the different operation modes [2]. The charging and discharging processes of the vehicle's battery are tested with a Matlab-SimPowerSystems-Simulink simulation. For the G2V operation mode test, the grid current which appears to be almost sinusoidal seems to be in phase with the grid voltage due to the AC/DC converter's control of the power factor correction (PFC). In V2G mode, the grid current and its voltage seem to be in opposite phases, as the grid is assumed to be a load in this case. In the active filter mode, where there isn't any power flow circulating between the grid and the battery, the grid voltage and current also seem to be in phase. In fact, the AC/DC converter can offer the grid a unity power factor, specifically in case there is no need for the battery to inject some power into the electric grid or when the vehicle's battery is fully charged [2]. The charger's active filter mode operates for elevated charging power [20]. The bi-directional charger's use aims to attain the limits that the standards have set in terms of power quality and appropriate charging and discharging of the vehicle's battery. In fact, all requirements can be satisfied by the charger through its control, which seems to be a promising background for the future experimental setups [2]. Briefly, the study described in [2] focuses on the electrical structure and functioning of bidirectional chargers. It controls the charging and discharging processes based on the battery's voltage and current variations. However, as the next chapters will show, our study allows a regulation of the energy flows based not only on the vehicles' state-of-charge, but also

on the electricity demand and supply.

Besides, in order to maximize the revenues of both the PHEV (Plug-in Hybrid electric vehicles) owners and the DSPs (Distribution Service Providers), and achieve a proper peak load shifting, the in-home PHEVs charging is investigated in [21]. A PHEV charging model of a leader-follower game based on the framework of Stackelberg game is presented to identify the revenue expectations and preference of each of the DSP and the vehicles' owners [21], [22], [23].

According to the pricing schedule that the leader or DSP has already set, the followers (vehicles' owners) take the decision concerning when to launch their vehicles' charging, and the DSPs have the possibility to incentivize the owners' charging so they prevent system peak load [24].

Eventually, once the charging process has started, the PHEV's charging costs remain stable without getting influenced by the charging price modification. Meanwhile, DSPs are able to optimize the schedule of pricing depending on the probability of PHEVs arrival and the residents' base load. A control scheme for PHEV charging based on realistic statistics and the IEEE 13-bus test feeder is proposed in [25]. All costs related to voltage regulation, power distribution and line loss are integrated into the model through power flow analysis. Extensive simulations have been performed in order to prove the effectiveness of the proposed control scheme [25]. The study has clearly shown that the distribution systems' power quality has improved considerably as the voltage fluctuations and peak load have been reduced. Particularly, the total consumption of electricity has declined by 14.9 % after voltage regulation, and the voltage fluctuations got remitted [21], [26]. The game-theoretic method highlights the affiliation between the PHEV owners' strategy of charging and the DSP's pricing strategy. Similarly to the Nash equilibrium game where the players do not have any tendency to modify their strategy of playing, the DSP would be able to analyze and assess the group performance of all customers. After applying approximate linear functions via power flow analysis, and validating the associated optimal algorithm, the distribution system's power quality has significantly improved with regards to reducing voltage fluctuations and the system's peak load. However, the stochastic base loads as well as the arbitrary arrival time of vehicles' owners and their random price

variation's tolerance are more likely to be taken into consideration in future works [21]. While driving, the specific energy consumption of EVs is lower and the transportation costs as well as the environmental pollution are reduced [3], [27], [28]. The impacts of the operation of several EVs on the distribution network have been investigated in [3] and a management algorithm has been suggested then the EV's impact on the grid gets reduced. In order to minimize the network's energy losses, and create a balance in the main feeders' electric load, a smart management approach for the charging process of a limited number of EVs and their impact on the low voltage network have been discussed in [29]. Therefore, a low voltage network and an IEEE 37-nodes test network that works at LV levels have been adopted in [3]. In addition, a distributed generation source (particularly a solar energy source, which is a three-phase generator with a 10 kW total power, assumed to function constantly at nominal power during the simulation) has been placed on one of the network's nodes in order to reduce energy and power losses.

Using the Digsilent Power Factory application [30], the power and the entire grid's losses have been further studied. Consequently, the power losses and the energy that is consumed from the main feeder follow the same pattern. In order to efficiently charge the electric vehicles, the peak load period is to be avoided and the nighttime period is to be adopted for charging [30]. Moreover, a large number of EVs contributes to the disappearance of the low load period of the night [3]. Concerning the network's voltage levels, it has been noted that the load profile and energy losses are at their highest values whenever the voltage levels are at their lowest and vice versa [3].

It is worth noting that there are four generations of V2G2V (or G2V2G):

The first generation reflects the current state of EVs and their charging stations. In this case, the EV is only an energy consumer and the communication with users is limited to orders and charging periods via a human-machine interface.

The second generation is characterized by the need for charging management. The power flow would still be unidirectional, and the charging management would require an improvement of the communication from both the network's side and the charging station's side.

The third generation involves bi-directional power flow chargers of a high rated power, with a significantly reduced charging time. Yet, the V2G operation is still rudimentary at this stage.

In the fourth generation, the EV becomes a distributed energy storage node that receives the network's energy when it is cheaper, or when it comes from renewable sources. In this case the EV is a consumer and producer of energy [31].

Consequently, the fourth G2V2G generation will be adopted in our study, as it will focus on the controlled bi-directional energy flows where a specified energy management strategy will be defined. Mainly, in our study the adopted energy source is renewable from solar panels and wind turbines. So, the first “G” in G2V2G refers to Home or building, while the second “G” refers to Grid, Home or Building.

#### **1.4 Energy systems modeling**

The modeling of energy systems supplied by renewable sources such as solar panels and wind turbines has been investigated, based on the available literature. Consequently, the energy systems' components have been modeled and represented separately. The separate modeling of each component might contribute to a global model of this study's energy system. In particular, the study's energy system will be modeled and sized in chapter 2.

##### ***1.4.1 Electric Vehicles, batteries, battery chargers and converters***

Electric vehicles are defined as automobiles powered by electric motors fueled by batteries or fuel cells. One of the main weaknesses of electric vehicles is their price and technical performance. In fact, all EVs models are more expensive than their thermal (conventional) equivalents, due to the high prices of batteries that are mostly rented by automobile manufacturers. As for the EVs' performance and capabilities, some aspects such as the top speed, the EVs' autonomy, the volume of their batteries, the aging and batteries' life, as well as the standard charging duration (ranging between 5 and 8 hours at a single phase 220V power source) still require some improvement.

The main difference between electric vehicles and the internal combustion engine

conventional vehicles is that the EVs' power supply is based on in-battery storage of electricity while in the conventional cars the internal combustion results in a mechanical power supply. The diesel or gasoline engine and the fuel tank of a conventional car are replaced by a battery pack and an electric motor which is empowered by a controller [4].

The main differences between gasoline powered vehicles and electric vehicles are stated in table 1.1:

**Table 1.1: Comparison between Gasoline powered vehicles and electric vehicles [4]**

GASOLINE POWERED VEHICLES	ELECTRIC VEHICLES
Cause of almost half the total atmospheric pollution via carbon monoxide, nitrogen oxides, and hydrocarbons.	97 % cleaner, no tailpipe emissions, no leakage of contaminated oil into water supplies, and no local pollution.
Engine must be running, even when the car is idle.	Silent as there isn't any internal combustion engine.
Higher maintenance costs	Lighter car, fewer parts, less maintenance.

The electric motors most used in electric and hybrid vehicles are the series motors, the motors with separate excitation, and the synchronous motors. Yet, the synchronous motors are the most used by the vehicles' manufacturers. However, despite all of their advantages, the electric vehicles' biggest problem resides in their low battery life, limiting the vehicles' scope to a travel distance of ten to hundred kilometers [1].

EVs are expected to replace the conventional ICE (Internal Combustion Engine) cars as the EVs purchasing is increasing by 10 % every year and the EV penetration is foreseen to grow at a faster rate. Therefore, some strategies, such as the grid reinforcement, need to be developed in order to support the EVs flow of energy into the electric grid. However, the grid reinforcement strategy requires long durations of upgrading and high investment costs [32].

AC motor installations tend to be more complex and expensive than DC installations. In a DC electric vehicle, the controller transports the electric power in a controlled way from the batteries to the engine. The frequency at which this power is transported is not included in the human hearing range of frequencies. That explains why the EVs seem to be so silent, and the implementation of a warning device in order to alert pedestrians of their presence seems to be a possible future EV requirement. In an AC electric vehicle, three pseudo-sine waves are created by the controller [4].

The EV storage medium is the battery. The vehicles' batteries seem to be the most challenging technology in EVs. There are several types of batteries. Despite their economical prices, lead acid batteries do not seem to be ideal for electric vehicles because of their huge size and weight, their limited capacity, their short life and long charging time. Nickel Metal-Hydrate (NiMH) or lithium-Ion batteries are mostly used as electric vehicles' storage batteries, despite the fact that these types of batteries are very expensive. Particularly, the Li-Ion battery keeps being the most used for the Plug-in Hybrid Electric Vehicles (PHEV) and the Battery Electric Vehicles (BEV). The NiMH battery is rather used for the Hybrid Electric Vehicles (HEV).

Additionally, each electric vehicle has a 12 Volts lead-acid battery which is mainly used to power the car accessories such as the lights, the radio, the power windows, etc.. Thus, a DC/DC converter is used to convert the main battery's voltage back to 12V and to keep the 12V battery charged. A Battery Management System (BMS) ensures the normal operation of all cells in a battery pack. To design a BMS system, a detailed model of the battery must be built as detailed in [4], [7].

Accordingly, the below table 1.2 lists the advantages and disadvantages of the most available battery technologies in the market. While table 1.3 shows a comparison between the different types of battery technologies based on their depth of discharge and performance.

**Table 1.2: Comparison between batteries types [33]**

Battery Type		Advantages	Disadvantages
Lead		Low cost	- Low density Wh/kg - Sudden death of battery
Ni/Cd		Reliability / Cyclability	- Low density Wh/kg
Ni/MH		Good energy density	- High cost of basic materials - Behavior in low temperature
Sodium Chloride Nickel		Good energy density	Limited power High auto-discharge
Li-ion	LiCoO <sub>2</sub>	Excellent specific energy and power	Expensive
	LiFePO <sub>4</sub>	- Good energy performance (Wh/kg), security and cyclability - low cost compared with LiCoO <sub>2</sub>	Charging at low temperatures
Li-metal	Polymer	Thin film batteries easy to accommodate	Expensive

**Table 1.3: Comparison between different battery technologies based on depth of discharge and performance [34]**

Battery type	Depth of Discharge	Performance
Lead-Acid	30 %	Most economical for huge applications where weight is not involved.
Nickel-Cadmium (Ni/Cd)	90 %	Low energy density. Adopted in applications where long life, low costs, and a high discharge rate are needed.
Nickel Metal Hydride (Ni/MH)	80 % to 100 %	Higher energy density but shorter life cycle than Ni/Cd.
Lithium-ion (Li-ion)	75 % - 80 %	Light weight and high energy density.



The above stated comparison, Table 1.3, shows that Lithium-ion batteries, that are nowadays the most used in electric vehicles technologies, seem to have the best performance. However, NiMH batteries will be adopted in this study for their storage capability, and this choice is further detailed in chapter 2.

As given in [7], the EV battery model is presented as follows:

$$E_0 = E - R_p \frac{Q}{it-0.1Q} i^* - R_p \frac{Q}{Q-it} it + A e^{-Bit} \quad (1.1)$$

$$\text{Whereas: } \begin{cases} E_0 = \text{Open circuit voltage (V)} \\ E = \text{constant voltage (V)} \\ R_p = \text{polarization resistance } (\Omega) \\ Q = \text{Nominal capacity of the battery (Ah)} \\ it = \text{instant load of the battery (Ah)} \\ i^* = \text{low - frequency filtered current} \\ A = \text{voltage factor ; amplitude of the exponential zone (V)} \\ B = \text{load factor ; load at the end of the exponential zone (Ah}^{-1}) \end{cases}$$

In addition to the batteries and the motors, the following converters and inverters are essential components of hybrid and electric vehicles:

- DC/DC converter: responsible for the voltage regulation at the terminals of the motor.
- DC/AC inverter: responsible for the torque, speed regulation, the three-phase AC motors power supply through the battery's energy and power control as of  $P = C \cdot \Omega$ .

DC/DC bidirectional converter: the charging of the 12 V on-board battery through the HV battery, and partial charging of the HV battery through the 12 V on-board battery.

Battery chargers are specified depending on the type of power supply, whether single-phase or three-phase, and the power transmission mode. In the case of supply by alternating current, the charging process involves two conversion steps:

- AC/DC conversion: the transformation of the AC current issued by the distribution network into a DC current is carried out either by a diode rectifier bridge, or by other systems such as a Thyristors Bridge or a converter with sinusoidal current absorption.
- DC/DC conversion: the direct current obtained at the end of the first conversion is

modified to match the battery charging profile.

The AC power drawn from the grid is converted into DC power through a recovery system and EMC filtering; the electric motor is used as a filter element; the traction converter (inverter) is used for the monitoring of the battery charging process. The power level provided by the converter would be a slow charging for single-phase and a fast charging for three-phase power supply [7], [35].

*i. DC/DC converter – boost chopper:*

The DC / DC boost chopper with non-reversible current is used to increase the voltage of the PV panels to reach the voltage of the stationary lead-acid battery [36]. Its wiring diagram is presented in Figure 1.2.

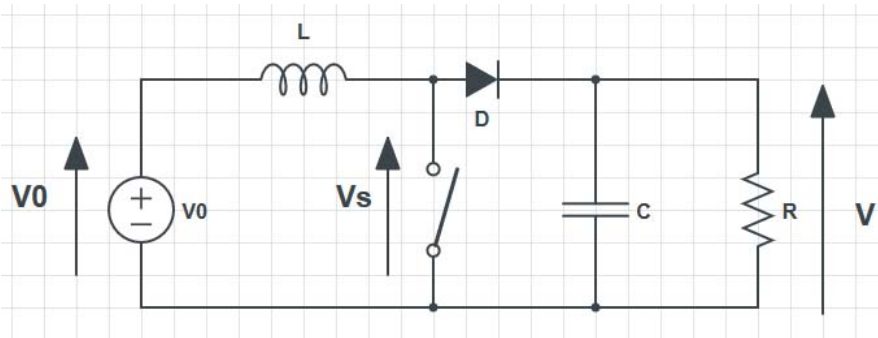


**Figure 1.2: DC/DC boost chopper wiring diagram**

Based on the wiring diagram of Fig. 1.2, and in order to assess each of the boost chopper's electrical components aside, the calculation is divided into two phases where the switch would be close then open respectively.

It is assumed that the circuit is ideal (no losses in the components, no voltage drop across the diode ...). In this wiring diagram, we distinguish the two following phases:

Phase 1:  $0 < t < \alpha T$  (with  $0 < \alpha = \text{cyclic ratio} < 1$ ;  $T = \text{period}$ ): this represents the energy accumulation phase where the switch is closed (Fig. 1.3).

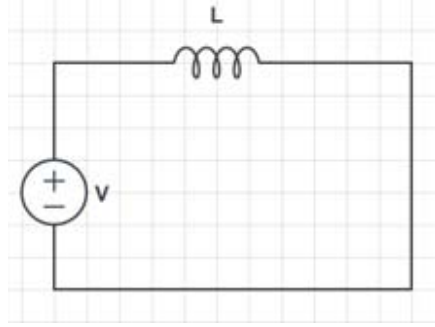


**Figure 1.3: Phase 1:  $0 < t < \alpha T$**

$$V_0 = L \frac{di_L}{dt} \quad (1.2)$$

At the end of the ON state:

$$\Delta I_{L,ON} = \int_0^{\alpha T} di_L = \int_0^{\alpha T} \frac{V_0}{L} dt = \frac{V_0 \alpha T}{L} \quad (1.3)$$

Phase 2:  $\alpha T < t < T$ : Switch open (Fig. 1.4):

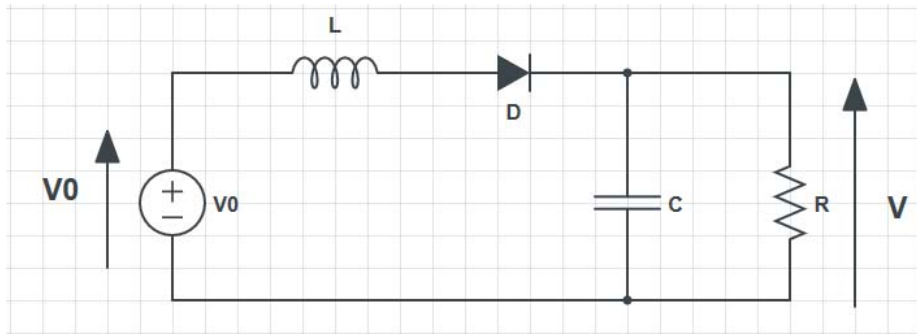


**Figure 1.4: Phase 2:  $\alpha T < t < T$**

$$V_0 - V = \frac{L di_L}{dt} \quad (1.4)$$

$$\Delta I_{L,OFF} = \int_{\alpha T}^T di_L = \frac{(V_0 - V)}{L} \int_{\alpha T}^T dt = \frac{(V_0 - V)(1 - \alpha)T}{L} \quad (1.5)$$

Summing up equations (1.3) and (1.5):

$$\Delta I_{L,ON} + \Delta I_{L,OFF} = \frac{V_0 \alpha T}{L} + \frac{(V_0 - V)(1 - \alpha)T}{L} = \frac{V_0 \alpha T + V_0 T - V_0 \alpha T - VT + V \alpha T}{L} = \frac{T(V_0 - V(1 - \alpha))}{L} \quad (1.6)$$

Therefore, for  $0 < t < T$ :

$$L \frac{di_L}{dt} = V_0 - (1 - \alpha)V \quad (1.7)$$

Permanent regime:

$$\text{Energy stored in the inductance: } E = \frac{1}{2} LI_L^2$$

The current flowing through the inductor at the beginning and at the end of the switching cycle is the same:

$$\Delta I_{L,ON} + \Delta I_{L,OFF} = 0$$

$$\Rightarrow \frac{V_0 \alpha T}{L} + \frac{(V_0 - V)(1 - \alpha)T}{L} = 0$$

$$\Rightarrow V_0 \alpha T + V_0 T - V_0 \alpha T - VT + V \alpha T = 0$$

$$\Rightarrow V_0 T - V(1 - \alpha)T = 0$$

$$\Rightarrow V_0 T = V(1 - \alpha)T$$

$$\Rightarrow \frac{V}{V_0} = \frac{1}{1 - \alpha} > 1 \tag{1.8}$$

Thus, equation (1.8) proves that the output voltage  $V_0$  exceeds the input voltage  $V$ .

ii. **Bidirectional DC/DC converter:**

Its wiring diagram is presented as follows [36] (Fig. 1.5):

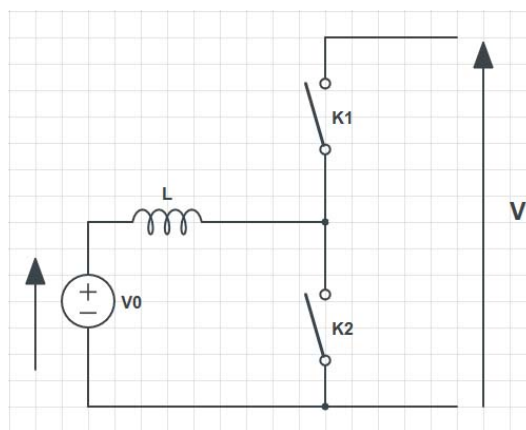
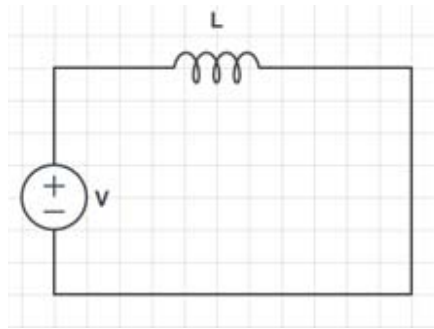


Figure 1.5: DC/DC bidirectional converter wiring diagram

Similarly, the calculations are estimated through two phases where the switches alternate between open and close positions.

Phase 1:  $0 < t < \alpha T$ : Switch K1 OFF, K2 ON (Fig. 1.6):



**Figure 1.6: Phase 1:  $0 < t < \alpha T$**

$$V_0 = L \frac{di_L}{dt} \quad (1.9)$$

$$\Delta I_{L,1} = \int_0^{\alpha T} dI_L = \int_0^{\alpha T} \frac{V_0}{L} dt = \frac{V_0 \alpha T}{L} \quad (1.10)$$

Phase 2:  $\alpha T < t < T$ : Switch K1 ON, K2 OFF (Fig. 1.7):

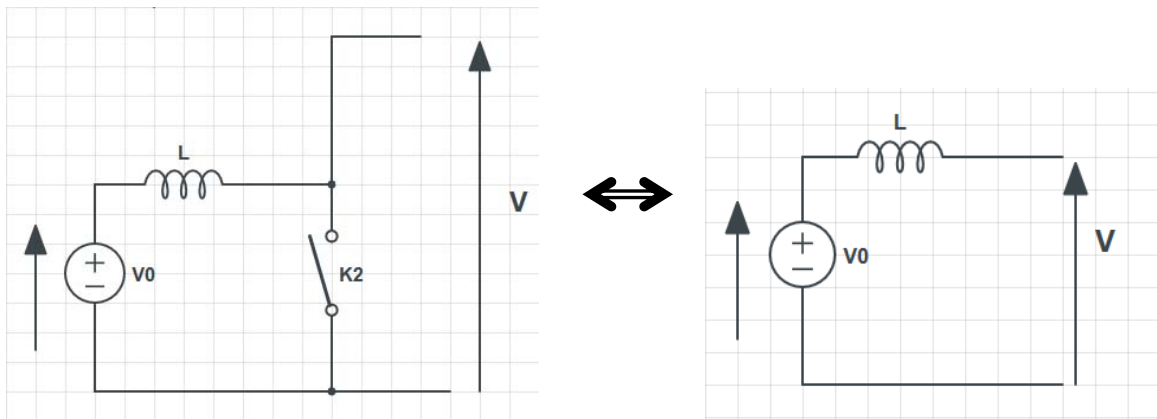


**Figure 1.7: Phase 2:  $\alpha T < t < T$**

The switching frequency and average duty cycle related to this application are embodied as follows:

Switching frequency:  $f = 20 \text{ kHz}$

$$\text{Average duty cycle: } \alpha = 1 - \frac{V_0}{V} \quad (1.11)$$

$$V = V_0 - L \frac{di_L}{dt} \quad (1.12)$$

$$\Delta I_{L,2} = \int_{\alpha T}^T dI_L = \frac{(V_0 - V)}{L} \int_{\alpha T}^T dt = \frac{(V_0 - V)(1 - \alpha)T}{L} \quad (1.13)$$

The sum of equations (1.10) and (1.13) would result into:

$$L \frac{di_L}{dt} = V_0 \alpha - (1 - \alpha)(V_0 - V) = V_0 - (1 - \alpha)V \quad (1.14)$$

The energy system adopted in this study highlights the renewable energy sources supply. And the energy supply by renewable sources involves wind turbines and photovoltaic panels that would allow inexhaustible energy generation with reduced GHG emissions. Yet, the choice of the most convenient wind turbine and PV panels for this study is presented in what follows.

#### 1.4.2 *Wind turbines*

Wind turbines have been annexed to the studied system to ensure enough energy production to feed the house and fulfill all its needs. In order to choose the right adjunct wind turbine to our system, the difference between both horizontal axis wind turbine (HAWT) and vertical axis wind turbine (VAWT) has been investigated.

Eventually, VAWTs could have several advantages over the HAWTs. In fact, VAWTs are easily controllable and they generate less noise than the HAWTs. Their installation also requires less space than the HAWTs.

However, it has been proven that HAWTs are widely more beneficial despite their slow activation and wind adaptation as they have an extensively better aerodynamic efficiency besides their easy implementation and maintenance [5].

**Table 1.4: Comparison between Horizontal Axis and Vertical Axis wind turbines**

<b>Horizontal Axis Wind Turbine</b>	<b>Vertical Axis Wind Turbine</b>
Better aerodynamic efficiency	Easily Controllable
Easy implementation and maintenance	Less noisy than HAWT
Slow activation and wind adaptation	Installation requires less space

The advantages and disadvantages of each type of wind turbines have been exposed in the comparison table 1.4.

Based on this comparison, a Horizontal Axis Wind Turbine is adopted in this study.

### **1.4.3 PV panels**

In order to choose the most adequate type of PV panels to be installed, a comparison between the different types of modules available in the market has been investigated in [37], [38]: High-grade Silicon is known as the most frequently used element for solar cells. It is processed with boron and phosphorous semi-conductors charged positively and negatively. Whenever the photovoltaic cell is hit by the sun's light energy, electrons start flowing freely from negative phosphorus to positive boron. The electric potential produces a current that can be connected through a metallic grid that covers the external circuit and the cell.

Actually, the types of cells used in PV systems are:

- A) silicon based cells (including mono-crystalline (c-Si), polycrystalline (p-Si), ribbon crystalline silicon (r-Si), amorphous Silicon (a-Si)),
- B) non-silicon based (including cadmium telluride (CdTe), copper indium gallium or diselenide (CIS/CIGS),
- C) new concept devices (including concentrated PV (CPV)).

In fact, the crystalline silicon technology, also called first generation solar technology, is mostly used in grid-connected applications with enough subsidies for its high cost offset, or in off-grid remote areas. Nevertheless, for this first generation technology, the potential for cost reduction in the long term is not enough to ensure affordable energy, and the processing is difficult due to the fragility of the silicon wafers.

Therefore, the second generation technology or thin film technology has appeared in order to reduce the high costs and simplify the manufacturing. In this technology, a thin-layer of photo-active material is placed on a flexible substrate using a-Si, CIGS or CdTe semi-conductor. Yet, even though the manufacturing got simpler, the efficiency of this technology remains relatively low.

And, in order to achieve high efficiency and low costs, the third generation technology has been developed. This last generation includes dye-sensitized titanium PV cells, as well as materials generating electron-hole pairs. Hence, the photovoltaic modules are classified in the Fig. 1.8 [37] as follows:

**Silicon based modules:** Silicon modules are of 3 types: mono-crystalline, polycrystalline and amorphous silicon.

- Mono-crystalline silicon modules, which generally are of a dark color (gray or black), are specified with the best efficiency, yet relatively high prices.
- Polycrystalline silicon modules are of a shiny blue color that derives from several small crystals. These modules are cheaper, yet they have a lower efficiency.
- Amorphous silicon cells (also known as thin-film cells) have a brown or a reddish brown color, and are constituted from a very thin layer of un-crystallized silicon.

**Non-silicon based modules** (that are also thin-film cells): CdTe – Cadmium Telluride, CIS /CIGS – Copper Indium Gallium Selenide, seem to be the best decentralized photovoltaic electricity production.

#### **Photovoltaic cells production:**

Solar cells are looped together in series of many strings of cells. The PV modules' cells are compressed between a weatherproof backing and a transparent cover.

The modules are formed by popping the cell material on a substrate of glass, stainless steel or polyamide, and the cells are interconnected to a module by laser.

Normally, crystalline silicon PV modules, especially mono-crystalline and poly-crystalline modules, are the most used of all types of modules as they have the highest efficiency, yet their high efficiency is often accompanied by high costs despite of the several strategies used by many countries in order to reduce the modules' costs. As for the other types of PV modules such as the amorphous silicon, even though they have a relatively low efficiency, they are flexible and have a noticeable aesthetical usage. Actually, despite of their high efficiency, mono-crystalline PV panels block the outside view of the buildings because of their opaqueness.



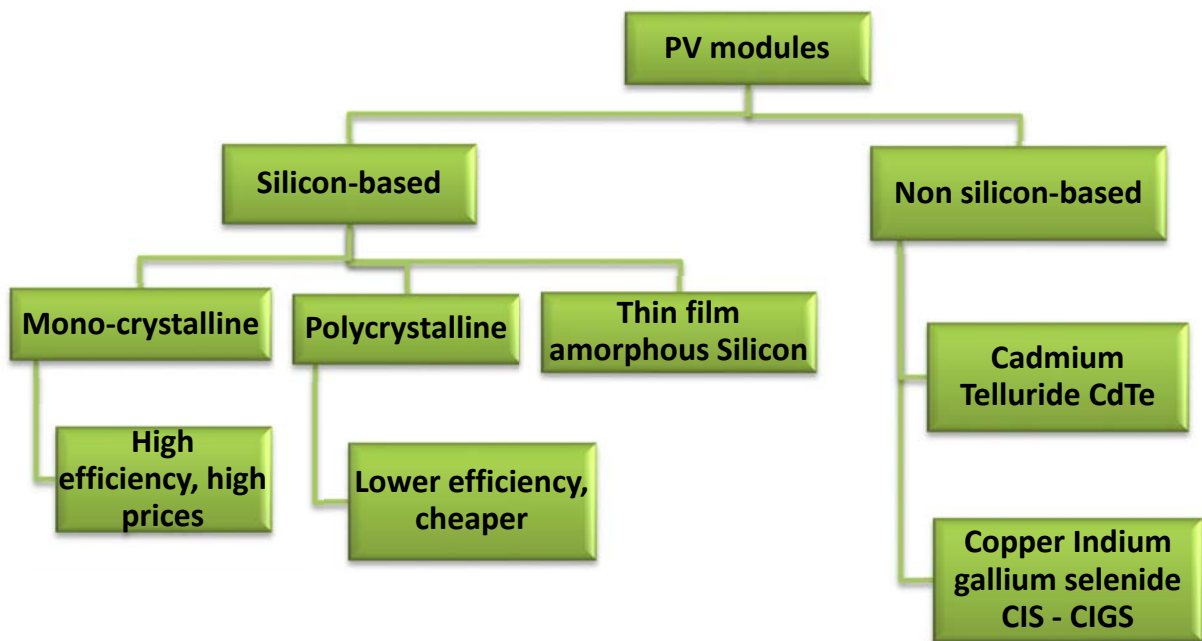


**Figure 1.8: Summary on the different types of PV modules**

The below table 1.5 shows the five most available types of PV modules in the market, with their efficiency [37], [38]:

**Table 1.5: PV modules efficiency**

<b>PV Module</b>	<b>Efficiency (%)</b>
<b>Single Crystalline Silicon m-Si</b>	18.5
<b>Poly-crystalline Silicon p-Si</b>	11.6
<b>Hydrogenated amorphous Silicon a-Si</b>	6.3
<b>Cadmium telluride CdTe</b>	6.9
<b>Copper indium gallium diselenide CIS</b>	8.2

Hence, based on the performed comparison, the mono-crystalline silicon PV modules with the highest efficiency will be adopted in this study.

Having assessed the energy systems' models and their components, it would be important to discuss the optimization of these systems that has become a vital feature for their adoption.

Indeed, choosing the most adequate solution for energy systems problems, especially those seeking several objectives at a time, is further discussed in section 1.5.

## **1.5 Multi-Objective Optimization**

In order to optimize energy systems involving several objectives simultaneously; many multi-objective methods can be adopted to acquire the most optimal solution. In fact, many optimization methods, particularly multi-objective ones have been discussed in details in the available literature [39], [40].

For instance, the charging process of electric vehicles is highlighted through the application of the genetic algorithm as a multi-objective optimization method [41].

In [32], an EV charging/discharging strategy is proposed for EVs located in a controlled environment such as a parking lot taking into consideration their mobility pattern and the market prices' variations. An efficient EV charging and discharging scheduling is investigated as a multi-objective optimization problematic with regards to the minimization of charging costs, maximization of aggregators' profits and maximization of the number of EVs with a target State-of-Charge (SoC) at the departure. For the EV model, the chosen pattern is that of a leisure parking lot located in Singapore, taking into consideration the uncertainty in parking durations [32].

A dynamic heuristic scheduling algorithm aiming to solve the scheduling problem is proposed [39], [42]. Extensive simulations are realized for 24 hours with intervals of 30 minutes each, for three aggregators of different sizes thus assessing the proposed technique's robustness and scalability [32].

Consequently, as compared with other algorithms [43], the proposed algorithm provides better results providing a trade-off between the different perspectives of EV and aggregator. In the stress test case study, with the proposed algorithm, 25 % more vehicles could depart with the target SoC at lower charging costs. In the realistic study, the results of the proposed approach were similar to the case study where the aggregator is small, and that proves the scalability of this approach. Furthermore, as the proposed approach provides sub-optimal results at a low computational time (less than 1 minute) it seems to perfectly fit the real world [32].

The table 1.6 summarizes the most used multi-objective optimization methods in [40], [41], [44], [45], [46], [47], [48], [49].

**Table 1.6: Multi-Objective optimization methods and procedures**

	<b>Classification</b>	<b>Idea</b>	<b>Advantages</b>	<b>Disadvantages</b>
<b>Global Criterion Method</b>	No preference method	Distance to the ideal objective vector is minimized.	- Simplicity - Effectiveness	- Definition of the desired goals - Non dominated solution only if the goals are chosen in the feasible domain (limited applicability)
<b>Weighted Sum method</b>	A priori method	Optimize a weighted sum of the objective functions, where the weights depend on the decision maker's preference.	- Positive weights' solution is Pareto-optimal - Easy to solve (only objective functions/no additional constraints)	- Can't find solutions for a concave shape of the Pareto-optimal set.
<b>Epsilon-constraint method</b>	A priori method	Optimize 1 objective function using the others as parametric constraints	- Easy implementation - All pareto-optimal solutions can be found (even for non-convex parts)	- Difficulty in the choice of upper bounds as they might not give feasible solutions - The choice of the objective to be optimized
<b>Genetic Algorithm</b>	Evolutionary Algorithm	Out of a number of solutions available, only the more fit solutions survive, while the less fit solutions are discarded.	- Pareto-optimal set can be accurately identified. - Easy manipulation and adaptability to different problems.	- Huge number of iterations - Long timing of computation
<b>Particle Swarm Optimization</b>	Evolutionary Algorithm	The population uses information gathered from each individual and the population as a whole to converge on the optimum.	- Pareto-optimal set can be accurately identified.	- Difficult constraint handling
Other evolutionary algorithms: evolutionary programming, genetic programming, differential evolution simulated annealing, tabu search, ant colony optimization, harmony search, etc.				

<b>Normal Boundary Intersection</b>	A posteriori method	- Find an equally spaced estimation of the solution	- Approximation of the Pareto front with equally spaced solutions.	- For concave problems, non Pareto-optimal solutions can be found.
<b>Simplex method</b>	Linear programming	Iterative optimization algorithm	Having adjusted the initial and slack variables correctly, the objective function will be optimized at the vertices of the feasible region.	- Difficult computation with thousands of constraints and decision variables. - Applicable only for linear constraints - Inaccuracy due to rounding errors
<b>Lexicographic ordering approach</b>	A priori method	- Classify the objective functions based on their importance	The priorities are not fixed, but they change throughout the search process	Practically, some Tolerance is used to get optimal values.
<b>Reference point method</b>	Interactive method	-The decision maker choses a reference point that is referred to in the scalarization of the problem.	- Multi-criterion decision making - Reliable solutions based on the decision maker's preferences	- Scalarized problem is not differentiable.
<b>Satisficing Trade-off method</b>	Interactive method	- Similar to reference point method, based on the classification of objectives (3 categories)	Easy implantation (decision makers only need to set the aspiration categories)	Limitation of available information
<b>NIMBUS method</b>	Interactive method	- Similar to reference point method, based on the classification of objectives (5 categories)	- Can solve non-convex and non-differentiable problems.	- Limited computer capacity. - Problematic software update and delivery.

Of all the investigated optimization methods, the evolutionary genetic algorithm stands out for its accurate identification of the Pareto-optimal solutions. This optimization method has an easy manipulation and adaptability to difficult problems where lies some ambiguity regarding the solution search space. In fact, it only allows the fittest solutions to survive and discards the least fit ones while minimizing the initial population until attaining the Pareto-front. Hence, our study focuses on the genetic algorithm as the multi-objective optimization approach to be adopted.

Further details concerning this heuristic method and its application within the context of this study are provided in chapters 3 and 4.

## **1.6 Energy management strategies**

The EV market is expanding and the number of the owned electric vehicles out of all the vehicles worldwide keeps getting bigger. Thus, EV batteries have the possibility to be potentially dispatched so they can be used by conventional organizations on a national level or in local micro-grids. Particularly, the charging/discharging schedule can be modified: charging would be enabled at times when pricing is low and discharging would be enabled at the high price period.

Consequently, with smart scheduling for the electric vehicles charging and discharging processes, the electricity prices fluctuation would be reduced and the demand curve flattened, in order to reach the battery's full potential aiming to stabilize the power grid. In fact, the decision regarding when to start charging or discharging the vehicles' battery is made either by utilities according to the curves of supply and demand, or by the consumers referring to the real-time and the sell-back market prices [9].

The combination of renewable energy production with the demand-side management has become a crucial trend for the energy storage and production systems where a balanced electricity demand and supply system is sought [50].

In [51], EVs have been integrated into the distribution grid through an EV infrastructure that involves multiple EVs operation which lessens the charging down-time. As the AC/DC buses power exchange was dealt with by a master control, the individual EVs control was decentralized, and G2V, V2G as well as the simultaneous G2V-V2G modes have been modeled using the Matlab/Simulink platform. It has been proved that the control of EV battery discharging (V2G) occurs in constant current strategy and EV battery charging (G2V) follows a constant voltage control strategy. As for the simultaneous G2V-V2G operation mode a balanced operation scheme enabling both the G2V and V2G modes at the same time has emerged. Consequently, the results which aim to a maximization of the AC power injection into the grid and a reduction in the load unbalance and the low order harmonic factor settle with the IEEE standards 1459-2010 [51].

The amount of energy that can be injected to the grid via V2G mechanism is investigated in [6]. In order to analyze the accurate transportation statistics while achieving the demand profile of EV and meet the daily driving needs, four kinds of EVs were taken into consideration in the study, representing large, midsize and small vehicles available in the market: BEV or Battery Electric Vehicles (the most dominating in the actual market, are comparable with the modern passenger cars and family cars), City-BEV (which seem to be similar to the civic transport subcompacts in terms of weight, size and energy consumption), PHEV 30 and 90 (which have an All Electric Range AER of 30 and 90 km where they have the possibility to be entirely driven in electrical mode without fuel oil) [5], [52].

The SoC of the battery is assessed for various mileages taking into consideration the energy consumption depending on the driving speed, period and cycles (whether on highway, road, urban or in traffic jam). The schedules for EV charging and discharging are identified according to the parking durations, arrival and travel time for power levels provided by the EPRI (Electric Power Research Institute) and the SAE (Society of Automotive Engineers) [5], [53], [54].

The results of the study have shown that as the charging power gets lower, the peak G2V load gets smaller and shifts to later hours at night, offering a tendency to fill the valley night time. Besides, after getting back from their last trip, the customers with a high left over state of charge have the possibility to postpone the charging to later hours and/or use a low charging power approach to avoid charging at peak time [5]. Eventually, the constant time approach beside the low charging power seems to be a smart strategy for EV charging [5]. Obviously, the charging peak load overlaps with the vehicles' arrival period and intensifies in the evening to surpass the conventional peak while the system's hourly demand is reduced in the morning period due to the V2G mechanism [5], [55].

In [11], the study involves the benefits of integrating EVs into the smart grid as distributed energy storage serving either as an aggregated generator or a controllable load depending on the grid's demand through the DSM program (Demand Side Management).

The distributed energy storage of using EVs batteries allows the control flexibility in smart distribution systems reducing the purchase costs of electricity for the vehicles' owners and customers [56], [57].

A smart system including RES (Renewable Energy Sources) in addition to the main electric grid and using hybrid vehicles PHEV as energy storage has been studied in [58]. Accordingly, the EV owners would be discharging the excessive energy of their vehicles' batteries in the grid at the hours of peak demand, and charging then within the off-peak hours. An energy management model has been created using HOMER Legacy software as well as a Graphical User Interface (GUI) specifying the exact charging and discharging time and the energy costs via smart metering [58], [59], [60].

In [16], an experimental vehicle to grid (V2G) platform has been developed in order to study the interactions that occur between the electric grid and the electric vehicle's load. The results of the experiments have been proved to comply with the national standards.

Moreover, it has been demonstrated that, the current harmonic distortion rate is affected (inversely proportional) by the charge and discharge power while the voltage harmonic distortion rate is not [61].

In [17], a micro-market for selling and purchasing energy has been introduced in the context of an electric vehicles parking facility in order to assess the minimization of electric energy costs, and increase the profits of the Parking Facility Operator PFO. In addition, the operator would introduce the electric vehicles into markets where electric energy is more expensive allowing them to sell the energy thus making benefits out of the energy transactions [3], [62].

A controlled G2V charging strategy has been investigated through the business models for EV integration in Austria and their economic analysis within the year 2020 and beyond. Studies have shown that the economic potential of the operation is better than that of V2G operation due to the several control energy calls and the absence of costs related battery degradation [17], [63].

A networking model has been designed for the assessment of the electric vehicles' mobility in V2G systems. It has been concluded that the demand response can be balanced in mobile energy networks through the transport of energy operated by the EV fleets achieving a synchronous stability in the demand level of the diverse network districts [19], [64], [65], [66].

In [67], the study involves two smart strategies of vehicles' charging through a V2G and G2V framework in order to integrate EVs into the existing infrastructure of a workplace car parks with the lowest PAR (Peak-to-Average Ratio) and daily costs possible. It has been shown that the strategy aiming the minimization of PAR is recommended whenever plug-in electric vehicles are needed to accommodate with longer delay in the upgrade of distribution infrastructure. Besides, it has been proven that the slow charging of plug-in electric vehicles is recommended for optimal economic and technical benefits for both strategies while fast charging would deteriorate both strategies' performances.

In [68], the EVs' optimal assignment to charging stations (taking into consideration both assignments under disturbed conditions such as traffic jam and slopes on roads and assignments under normal conditions) is proven to occur at the highest level of the EV battery's State of Charge (SoC) whenever it is possible. This decreases the EV's charging time and energy consumption.

In [69], in order to improve the fuel consumption of hybrid electric vehicles, an Energy Management System (EMS) has been built and computed using a Sequential Approximate Optimization (SAO) and a Radial Basis Function network (RBF). It has been shown that this EMS algorithm allows a significant reduction of fuel consumption.

In [70], the SPSA method (Simultaneous Perturbation Stochastic Approximation) is used for a model free tuning of hybrid electric vehicle's state of charge. This method is based on the optimization of a linear equation between the actual speed of the vehicle and a SoC target. The study has shown an improvement of 28 % in the efficiency of fuel consumption and 100 % in drivers' satisfaction.

The energy management system of the power unit of a Formula 1 racecar has been optimized in [71]. Therefore, a nonlinear program has been conceived in order to optimize the tuning and implementation of a control policy matching the system's limitations with regards to battery usage and fuel consumption. The resulting controls are tested using a forward simulator. These controls seem to be compatible with the optimal trajectories thus validating the proposed supervisory algorithm. PHEVs do benefit from the fuel-switching feature converting some of the vehicles' energy into electricity thus reducing its fuel consumption. Eventually, they



have the possibility to operate in charge-depleting mode (CD mode) where the electrical energy is consumed until a minimum predetermined level of the SoC is reached, and then switch to the charge-sustaining mode (CS mode) [72].

Several energy management approaches and controlled scheduling strategies have been proposed in the literature [73], [74], [75], [76], [77] and [78]. It is because of the successful energy management systems that a big number of electric vehicles can be handled by the distribution networks. In fact, as a large number of vehicles have the possibility to affect the electricity demands of the networks on the country scale, the whole sector of electric transportation might get affected as well [3]. The charging needs of vehicles have been investigated through the implementation of a predictive model that foresees the time for multiple requests of charging and the changing rate [79].

The bi-directional exchange created between electric vehicles and the grid would allow the charging of their batteries as well as the power injection back to the grid. Then, the power grid gets stabilized in terms of frequency and voltage regulation and power demands would be fulfilled particularly during peak hours [2].

In order to supervise a household's energy consumption closely and trigger new energy saving incentives, the household's aggregate consumption has been decomposed into the individual consumption of each home appliance aside through a splitting approach of the convenient clusters [80], [81].

Moreover, the charging profiles and daily trips scheduling of an electric vehicles population has been generated using real-time vehicles' charging data through a stochastic simulation procedure [82]. Besides, the charging process related to hybrid-electric vehicles based on electricity supply and demand has also been assessed using imperialist competitive algorithm, particle swarm optimization and teaching-learning algorithm. The comparison between all three methodologies showed that training-learning algorithm widely outperforms the other methods in terms of load peak prevention, yet, the imperialist competitive algorithm could considerably outshine with regards to performance costs reduction [83], [84].

The energy flows from/to the electric vehicles might contribute to better efficiency, stability and reliability with regards to the grid's performance. Yet, without setting a rational scheduling, serious problems might occur due to deregulated charging or discharging, especially for a fleet of electric vehicles. Nevertheless, the power transmission over a long distance and the market price fluctuation might cause a huge energy waste referred to as battery operation convergence. Thus, it is recommended to plan a hierarchy between the EV owners and the grid. It is to be noted that, if all EV owners start using the same real-time price and sell back market price, the resulting synchronous activity would create new demand peaks and different price curves. The big number of electric vehicles getting integrated to the market might bring unstable factors to the grid. Thus, in order to treat the excessive vehicles' energy properly, the price trend and future electricity consumption would be predicted by the central grid. The decision concerning the amount of energy needed and when to charge is then made by the central grid, and the discharge process would occur only when needed [9].

As electric vehicles can supply energy storage to the power grid, their opportunities for services related to grid balancing and storage are increasing. This allows EV owners to make revenues; therefore compensating a part of the electric vehicles high costs that stop some of the consumers from adopting EV [6].

Three potential energy management strategies are stated and compared as mentioned in table 1.7:

**Table 1.7: Types of Energy Management Strategies**

<b>Energy Management Strategy</b>	<b>Description</b>
All-Electric Range AER- focused strategy	PHEV is purely electric driven.
Engine-dominant blended strategy	Stored electric energy is used to support engine operation and optimize the system efficiency dominated by the engine.
Electric-dominant blended strategy	A strategy that is similar to the purely electric driven strategy without prioritizing a significant all-electric driven distance within CD operating mode.

The above-mentioned strategies could be used separately or mixed depending on the decision of the controller based on the duty cycle's distance and the aggressiveness context seeking lower fuel consumption. For instance:

- for a long distance trip, the engine-dominant blended strategy would be recommended.
- for trips where the vehicle would travel a short distance before its next recharging cycle, the electric-dominant blended strategy would be recommended.
- for trips where the upcoming cycle is predefined, an alternative mix between the engine-dominant and electric-dominant blended strategies would be recommended.

## **1.7 Conclusion**

Electric vehicles seem to be of a huge interest nowadays for their huge share in the pollution reduction resulting from the transportation sector. Consequently, in this chapter, electric vehicles, as well as energy systems and their components have been investigated based on the available literature. Besides, multi-objective optimization and its numerous approaches have been discussed. Some of the literature's energy management strategies related to electric vehicles' charging and discharging scheduling have also been reviewed.

The following chapter will then describe a specific energy system conceived in this study and will present its detailed configuration and modeling as well as the sizing of its components. The complete study focuses on the electric energy flowing into and out of electric vehicles and the control and regulation of this energy based on the electricity supply and demand.

## **Chapter 2 - Energy System's modeling and sizing**

2.1	Introduction.....	61
2.2	Energy System's definition.....	61
2.2.1	Energy System's global architecture.....	61
2.2.2.	Energy System's topology .....	64
2.3	Modeling and sizing of the system's components .....	65
2.3.1	Energetic model of EV's propulsion.....	66
2.3.2	Sizing of the vehicle's batteries .....	69
2.3.2.1	Sizing of the Ni/MH on-board batteries.....	70
2.3.2.2	Sizing of the stationary lead-acid batteries.....	71
2.3.3	Sizing of the photovoltaic panels .....	72
2.3.4	Sizing of the wind turbine.....	75
2.3.5	Sizing of power converters .....	77
2.3.5.1	DC/DC converter – boost chopper (wiring diagram presented in Fig. 1.2).....	77
2.3.5.2	Bidirectional DC/DC converter (wiring diagram presented in Fig. 1.5).....	78
2.3.5.3	AC/DC inverter .....	78
2.4	System's energetic modeling .....	79
2.5	Conclusion .....	83

## **2.1 Introduction**

The avoidance of greenhouse gases emissions and reduction of pollution related to the transportation sector involve the adoption of vehicular electrification. This study mostly aims to control the energy flows between the electric vehicle, the electric grid and homes in a way to reduce the habitats' dependency on the electric grid hence to minimize the flows from the grid into homes, in order to reduce the greenhouse gases emissions. So the house needs would be directly produced from renewable energy sources (photovoltaic panels and wind turbine), and the vehicle's excess of energy would be implemented into the house or the grid when needed, depending on the supply and demand of electricity.

Particularly, the system's composition and the sizing of each of its components are further studied in details in this chapter, as well as the energetic modeling of the whole system with regards to the production and consumption variations. Mainly, this chapter includes the definition of the study's energy system and its global architecture and topology. It also exhibits the energetic global model of the system, and the mathematical modeling and sizing of the vehicle's batteries, the stationary batteries, and power converters. The sizing of renewable sources is also studied, and the calculations related to the photovoltaic panels and wind turbine are exposed.

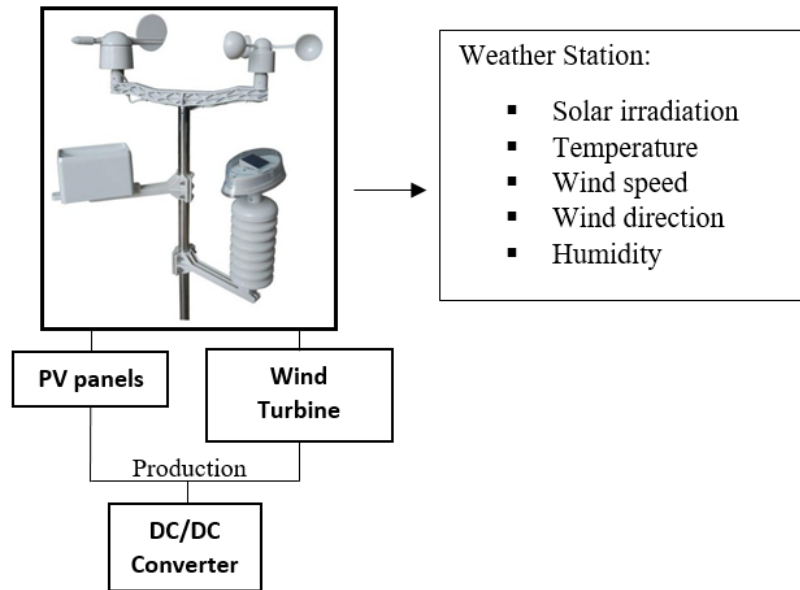
## **2.2 Energy System's definition**

In order to control the energy flows between electric vehicles, the grid and houses; and to adapt the vehicles' charging and discharging features based on the electricity supply and demand, the energy system investigated in this study is first defined. It includes a domestic household supplied by renewable energy sources (particularly photovoltaic panels and a wind turbine), as well as a fleet of electric vehicles used not only for personal travel needs but also for energy storage and retrieval.

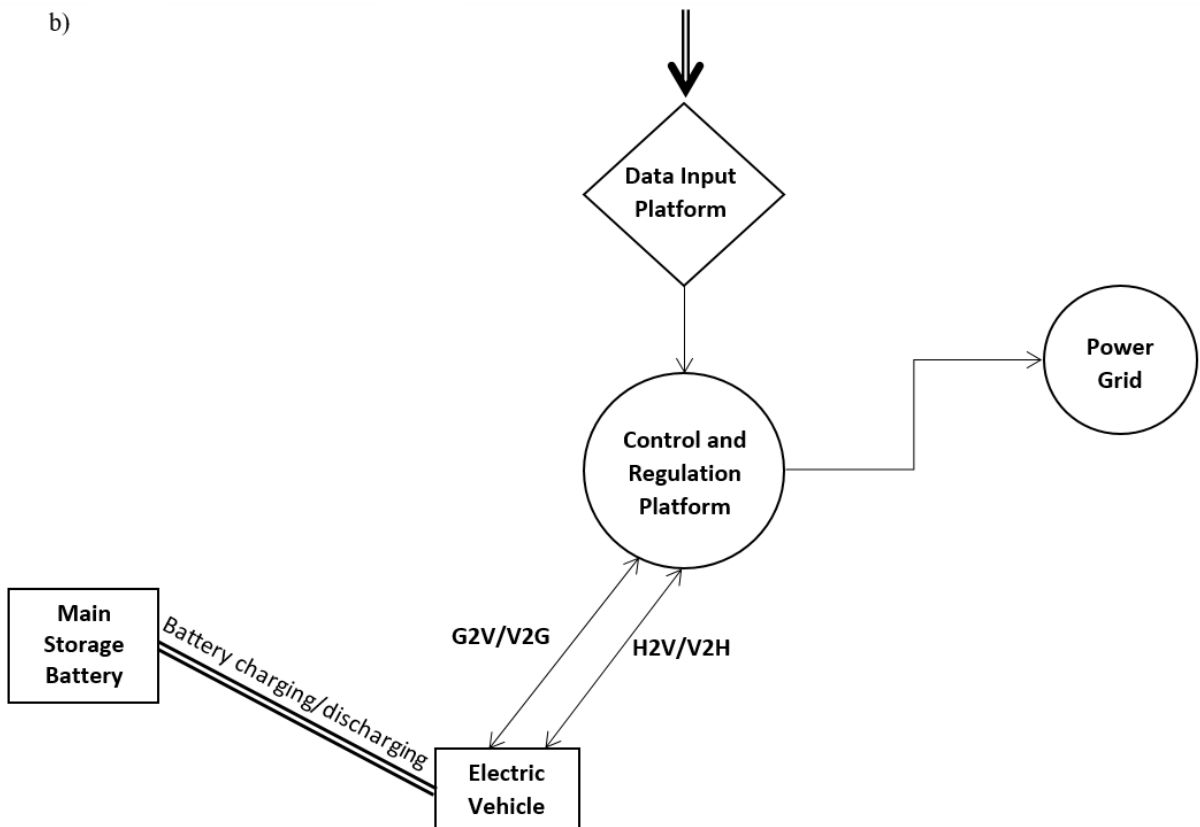
### ***2.2.1 Energy System's global architecture***

The global architecture related to the energy system defined in this study is illustrated in Fig. 2.1 – a), b) and c).

a)



b)



c)

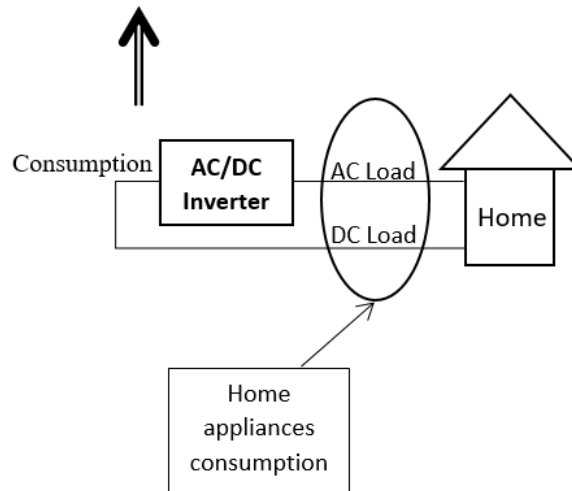


**Figure 2.1: Energy System's global architecture**

Based on the energy system's global model, the electricity production and consumption are first gathered before being implemented into a control and regulation platform. The electricity production, represented in section a) of Fig. 2.1, is collected through the solar energy and wind power resulting from the weather station data input. The energy consumption, represented in Fig. 2.1, section c), is defined by the functional household appliances. As illustrated in the Fig 2.1, section b), the control and regulation platform takes in charge the charging and discharging of the available electric vehicles according to the margin of difference between the energy produced or consumed, and the lack or excess of energetic needs.

The aim of the study is to suppress, as much as possible, the grid supply to the houses for economic and environmental purposes. Thus, the energy flows between the vehicles, houses, renewable sources and the grid are presented in Fig 2.2.

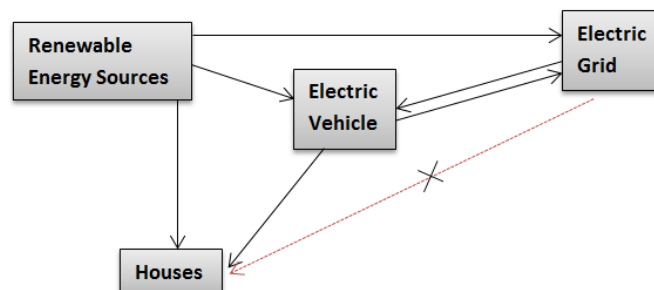


**Figure 2.2: Energy flow block diagram**



### 2.2.2. Energy System's topology

The detailed system's topology is presented in the following Fig 2.3.

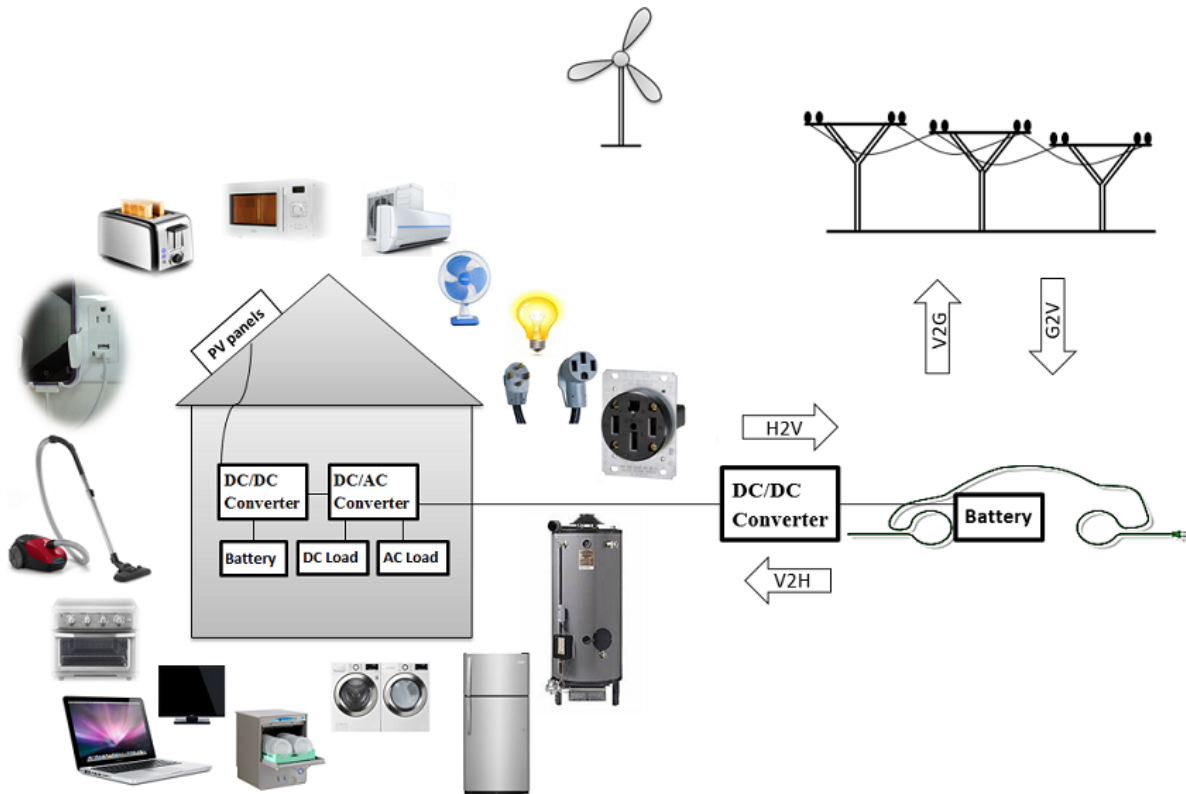


Figure 2.3: The studied energy system's topology

The system includes two DC/DC converters and a DC/AC inverter in addition to the electrical equipment and the home appliances and loads.

Electrically speaking, the electric vehicle's configuration is presented in the following Fig. 2.4.

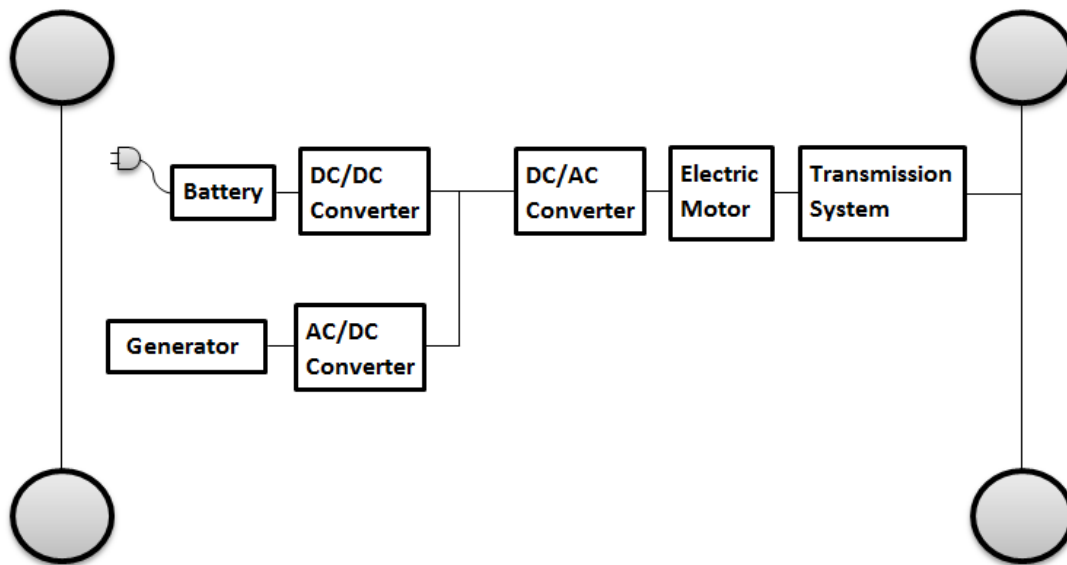


Figure 2.4: Electric vehicle's configuration

### 2.3 Modeling and sizing of the system's components

First, in order to investigate a realistic prototype, the study has been made based on a real existing electric vehicle; the technical specifications of which are listed below:

#### Vehicle's specifications:

- Vehicle's mass = 1468 kg
- Maximum speed = 135 km/h
- Motor type: synchronous wound rotor motor
- Average speed = 50 km/h
- Acceleration = 0 to 100 km/h in 13.5 seconds
- Maximum power = 65 kW
- Maximum torque = 220 N.m
- Front surface = 2.07 m<sup>2</sup>
- Autonomy = 100 km.
- Coefficient of air penetration:  $C_x = 0.28$
- Density of air:  $\rho = 1.225 \text{ kg/m}^3$
- Acceleration of gravity:  $g = 9.81 \text{ N / kg}$

- Rolling resistance coefficient:  $C_r = 0.01$  for an inflation pressure ranging between 1.2 N/cm<sup>2</sup> and 2.2 N/cm<sup>2</sup>.

Thus, these technical specifications are adopted in the rest of this study for all the calculations where electric vehicles technical data are needed.

### 2.3.1 Energetic model of EV's propulsion

The calculation of the energy and power required for the vehicle's propulsion is performed through the definition of the energetic model of the EV.

Referring to the Newton's second law of motion, the sum of the forces applied on the EV is described by the following equation:

$$\sum \vec{F} = m \times \vec{a} = \vec{F}_p + \vec{F}_f + \vec{F}_a + \vec{F}_g \quad (2.1)$$

$$\text{with: } \begin{cases} m = \text{mass of the vehicle} \\ \vec{a} = \text{acceleration of the vehicle} \\ \vec{F}_p = \text{Propulsive force of the vehicle} \\ \vec{F}_f = \text{Friction force of the wheels} \\ \vec{F}_a = \text{Aerodynamic force} \\ \vec{F}_g = \text{Force of gravity} \end{cases}$$

Noting that the direction of the friction force of the wheels, the aerodynamic force and the force of gravity are opposite to that of the propulsive force:

$$\vec{F}_p = ma + \vec{F}_f + \vec{F}_a + \vec{F}_g \quad (2.2)$$

The friction force of the wheels  $F_f$  can be calculated as follows:

$$F_f = C_r \times m \times g \times \cos \alpha \quad (2.3)$$

$$\text{whereas: } \begin{cases} C_r = \text{coefficient of rolling resistance} \\ g = \text{gravity acceleration} \\ \alpha = \text{angle of inclination of the vehicle with respect to the horizontal} \end{cases}$$

The rolling resistance coefficient  $C_r$  is estimated to be 0.01 at an inflation pressure ranging between 1.2 N/cm<sup>2</sup> and 2.2 N/cm<sup>2</sup>

The aerodynamic force  $F_a$  can be presented by the equation:

$$F_a = \frac{1}{2} \rho S C_x V^2 \quad (2.4)$$

whereas:  $\begin{cases} \rho = \text{Air density} = 1.225 \text{ Kg/cm}^3 \\ S = \text{Frontal section} \\ C_x = \text{coefficient of air penetration} \\ V = \text{Relative speed of the vehicle} \end{cases}$

As for the force of gravity  $F_g$ , it can be estimated as per the equation:

$$F_g = m g \sin \alpha \quad (2.5)$$

Therefore, the equation (2.2) of the vehicle's propulsive force is detailed in the following model:

$$\rightarrow F_p = ma + C_r \times m \times g \times \cos \alpha + \frac{1}{2} \rho S C_x V^2 + m g \sin \alpha \quad (2.6)$$

Furthermore, the power required to propel the vehicle (in Watts) is given by the equation:

$$P_p = F_p \times V \quad (2.7)$$

The energy required to propel the vehicle (in Wh) is given by:

$$E_p = \frac{A}{V} \times P \quad (2.8)$$

Where A represents the autonomy of the vehicle in km, and P is the total power absorbed by the vehicle.

$$\text{However: } P = P_p + P_{\text{aux}} = F_p \times V + P_{\text{aux}} \quad (2.9)$$

whereas  $P_{\text{aux}}$  represents the auxiliary power related to the on-board electric accessories.

Thus, referring to equations (2.8) and (2.9), the energy required to propel the vehicle can be expressed as follows:

$$E_p = \frac{A}{V} \times (F_p \times V + P_{\text{aux}}) \quad (2.10)$$

Besides, the amount of energy that should be put into the vehicle's battery when charging is expressed by:  $P_{\text{batterie}}(t) = \frac{P(t)}{\rho_p}$ ; where  $\rho_p$  represents the efficiency of the chain of electric

traction of the vehicle's battery (which depends on the temperature, the state of charge and the discharge power).

On the other hand, the electrochemical energy that would be contained in the battery during a trip of duration T seconds:  $E_{battery} = \int P_{battery}(t)dt$

The amount of energy supplied to recharge the battery after a trip of duration T seconds is also expressed by:  $E_{charge} = \frac{E_{battery}}{\rho_c}$ ; where  $\rho_c$  represents the charge efficiency that helps evaluate the losses during discharge.

Also, since the amount of energy to be recharged and the charging power are known, the charging time can be deduced according to the equation:  $E_{ch} = P_{ch} \times T_{ch}$

Therefore, referring to the vehicle's specifications, some numerical examples of energy calculations are presented as follows:

1. For  $\alpha = 0$  (straight road),  $a = 0$ , and  $V =$  average speed = 50 km/h = 13.8 m/s; and assuming that  $P_{aux} = 5kW$ :

$$F_f = C_r \times m \times g \times \cos \alpha = 0.01 \times 1468 \times 9.81 \times \cos 0^\circ = 144 \text{ N}$$

$$F_a = \frac{1}{2} \rho S C_x V^2 = \frac{1}{2} \times 1.225 \times 2.07 \times 0.28 \times 13.8^2 = 67.6 \text{ N}$$

$$F_g = m g \sin \alpha = 1468 \times 9.81 \times \sin 0^\circ = 0$$

$$\rightarrow F_p = ma + F_f + F_a + F_g = 0 + 144 + 67.6 + 0 = 211.6 \text{ N}$$

$$\rightarrow P = F_p \times V + P_{aux} = 211.6 \times 13.8 + 5 = 2.92 \text{ kW}$$

$$\rightarrow E_p = \frac{A}{V} \times P = \frac{100}{50} \times 2.92 = 5.84 \text{ kWh}$$

2. For  $\alpha = 30^\circ$  (inclined road), and  $V =$  average speed = 50 km/h = 13.8 m/s:

$$F_f = C_r \times m \times g \times \cos \alpha = 0.01 \times 1468 \times 9.81 \times \cos 30^\circ = 124.7 \text{ N}$$

$$F_a = \frac{1}{2} \rho S C_x V^2 = \frac{1}{2} \times 1.225 \times 2.07 \times 0.28 \times 13.8^2 = 67.6 \text{ N}$$

$$F_g = m g \sin \alpha = 1468 \times 9.81 \times \sin 30^\circ = 7200.54 \text{ N}$$

$$\rightarrow F_p = ma + F_f + F_a + F_g = 0 + 124.7 + 67.6 + 7200.54 = 7392.84 \text{ N}$$

$$\rightarrow P = F_p \times V + P_{\text{aux}} = 7392.84 \times 13.8 + 5 = 107 \text{ kW}$$

$$\rightarrow E_p = \frac{A}{v} \times P = \frac{100}{50} \times 107 = 214 \text{ kWh}$$

As noticed in the numerical applications of the energy calculation in examples 1) and 2), the higher the inclination angle of the road contributes to excessive propulsion of the vehicle.

### 2.3.2 *Sizing of the vehicle's batteries*

As the objective of the study is to be able to use the EV's battery for the energy storage and restitution, the choice of the battery technology is directly linked to its capacity of storage. Thus, the battery with the highest depth of discharge and lowest reachable state of charge should be adopted.

Based on the comparison between the different battery technologies and their depth of discharge and performance (table 1.3), the Lithium-ion batteries, that are nowadays the most used in electric vehicles technologies, beat the other types of batteries in terms of performance. The Nickel Metal Hydride batteries also seem to have a good performance. Indeed, even though the Li-ion batteries do have higher energy density and specific energy than the rest of battery types, the Ni/MH batteries are still adopted by some car manufacturers. For instance, the electric vehicles Prius Lexus of Toyota, Civic insight of Honda, Altima of Nissan and Escape Fusion MKZ HEV of Ford all include Ni/MH batteries. And the vehicles Leaf EV of Nissan, Mini E of BMW, Escape PHEV of Ford and Chrysler 200C EV do include Li-ion batteries. However, even though the Li-ion batteries seem to have the best performance, the Ni/MH would guarantee the best use as their depth of discharge surpasses the other types. And noting that, in this study, the vehicles' on-board batteries are used for storage, the depth of discharge would be an important factor for the maximum possible restitution of energy into the electric grid. Therefore, the Ni/MH technology will be adopted for the vehicles' on-board batteries of this study. As for the system's stationary batteries, the lead-acid technology will be adopted as this type of batteries remains the most economical, and their weight is not an important factor in this application [85], [86].

### 2.3.2.1 Sizing of the Ni/MH on-board batteries

The capacity of the pack of batteries is defined as per the equation: Capacity (pack) =  $\frac{P}{U_{pack}}$  whereas  $U_{pack}$  is the voltage of the battery pack set to 250 V.

For  $\alpha = 0$  (straight road),  $a = 0$  and  $V = \text{maximum speed} = 135 \text{ km/h} = 37.5 \text{ m/s}$ , and assuming that  $P_{aux} = 2 \text{ kW}$ , the equations (2.3) through (2.9) can be interpreted as follows:

$$F_f = C_r \times m \times g \times \cos \alpha = 0.01 \times 1468 \times 9.81 \times \cos 0^\circ = 144 \text{ N}$$

$$F_a = \frac{1}{2} \rho S C_x V^2 = \frac{1}{2} \times 1.225 \times 2.07 \times 0.28 \times 37.5^2 = 499.2 \text{ N}$$

$$F_g = m g \sin \alpha = 1468 \times 9.81 \times \sin 0^\circ = 0$$

$$F_p = ma + F_f + F_a + F_g = 0 + 144 + 499.2 + 0 = 643.2 \text{ N}$$

$$P = F_p \times V + P_{aux} = 643.2 \times 37.5 + 2000 = 26.1 \text{ kW}$$

$$E_p = \frac{A}{V} \times P = \frac{100}{135} \times 26.1 = 19.3 \text{ kWh}$$

Consequently, the capacity of the needed pack of batteries would be:

$$\text{Capacity} = \frac{P}{U_{pack}} = \frac{26100}{250} = 77 \text{ Ah}$$

Having chosen the Ni/MH battery of the Fig 2.5, Panasonic BK1100FHU 1.2 V – 11 Ah of 0.3 kg (the technical specification of which is given in Appendix A.1):

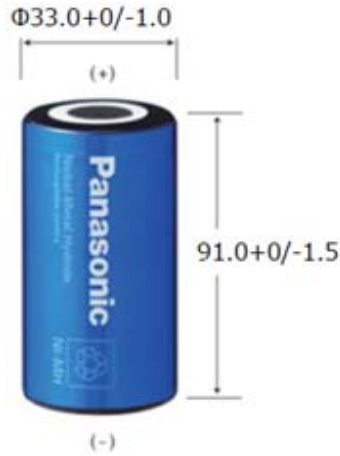


Figure 2.5: Ni/MH Battery Panasonic BK1100FHU [87]

The pack of batteries would be defined as follows:

- Number of modules in series:  $N_s = \frac{U_{pack}}{U_{element}} = \frac{250}{1.2} = 208.3 \rightarrow 209 \text{ modules}$
- Number of modules in parallel:  $N_p = \frac{C_{pack}}{C_{element}} = \frac{77}{11} = 7 \rightarrow 7 \text{ modules}$

The nominal/usable capacity of the on-board battery is assumed to be 75Ah for the rest of the study.

### 2.3.2.2 Sizing of the stationary lead-acid batteries

In order to choose the most convenient stationary lead-acid batteries, their capacity is first specified in the following equation:

$$\text{Capacity (lead – acid batteries)} = \frac{E_c \times N}{L \times U} \quad (2.11)$$

whereas  $\left\{ \begin{array}{l} E_c = \text{Daily consumption of energy} = 31.1 \text{ kWh/day} \\ N = \text{number of days of battery life estimated at 3 days without charging} \\ U = \text{Battery pack voltage} \\ L = \text{maximum discharge of the battery estimated at 65 \%} \end{array} \right.$

Concerning the voltage of the battery pack U, the storage voltage recommended by the suppliers for a rated power of PV exceeding 1600 Wp is 48 V, this value of the voltage is therefore adopted in this study (Wp is the unit of measure of the peak power).



It should be mentioned that overcharging or over-discharging of the battery will damage it and decrease its life.

Consequently, the lead-acid batteries capacity is calculated as per equation (2.11) as follows:

$$\text{Capacity (lead - acid batteries)} = \frac{E_c \times N}{L \times U} = \frac{31.1 \times 3}{0.65 \times 48} = 2990 \text{ Ah}$$

→ Adopted Lead-Acid Battery: Motoma power 48 V 3000 Ah (technical specifications is given in Appendix A.2), and maximum load current = 20% x rated capacity = 3000/5 = 600 A (Fig. 2.6).



Figure 2.6: Lead-acid batteries Motoma MS48V3000 [88]

### 2.3.3 Sizing of the photovoltaic panels

The next component of the study's energy system to be sized is the photovoltaic panels. The size of the most convenient PV panels to adopt is defined based on the following equation:

$$E_c = N_H \times P_o \quad (2.12)$$

$$\text{whereas: } \begin{cases} E_c = \text{Daily energy consumption} \\ N_H = \text{Number of hours of use per day} \\ P_o = \text{Operating power} \end{cases}$$

#### Daily consumption of energy in the home:

Table 2.1: Daily home appliances energy consumption

Heating/Ventilation	Air conditioner	3 hours/day	3.5 kWh	4.75 kWh
---------------------	-----------------	-------------	---------	----------

	<b>Fan</b>	<b>5 hours/day</b>	<b>250W*5 = 1.25 Kwh</b>	
<b>Water heating</b>		<b>20 minutes/day</b>		<b>1.75 kWh</b>
<b>Lighting</b>	<b>4 Light bulbs</b>	<b>9 hours/day</b>	<b>4*80W*9= 2.88 kWh</b>	<b>2.88 kWh</b>
<b>Audiovisual Appliances</b>	<b>200W TV</b>	<b>6 hours/day</b>		<b>1.2 kWh</b>
<b>Cooking</b>	<b>Oven</b>		<b>2 kWh</b>	<b>3.5 kWh</b>
	<b>Microwave</b>	<b>15 minutes/day</b>	<b>0.36 kWh</b>	
	<b>Grill + electric kettle + toaster</b>	<b>Non-recurrent use on a daily basis.</b>	<b>Estimated daily average: 1.14 kWh</b>	
<b>Washing/drying</b>	<b>Dish washer + dryer + washing machine</b>	<b>Non-recurrent use on a daily basis.</b>		<b>Estimated daily average: 2 kWh</b>
<b>Electronics use</b>	<b>Laptop + vacuum cleaner + phone charger</b>	<b>Non-recurrent use on a daily basis.</b>		<b>Estimated daily average: 0.7 kWh</b>
<b>Refrigerator</b>	<b>180 W</b>	<b>24 hours</b>		<b>4.32 kWh</b>
<b>Electric outlet for the vehicle</b>		<b>100km/day</b>		<b>10 kWh/100 km</b>

Based on the above listed energy consumption of the household appliances, the daily consumption of energy in the home would be of approximately 31.1 kWh. It is to be noted that the energy consumption considered for the electric vehicle's in-home outlet is a lump sum corresponding to 100km/day; yet, it does not take into consideration the EV owners' individual travel needs.

Thus, the energy production related to the PV panels would be calculated as follows:

$$E_p = E_c \times k \quad (2.13)$$

$$\text{whereas } \begin{cases} E_p = \text{Energy production} \\ E_c = \text{Daily energy consumption} \\ k = \text{correction coefficient} = 1.3 \end{cases}$$

$$E_p = E_c \times k = 31.1 \times 1.3 = 40.43 \text{ kWh/day}$$

As mentioned in chapter 1 section 1.4.3, the mono-crystalline silicon PV modules with the highest efficiency are adopted in this study.

Calculation of the peak power of the PV panels that should be installed:

Noting that the South East orientation is proven to ensure the highest solar radiation [89], the photovoltaic panels are assumed to be oriented in the South-East direction with an inclination angle of 30° under standard conditions where solar radiation is estimated at 1000 W/m<sup>2</sup> with an ambient temperature of 25°C.

The peak power of the PV modules is calculated as per the equation:

$$Peak\ power = \frac{E_p}{N} \quad (2.14)$$

whereas N represents the number of hours of sun exposure per day, estimated to 4.5 hours/day in this study, particularly in Quebec, Canada. In fact, the choice of the city was made based on varied meteorological conditions where the climate is characterized by wide ranges between maximal and minimal solar and wind data.

In Quebec, the climate can be very sunny and windy at times, and can alternate between either sunny or windy at others, and this meteorological variety projects diverse maximal and minimal renewable energy productions.

$$\text{Therefore: } Peak\ power = \frac{E_p}{N} = \frac{40.43}{4.5} = 8.98\ kW_p$$

Consequently, 33 monocrystalline PV modules with rated power 280Wp, Fig. 2.7, under standard conditions STC are to be installed; thus the installation of 54.79 m<sup>2</sup> of DualSun panels 990 mm x1677 mm, thickness = 45 mm. The voltage of the modules at rated power is of 31.95 V; its intensity at rated power is of 8.77 A.



**Figure 2.7: Monocrystalline PV module DualSun 280 Wp [90]**

(More details about technical data sheet of PV panels are given in appendix A.3).

#### **2.3.4 Sizing of the wind turbine**

As already stated in chapter 1 section 1.4.2., a Horizontal Axis Wind Turbine is adopted in this study.

As the in-home daily consumption has been estimated to:  $E_C = 31.1$  kWh/day, the yearly consumption would be :  $E_C = 31.1 \times 365 = 11351.5$  kWh/yr.

In order to indicate the technical specifications of the wind turbine, the system is assumed to be located in Quebec, where the average wind speed is of 9.8 miles per hour, thus of 4.38 m/s.

The power output of the wind turbine is provided by the following equation:

$$P = \frac{1}{2} \times k \times \rho \times C_p \times A \times V^3 \quad (2.15)$$

whereas:  $\left\{ \begin{array}{l} P = \text{output power (kW)} \\ k = \text{constant to yield power (kW)} = 0.000133 \\ \rho = \text{Air density (lb/ft}^3\text{)} \\ C_p = \text{maximum power coefficient, theoretically estimated as 0.59} \\ A = \text{Rotor swept area (ft}^2\text{)} = \frac{\pi D^2}{4}, D \text{ is expressed in ft} \\ V = \text{wind velocity (mph)} \end{array} \right.$

The Annual Energy Output AEO (expressed in kWh/year) is provided by the following equation:

$$AEO = 0.01328 \times D^2 \times V^3 \quad (2.16)$$

whereas:  $\begin{cases} D = \text{Rotor Diameter (ft)} \\ V = \text{Annual average wind velocity (mph)} \end{cases}$

$$\text{Thus, } D = \sqrt{\frac{AEO}{0.01328 \times V^3}} = \sqrt{\frac{11351.5}{0.01328 \times 9.8^3}} = 30.14 \text{ ft}$$

Consequently, the equation (2.15) results in the following calculations:

$$P = \frac{1}{2} \times 0.000133 \times .077 \times 0.59 \times 713.47 \times 9.8^3 = 2.03 \text{ kW} \quad (2.17)$$

$$\text{with } \begin{cases} k = 0.000133 \\ \rho = 1.23 \text{ Kg/m}^3 \text{ at sea level} = 0.077 \text{ lb/ft}^3 \\ C_p = 0.59 \\ A = \frac{\pi D^2}{4} = \frac{\pi \times 30.14^2}{4} = 713.47 \text{ ft}^2 \\ V = 9.8 \text{ mph} \end{cases}$$

Consequently, the horizontal axis wind turbine ETNEO AN3000 (technical specifications of which are given in appendix A.4) with 2.8 kW of power is adopted in this study (Fig. 2.8).

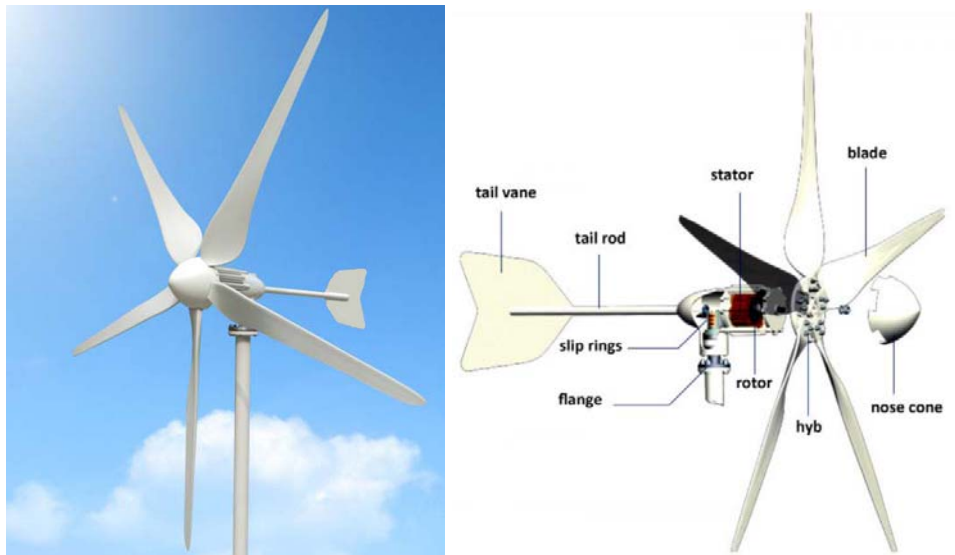


Figure 2.8: ETNEO AN3000 wind turbine [91]

### 2.3.5 Sizing of power converters

Referring to the converters' modeling operated in chapter 1, their parameters' identification is calculated in the following sub-section.

#### 2.3.5.1 DC/DC converter – boost chopper (wiring diagram presented in Fig. 1.2)

The inductance L and capacitance C of the DC/DC boost chopper are given by:

$$\begin{cases} L = \frac{\alpha V_0}{f \Delta I} \\ C = \frac{\alpha I_{max}}{f \Delta V} \end{cases} \quad (2.18)$$

whereas: 
$$\begin{cases} f = \text{switching frequency} \\ \alpha = \text{average duty cycle} \\ V_0 = \text{Input voltage} \\ \Delta I = \text{current oscillation in the inductance} \\ \Delta V = \text{Oscillation of the output voltage} \end{cases}$$

In our case, the parameters of equation (2.18) can be estimated as follows:

$$\begin{cases} V_0 = 31.95 \text{ V} \\ I_0 = 8.77 \times 36 = 315.72 \text{ A (assuming 36 modules connected in parallel)} \\ V = 48 \text{ V} \\ I = 600 \text{ A} \\ \Delta V = V - V_0 = 48 - 31.95 = 16.05 \text{ V} \end{cases}$$

$$\rightarrow I_{0,max} = \sqrt{2} \times 315.72 = 446.5 \text{ A}$$

$$\rightarrow \Delta I = 15 \% \times I_{0,max} \text{ in order to reduce the hysteresis losses}$$

$$= 0.15 \times 446.5 = 67 \text{ A.}$$

The duty cycle can be calculated through the equation: 
$$\frac{V}{V_0} = \frac{1}{1-\alpha} \quad (2.19)$$

$$\rightarrow \alpha = 33 \%$$

Numerical application for a switching frequency  $f = 20 \text{ KHz} = 20000 \text{ Hz}$ :

$$\begin{cases} L = \frac{\alpha V_0}{f \Delta I} = \frac{0.33 \times 31.95}{20000 \times 67} = 7.9 \times 10^{-6} H = 7.9 \mu H \\ C = \frac{\alpha I_{max}}{f \Delta V} = \frac{0.33 \times 600}{20000 \times 16} = 6.17 \times 10^{-4} = 61.7 mF \end{cases}$$

A MPPT controller is adopted to achieve the maximum output power of the PV panels.

### 2.3.5.2 Bidirectional DC/DC converter (wiring diagram presented in Fig. 1.5)

Similarly, the identification of the bidirectional DC/DC converter's parameters is calculated in what follows.

At the converter's input (inductance side) are installed the lead-acid batteries of a capacity of 3000Ah with a 48V voltage and a maximal load current of 600A.

At the converter's output side 209 modules in series and 7 modules in parallel of Ni/MH batteries of 1.2 V of voltage and 75Ah of capacity. The total voltage of the pack on the output side would then be:  $V = 209 \times 1.2 = 250.8 V$

The average duty cycle can be calculated as per equation (2.19) as follows:

$$\alpha = 1 - \frac{V_0}{V} = 1 - \frac{48}{250.8} = 1 - 0.19 = 0.81 \Rightarrow \alpha = 81\%$$

$$L = \frac{\alpha \times V_0}{f \times \Delta I} \quad \text{whereas} \quad \begin{cases} \alpha = 0.81 \\ V_0 = 48V \\ f = 20000Hz \\ \Delta I = 0.15 \times 600 = 90 A \end{cases}$$

$\Delta I$  has been assumed as 15% of the maximal load current taking into consideration the current oscillation within the inductance in order to reduce the hysteresis losses.

$$\text{Therefore, } L = \frac{\alpha \times V_0}{f \times \Delta I} = \frac{0.81 \times 48}{20000 \times 90} = 2.16 \times 10^{-5} H = 21.6 \mu H$$

### 2.3.5.3 AC/DC inverter

As the energy needs of the house are estimated as:  $P = 8.7 kW_c$ ; an inverter of 9kW power is adopted in the study, particularly, the SolarEdge inverter SE9KUS 3 $\phi$  universal 9kW (for datasheet we refer to Appendix A.5) (Fig. 2.9).



Figure 2.9: AC/DC inverter SolarEdge SE9KUS 9kW [92]

## 2.4 System's energetic modeling

The establishment of the electric model of each of the system's components would not lead to a global model of the system that includes all its components due to the huge diversity of the components' different variables. Therefore, the energetic model of the system is embodied based on the production and consumption of electric energy and the system's interaction to the energetic excess or insufficiency; the production and consumption being defined by renewable energy sources, the vehicle and household appliances.

Thus, three case studies would be investigated:

- a- The production of energy would surpass the demand of electricity, and there would be an excessive amount of energy for the electric vehicles to charge their batteries.

$$E_{pr} > E_c$$

$$E_{pr} = E_c + \Delta$$

whereas  $\Delta$  = the excess of energy that can be partially or completely used by the vehicle for charging and  $E_{pr}$  and  $E_c$  represent the production and consumption of energy progressively.

Energy produced by renewable sources > Energy consumed by the home and the vehicle

$$E_{pr}(\text{Renewable sources}) > E_c(\text{Home}) + E_c(\text{vehicle})$$



$$E_{pr}(PV) + E_{pr}(WT) > E_c(Home) + E_c(vehicle) \quad (2.20)$$

where  $E_{pr}(PV)$  and  $E_{pr}(WT)$  are the energy produced by the photovoltaic panels and the wind turbine progressively.

- The energy produced by photovoltaic panels is embodied as follows:

$$E_{pr}(PV)_{Wh/day} = N_{H_j} \times P_f \times k$$

$$\text{Whereas } \begin{cases} N_{H_j} = \text{number of hours of use per day (in hours)} \\ P_f = \text{Operating power (in watts)} \\ k = \text{correction factor} = 1.3 \end{cases}$$

- The energy produced by the wind turbine is also summarized by:

$$E_{pr}(WT) = \frac{\text{wind turbine annual energy output}}{\text{number of days/year}} = \frac{0.01328 \times D^2 \times v^3}{365.25}$$

$$\text{whereas } \begin{cases} D = \text{Rotor diameter (ft)} \\ v = \text{annual average wind speed (mph)} \end{cases}$$

- The energy consumed by the vehicle:  $E_c(vehicle) = E_o \times d = E_p$

$$\text{whereas } \begin{cases} E_o = \text{Energy linked to the on – board electric outlet (kWh/km)} \\ d = \text{travelled distance (km)} \\ E_p = \text{propulsive energy of the vehicle} \end{cases}$$

$$\begin{aligned} E_c(vehicle) &= E_o \times d = E_p = \frac{A}{V} (F_p \times V + P_{aux}) \\ &= \frac{A}{V} \left[ (ma + C_r \times m \times g \times \cos \alpha + \frac{1}{2} \rho S C_x V^2 + m g \sin \alpha) V + P_{aux} \right] \end{aligned}$$

- The energy consumed by the functional household appliances  $E_c(Home)$ :

$$\begin{aligned} E_c(Home) &= \sum_{\text{home appliances}} N_{H_j} \times P_f = (N_{H_j} \times P_f)_{\text{heating/ventilation}} + \\ &(N_{H_j} \times P_f)_{\text{water heating}} + (N_{H_j} \times P_f)_{\text{lighting}} + (N_{H_j} \times P_f)_{\text{audiovisual appliances}} + \\ &(N_{H_j} \times P_f)_{\text{cooking}} + (N_{H_j} \times P_f)_{\text{washing/drying}} + (N_{H_j} \times P_f)_{\text{electronics use}} + \\ &(N_{H_j} \times P_f)_{\text{refrigerator}} \end{aligned}$$

Therefore, the equation (2.20) can be represented by:

$$N_{H_j} \times P_f \times k + \frac{0.01328 \times D^2 \times v^3}{365.25} > \sum_{\text{home appliances}} N_{H_j} \times P_f + E_o \times d$$

$$N_{H_j} \times P_f \times k + \frac{0.01328 \times D^2 \times v^3}{365.25} > \sum_{\text{home appliances}} N_{H_j} \times P_f + \frac{A}{V} [(ma + C_r \times m \times g \times \cos \alpha + \frac{1}{2} \rho S C_x V^2 + m g \sin \alpha) V + P_{\text{aux}}] \quad (2.21)$$

b- The consumption of energy exceeds its production. In this case, the demand of energy exceeds the electricity supply and the amount of energy available is insufficient. In order to compensate this insufficiency, it would be recommended to refer to complementary sources of energy, or to use the available energy stored. Thus, at this stage, the energy stored in the electric vehicles' battery could be used; hence the vehicles would be discharging.

$$E_{pr} < E_c$$

$$E_{pr} = E_c - \Delta$$

whereas  $\Delta$  = the lack of energy that is partially or completely compensated by the storage of the vehicles' battery.

The energy produced by renewable sources and the vehicle is less than the energy consumed by the home:

$$E_{pr}(\text{Renewable sources}) + E_{pr}(\text{vehicle}) < E_c(\text{Home})$$

$$E_{pr}(PV) + E_{pr}(WT) + E_{pr}(\text{vehicle}) < E_c(\text{Home})$$

$$N_{H_j} \times P_f \times k + \frac{0.01328 \times D^2 \times V^3}{365.25} + E_{pr}(\text{vehicle}) < \sum_{\text{home appliances}} N_{H_j} \times P_f$$

$$N_{H_j} \times P_f \times k + \frac{0.01328 \times D^2 \times V^3}{365.25} + E_{pr}(\text{vehicle}) < (N_{H_j} \times P_f)_{\text{heating/ventilation}} +$$

$$(N_{H_j} \times P_f)_{\text{water heating}} + (N_{H_j} \times P_f)_{\text{lighting}} + (N_{H_j} \times P_f)_{\text{audiovisual appliances}} +$$

$$(N_{H_j} \times P_f)_{\text{cooking}} + (N_{H_j} \times P_f)_{\text{washing/drying}} + (N_{H_j} \times P_f)_{\text{electronics use}} +$$

$$(N_{H_j} \times P_f)_{\text{refrigerator}} \quad (2.22)$$

$$\text{with } E_{pr}(\text{vehicle}) = \frac{A}{V}(F_p \times V + P_{aux}) = E_o \times d$$

The value of  $E_{pr}(\text{vehicle})$  to be discharged from the vehicle can be estimated based on the SoC available, and the distance that could be travelled using the SoC's amount of energy. However, all the energy stored in the battery may not be fully returned to supply the needs of the house.

- c- The energy production and consumption are equivalent. In this case, there's no need to refer to new sources of energy to compensate the insufficiency, yet, there's no excessive energy to be used for extra consumption. Thus, the fleet remains unused, and the vehicles would be neither charging nor discharging. They would neither be storing nor restituting energy, yet they would rather be waiting until an imbalance between the demand and supply of electricity strikes again, which will trigger a new storage or retrieval cycle

$$E_{pr} = E_c$$

$$E_{pr} = E_c \pm \Delta \quad \text{whereas } \Delta = 0$$

$$E_{pr}(\text{Renewable sources}) = E_c(\text{Home})$$

$$E_{pr}(\text{PV}) + E_{pr}(\text{WT}) = E_c(\text{Home})$$

$$N_{H_j} \times P_f \times k + \frac{0.01328 \times D^2 \times V^3}{365.25} = \sum_{\text{home appliances}} N_{H_j} \times P_f$$

$$N_{H_j} \times P_f \times k + \frac{0.01328 \times D^2 \times V^3}{365.25} = (N_{H_j} \times P_f)_{\text{heating/ventilation}} + (N_{H_j} \times P_f)_{\text{water heating}} + (N_{H_j} \times P_f)_{\text{lighting}} + (N_{H_j} \times P_f)_{\text{audiovisual appliances}} + (N_{H_j} \times P_f)_{\text{cooking}} + (N_{H_j} \times P_f)_{\text{washing/drying}} + (N_{H_j} \times P_f)_{\text{electronics use}} + (N_{H_j} \times P_f)_{\text{refrigerator}} \quad (2.23)$$

Accordingly, all the three proposed cases can be summarized by the following equation:

$$E_{pr} = E_c \pm \Delta \quad (2.24)$$

$$\text{whereas } \Delta = \begin{cases} 0 & \text{if } E_{pr} = E_c \\ \text{excess of energy} & \text{if } E_{pr} < E_c \\ \text{lack of energy} & \text{if } E_{pr} > E_c \end{cases}$$

## **2.5 Conclusion**

In this chapter, the main objective of this study of modeling the treated system has been defined and the considered energy system has been exposed and discussed. More precisely, each component of the described system has been investigated, and a choice of its type as well as its detailed sizing has been performed. Custom parameters have been calculated and particular technical specifications have been assigned to all of the system's components. Besides, the global energetic modeling of the system has been embodied through three case studies where the margin of difference between energy production and consumption varies. Furthermore, a multi-objective optimization of the vehicles' charging and discharging is performed in chapters 3 and 4 in order to fulfill the system's energetic needs.

## **Chapter 3 - Energy Storage multi-objective optimization**

3.1	Introduction.....	86
3.2	Multi-Objective Optimization for charging.....	87
3.2.1	Objectives definition and modeling.....	87
3.2.2	Multi-objective optimization – Genetic Algorithm.....	91
3.2.2.1	Objective 1: Optimization of the State-of-Charge.....	91
3.2.2.2	Objective 2: Optimization of the Valley Energy.....	96
3.2.2.3	Objective 3: Optimization of the Propulsive Energy.....	99
3.2.2.4	Objective 4: Optimization of the losses.....	101
3.3	Optimization Scenarios.....	104
3.4	Weighted Sum Approach.....	107
3.5	Computation and Verification.....	110
3.6	Conclusion.....	115

### **3.1 Introduction**

As mentioned in chapter 2, the studied system involves an electric vehicles fleet with a Nickel Metal Hydride (NiMH) on-board battery of a capacity of 75 Ah and an 80 % depth of discharge, thus a significant storage capacity. The investigated domestic household has an average daily consumption of 31.1 kWh that is entirely or partially compensated with the energy production of 33 mono-crystalline photovoltaic modules with a rated power of 280Wp under standard conditions, as well as the production of a horizontal axis wind turbine with a power of 2.8 kW. The calculated household daily consumption includes the energy consumed for heating/ventilation, water heating, lighting, audio-visual appliances, cooking, washing/drying, electronics use, the refrigerator, as well as the vehicle's electric outlet.

While electric vehicles have been immensely taking part in the worldwide pollution reduction, their on-board batteries can also be used as means of storage and retrieval of electrical energy which does not seem to be easily stored in huge quantities. To do so, the charging of vehicles can be scheduled based on the supply and demand of electricity and their alternative energy needs. Thus, as long as the electricity supply by the electric grid exceeds its demand, the vehicles batteries would be used for storage means. Thus, the vehicles would charge their batteries where energy would be stored. Then, the energy storage is proposed through a multi-objective optimization of the flow of energy coming into the vehicle during its charging process. For this end, this chapter first describes the objective functions linked to the vehicles' charging optimization. The multi-objective genetic algorithm is adopted as an optimization approach to calculate the optimized solutions to the fitness functions. Subsequently, in order to combine the resulting solutions into a final combined optimized solution, each fitness function is normalized and the weighted sum approach is applied through different optimization scenarios where random weights are assigned based on the decision maker's priorities. Finally, the optimized values resulting from the calculation are computed and verified by simulation using Matlab software.

The originality of this optimization study appears in the application of the genetic algorithm method for electric vehicles' energy storage and retrieval and the validation of optimized results through Matlab simulations.

## 3.2 Multi-Objective Optimization for charging

In order to define the optimized solutions related to several objective functions of the same system, many optimization approaches can be referred to. An efficient optimization method to use is the heuristic genetic algorithm approach where the fittest solutions are selected through the reproduction of offsprings in consecutive generations. Thus, the multi-objective genetic algorithm optimization method is adopted to find the most optimized solutions of the defined objective functions [93], [94].

In this study, the optimization model is defined as follows:

$$\begin{cases} \min/\max F(X) = [f_1, f_2, \dots, f_n] \\ g_i(X) \geq 0, i = 1, 2, \dots, m \end{cases} \quad (3.1)$$

where  $F$ ,  $f_n$  and  $g_i$  are the global function to optimize, the objective functions and the constraints of the system respectively.

Whenever the production tops the consumption, the energy storage in the vehicles' batteries gets launched in order to recover the excess of energy and redirect it towards a beneficial usage of the unused energy that is wasted vainly. The vehicles' charging is then launched with the optimization of the energy flows through several objective functions that representing the system performances. The corresponding solutions are calculated for an optimized charging of the vehicles using genetic algorithm method as a multi-objective approach for optimization.

Further details concerning the charging model are provided in the following sections of this chapter, and those of the discharging model are provided in chapter 4.

### 3.2.1 Objectives definition and modeling

The charging optimization is assessed in order to accomplish the most optimized energy flows control. In order to attain the inquired optimality, the main objectives that the optimization aims to satisfy are first enumerated:



- i. Maximization of the longevity of vehicles' batteries and the optimization of their life cycles through the maximization of their state-of-charge.
- ii. Control of the vehicles' charging by switching the charging loads towards off-peak hours whenever the vehicles are connected to the electric grid, so that the demand curve gets as flattened as possible.
- iii. Optimization of the vehicles' needs by controlling their autonomy in numerous trip circumstances such as the functional on-board accessories and the type of roads.
- iv. Fulfillment of the infrastructural energetic needs.

In order to fulfill the objectives sought, the vehicles' modeling, as well as that of the charging process, has been established with the following objectives functions:

- i. The vehicles' state-of-charge SoC during the charging process should be maximized. It is generally presented by the following equation :

$$SoC(t) = SoC(t - 1) + \eta_{ch} \frac{P_{ch}}{E_b} \quad (3.2)$$

whereas  $\eta_{ch}$ ,  $P_{ch}$  and  $E_b$  consecutively represent the vehicles' charging efficiency, their charging power, and batteries' capacity. However, this objective is complemented with a SoC constraint limit that would not fall short of a minimal value  $SoC_{min}$  or surpass a maximal value  $SoC_{max}$ , in order to avoid any batteries' damage:  $SoC_{min} < SoC < SoC_{max}$  [95].

- ii. In order to avoid the significant energy losses and voltage fluctuations and in some cases the network infrastructure's reinforcements, the integration of EVs into the electric grid involves the need for a management system where the demand curve tends to be flattened. Thus the charging loads shift to off-peak hours through a coordinated charging strategy with lower electricity prices and demand load. Whenever the electric vehicles would be grid-connected, the avoidance of voltage fluctuations and energy losses requires a relatively flat demand curve achieved through a charging loads' shift towards off-peak hours.

So, whenever the electric vehicles are grid connected, it happens that, sometimes, they all get linked to charging stations simultaneously in order to fill their batteries. Hence, a huge electricity demand occurs during peak hours when the grid supply might become insufficient. On the other hand, the electricity demand is negligible during valley times where very few vehicles are charging and the grid energy is not extensively consumed. Generally, it is highly recommended to establish a balance between peak and valley periods in order to avoid the huge voltage and

power fluctuations as well as the oscillations of the charging demand profile. This balance, often acquired through economic incentives encouraging vehicles' owners to shift their charging towards the valley times where the electricity demand is lower and with reduced prices. This demand load shift would balance the grid through flattening the charging curve, hence maximizing the valley energy until omitting the unwanted fluctuations. Thus, the maximization of valley energy  $E_{\text{valley}}$  would balance the electricity demand and the network avoiding considerable fluctuations, energy waste and infrastructure reinforcements in case of long transmission lines insufficiently supplied by the grid. In fact, vehicles would connect for charging as soon as they are available, and their batteries are not completely full. The demand profile valley is mostly caused by the huge number of vehicles ready for charging. Yet, through the maximization of the valley energy, the charging demand curve gets flattened and the charging processed gets managed.

Consequently, the valley energy  $E_{\text{valley}}$ , depicted by the following equation should be maximized:

$$E_{\text{valley}} = \frac{Q \times (1 - \text{SoC}(t))}{P_{\text{ch}}} \times P_{\text{valley}} \quad (3.3)$$

whereas  $Q$ ,  $P_{\text{ch}}$  and  $P_{\text{valley}}$  correspond consecutively stand for the rated batteries' capacity, the charging power, and the valley power [96], [97].

iii. The optimization of the vehicles' needs involves the modeling of their propulsive energy  $E_p$  represented by the equation:

$$E_p = \frac{A}{V} \times (P_p + P_{\text{aux}}) \quad (3.4)$$

whereas  $A$ ,  $V$ ,  $P_p$  and  $P_{\text{aux}}$  respectively denote the vehicles' autonomy, their relative speed, their propulsive power and the auxiliary power. These parameters are linked to the functional on-board electrical accessories such as the headlights, windshield wipers, air conditioning, etc. It is to be noted that the vehicles' autonomy widely fluctuates depending on the types of roads they are travelling (whether in urban or rural areas) and their inclination angle  $\alpha$ , as well as the traffic on roads, the waiting line time and the energy consumption related to the use of on-board accessories (air conditioning/heating, headlights, radio, wipers...). Therefore, all these factors need to be taken into consideration within the optimization algorithm's charging and discharging

processes so that the vehicle always fulfills its personal trips' needs [98], [99], [100], [101], [102].

iv. In some areas where the infrastructure reinforcement would be complicated due to the huge length of transmission lines, the EVs grid integration would be intricate. Particularly, the network's reinforcement would be more complex in urban areas than in rural areas [103], [104], [105]. As the network's reinforcement would vary depending on the transmission lines' length, and the difficulty of vehicles' grid integration, the fulfillment of the infrastructural energetic needs is directly linked to the minimization of energy losses expressed by:

$$l = 100 \times \frac{P_{ch} - (P_p + P_{aux})}{P_{ch}} \quad (3.5)$$

Whereas the coefficient 100 allows the losses' embodiment in percentage %.

It is to be mentioned that this minimization concerns the energy losses linked to the power transmission lines' length, yet, it does not involve the power lines capacity and their resulting losses.

Therefore, the multi-objective optimization program is represented by a mathematical system where all objective functions highlight the mathematical model for each of the study's objectives already mentioned that are the state of charge, the charging power, the propulsive energy of the vehicle and the energy losses. The study is first carried out for the charging phase [106], [107], [108]. Hence, the charging optimization's modeling of equation (3.1) is summed up by the following system highlighting the objectives' mathematical models:

$$\bullet \begin{cases} \min/\max F(X) = [f_1, f_2, f_3, f_4] \\ g_i(X) \geq 0, i = 1, 2, \dots \end{cases} \quad (3.6)$$

•  $f_i$  (for  $i = 1, 2, 3, 4$ ) are objective functions:

$$\begin{cases} f_1 = SoC(t) = SoC(t-1) + \eta_{ch} \frac{P_{ch}}{E_b} \\ f_2 = E_{valley} = \frac{Q \times (1 - SoC(t))}{P_{ch}} \times P_{valley} \\ f_3 = E_p = \frac{A}{V} \times (P_p + P_{aux}) \\ f_4 = l = 100 \times \frac{P_{ch} - (P_p + P_{aux})}{P_{ch}} \end{cases} \quad (3.7)$$

Likewise, the constraints of this optimization would involve the maximal or minimal boundaries defined by the vehicle's charge or discharge, as well as the charging power that must surpass the summed up auxiliary and propulsive powers in order for the vehicle to circulate. These constraints are expressed in what follows.

- $g_i = \text{Constraint functions:}$

$$\begin{cases} g_1 \rightarrow SoC_{min} \leq SoC \leq SoC_{max} \\ g_2 \rightarrow P_{ch} \leq P_{ch_{max}} \\ g_3 \rightarrow E_{p_{min}} \leq E_p \leq E_{p_{max}} \\ g_4 \rightarrow l \geq l_{min} \\ g_5 \rightarrow P_{ch} > P_p + P_{aux} \end{cases} \quad (3.8)$$

Whereas  $P_{ch_{max}}$  and  $l_{min}$  respectively represent the maximal boundary for the charging power and the minimal value of the losses.

### 3.2.2 Multi-objective optimization – Genetic Algorithm

Once the multi-objective optimization model has been set, the heuristic genetic algorithm approach has been adopted to assess the optimized values related to each objective function. In order to unify the parameters and calculations, the mathematical model involves one electric vehicle instead of a fleet.

#### 3.2.2.1 Objective 1: Optimization of the State-of-Charge

$$f_1(SoC(t-1), P_{ch}) = SoC(t) = SoC(t-1) + \eta_{ch} \frac{P_{ch}}{E_b} \quad (3.9)$$

Taking into consideration the aim to maximize the battery's life cycle, its longevity and to avoid its deterioration and lifetime decrease, its SoC is limited within 10% to 90% range. Thus, considering the SoC limitation boundaries with an 80% depth of discharge for the vehicle, the maximum SoC allowed value is set at 90%. This value is adopted as a reference for an ideal optimization. Therefore, as the study aims to maximize the value of  $f_1 = SoC(t)$ , and noting that the applied multi-objective Genetic Algorithm GA is heuristic providing approximate values that are the closest possible to the optimal solution,  $SoC(t) = 90\%$  is adopted as the maximal reference value that the optimization aims to reach (theoretical value). Therefore, the GA aims

the get the closest possible value to 90 %. Thus, with reference to predefined vehicles' technical specification,  $E_b$  has been fixed at 75 Ah, and  $\eta_{ch}$  at 85%. The decision variables related to this objective function being  $SoC(t - 1)$  and  $P_{ch}$ , the genetic chromosome has been set as  $[SoC(t - 1), P_{ch}]$ . The optimized solution's calculation have been operated with an initial population of 12 randomly picked chromosomes, reduced into 6 chromosomes via a 50% selection rate of the most adequate values (table 3.1).

**Table 3.1: The optimization's initial population of 12 chromosomes with their solution and ranking**

<b><math>SoC(t - 1)</math> (%)</b>	10	20	30	40	45	50	<b>60</b>	<b>65</b>	<b>70</b>	<b>75</b>	<b>80</b>	<b>88.57</b>
<b><math>P_{ch}</math> (kW)</b>	95	100	104	108	112	116	<b>120</b>	<b>123</b>	<b>125</b>	<b>126</b>	<b>128</b>	<b>130</b>
<b><math>SoC(t)</math> (%)</b>	11.05	21.1	31.14	41.2	46.23	51.28	<b>61.32</b>	<b>66.35</b>	<b>71.38</b>	<b>76.39</b>	<b>81.4</b>	<b>90</b>
<b>Rank</b>	12	11	10	9	8	7	<b>6</b>	<b>5</b>	<b>4</b>	<b>3</b>	<b>2</b>	<b>1</b>

The survival population after a 50% selection rate involves the fittest 6 chromosomes out of 12, below listed:

$$\text{Chromosomes with ranks } 1 \rightarrow 6: \begin{cases} chr_1 = [88.57, 130] \\ chr_2 = [80, 128] \\ chr_3 = [75, 126] \\ chr_4 = [70, 125] \\ chr_5 = [65, 123] \\ chr_6 = [60, 120] \end{cases}$$

Rank weighting:

The probability  $P_n$  for the  $n^{\text{th}}$  place chromosome to be a parent:

$$P_n = \frac{N_{kept} - n + 1}{\sum_{i=1}^{N_{kept}} i} = \frac{6 - n + 1}{1 + 2 + 3 + 4 + 5 + 6} = \frac{7 - n}{21}$$

$$\text{Therefore, } \begin{cases} P(chr_1) = \frac{6}{21} \\ P(chr_2) = \frac{5}{21} \\ P(chr_3) = \frac{4}{21} \\ P(chr_4) = \frac{3}{21} \\ P(chr_5) = \frac{2}{21} \\ P(chr_6) = \frac{1}{21} \end{cases}$$

Two offsprings would be produced out of each mating. Therefore, in order to produce 6 new offsprings to fill the next generation, 3 pairs of parent chromosomes / 3 matings are needed. Hence, based on Haupt's method (Haupt et al., 2004), and assuming that the mutation rate  $\beta$  is of 0.35, the offspring chromosomes are defined as follows, whereas  $x$  represents a parent chromosome  $[m, d]$ 's crossover point:

$$\begin{cases} \text{offspring 1} = [x_{new_1}, y_m] \\ \text{offspring 2} = [x_{new_2}, y_d] \end{cases} \text{ with } \begin{cases} x_{new_1} = (1 - \beta)x_m + \beta x_d \\ x_{new_2} = (1 - \beta)x_d + \beta x_m \end{cases}$$

In order to define the parent chromosomes that would recombine and produce new offsprings for the succeeding generations, even though picking the chromosomes with the highest ranks as parents would provide fitter solutions, that must be avoided in order to maintain a good diversity of the successive populations and prevent a premature convergence where an extremely fit solution would take over the population [109] [110]. Consequently, 6 chromosome offsprings are generated through 3 parent matings, and the survival population of 6 has then been reduced into 4 chromosomes by the elimination of the two lowest ranks.

#### **A- First mating:**

If we suppose that  $chr_1 = [88.57, 130]$ , and  $chr_4 = [70, 125]$  are a pair of parent chromosomes:

$$\begin{cases} \text{offspring 1} = [0.65 \times 88.57 + 0.35 \times 70, 130] = [82, 130] \\ \text{offspring 2} = [0.65 \times 70 + 0.35 \times 88.57, 125] = [76.5, 125] \end{cases}$$

#### **B- Second mating:**

If we suppose that  $chr_2 = [80, 128]$ , and  $chr_5 = [65, 123]$  are a pair of parent chromosomes:

$$\begin{cases} \text{offspring 1} = [0.65 \times 80 + 0.35 \times 65, 128] = [74.75, 128] \\ \text{offspring 2} = [0.65 \times 65 + 0.35 \times 80, 123] = [70.25, 123] \end{cases}$$

#### **C- Third mating:**

If we suppose that  $chr_3 = [75, 126]$ , and  $chr_6 = [60, 120]$  are a pair of parent chromosomes:

$$\begin{cases} \text{offspring 1} = [0.65 \times 75 + 0.35 \times 60, 126] = [69.75, 126] \\ \text{offspring 2} = [0.65 \times 60 + 0.35 \times 75, 120] = [65.25, 120] \end{cases}$$

The genetic algorithm implies the elimination of the solutions with the lowest ranks in order for the highest ranks to survive. In this application the survival selection rate is of  $2/3^{\text{rd}}$ .

Thus, the two lowest ranks being eliminated, the survival population would be (table 3.2):

$$\text{Chromosomes with ranks } 1 \rightarrow 4: \begin{cases} chr_1 = [82, 130] \\ chr_2 = [76.5, 125] \\ chr_3 = [74.75, 128] \\ chr_4 = [70.25, 123] \end{cases}$$

**Table 3.2: Second generation of 6 chromosomes with their solution and ranking**

<b>SoC(t - 1)</b> (%)	<b>82</b>	<b>76.5</b>	<b>74.75</b>	<b>70.25</b>	69.75	65.25
<b>P<sub>ch</sub></b> (kW)	<b>130</b>	<b>125</b>	<b>128</b>	<b>123</b>	126	120
<b>SoC(t)</b> (%)	<b>84.43</b>	<b>78.38</b>	<b>76.16</b>	<b>71.6</b>	71.4	66.57
<b>Rank</b>	<b>1</b>	<b>2</b>	<b>3</b>	<b>4</b>	5	6

Rank weighting:

The probability for the  $n^{\text{th}}$  place chromosome to be a parent:

$$P_n = \frac{N_{\text{kept}} - n + 1}{\sum_{i=1}^{N_{\text{kept}}} i} = \frac{4 - n + 1}{1 + 2 + 3 + 4} = \frac{5 - n}{10}$$

$$\text{Therefore, } \begin{cases} P(chr_1) = \frac{2}{5} \\ P(chr_2) = \frac{3}{10} \\ P(chr_3) = \frac{1}{5} \\ P(chr_4) = \frac{1}{10} \end{cases}$$

#### **A- First mating:**

If we suppose that  $chr_1 = [82, 130]$ , and  $chr_3 = [74.75, 128]$  are a pair of parent chromosomes:

$$\begin{cases} \text{offspring 1} = [0.65 \times 82 + 0.35 \times 74.75, 130] = [79.46, 130] \\ \text{offspring 2} = [0.65 \times 74.75 + 0.35 \times 82, 128] = [77.29, 128] \end{cases}$$

#### **B- Second mating:**

If we suppose that  $chr_2 = [76.5, 125]$ , and  $chr_4 = [70.25, 123]$  are a pair of parent chromosomes:

$$\begin{cases} \text{offspring 1} = [0.65 \times 76.5 + 0.35 \times 70.25, 125] = [74.3, 125] \\ \text{offspring 2} = [0.65 \times 70.25 + 0.35 \times 76.5, 123] = [72.4, 123] \end{cases}$$

The two lowest ranks being eliminated, the survival population would be (table 3.3):

$$\begin{cases} chr_1 = [79.46, 130] \\ chr_2 = [77.29, 128] \end{cases}$$

**Table 3.3: Surviving population of 4 chromosomes**

<b><math>SoC(t - 1)</math> (%)</b>	<b>79.46</b>	<b>77.29</b>	74.3	72.4
<b><math>P_{ch}</math> (kW)</b>	<b>130</b>	<b>128</b>	125	123
<b><math>SoC(t)</math> (%)</b>	<b>80.89</b>	<b>78.7</b>	75.7	73.8
<b>Rank</b>	<b>1</b>	<b>2</b>	3	4

The two lowest ranks being eliminated, the survival population would be:  $\begin{cases} chr_1 = [79.46, 130] \\ chr_2 = [77.29, 128] \end{cases}$

Rank weighting:

The probability for the  $n^{\text{th}}$  place chromosome to be a parent:

$$P_n = \frac{N_{kept} - n + 1}{\sum_{i=1}^{N_{kept}} i} = \frac{2 - n + 1}{1 + 2} = \frac{3 - n}{3}$$

$$\text{Therefore, } \begin{cases} P(chr_1) = \frac{2}{3} \\ P(chr_2) = \frac{1}{3} \end{cases}$$

If we suppose that  $chr_1 = [79.46, 130]$ , and  $chr_2 = [77.29, 128]$  are a pair of parent chromosomes:

$$\begin{cases} \text{offspring 1} = [0.65 \times 79.46 + 0.35 \times 77.29, 130] = [78.7, 130] \\ \text{offspring 2} = [0.65 \times 77.29 + 0.35 \times 79.46, 128] = [78, 128] \end{cases}$$

**Table 3.4: fittest 2 chromosomes of the population**

	$SoC(t - 1)$ (in %)	$P_{ch}$ (in kW)	Fitness function: $SoC(t)$ (in %)
<b>1</b>	<b>78.7</b>	<b>130</b>	<b>80.13</b>
2	78	128	79.4

Thus, parent chromosomes are crossed to generate offsprings, and the population of 4 is decreased again into a population of 2 chromosomes that mate again to end up with a final



optimized chromosome of a  $P_{ch}$  of 130 kW and a  $SoC(t - 1)$  of 78.7% to end up with an optimized solution of 80.13% for  $f_1 = SoC(t)$ .

So the optimized solution for the first objective function  $f_1 = SoC(t)$  is given by:

$$\left. \begin{array}{l} P_{ch} = 130kW \\ SoC(t - 1) = 78.7\% \end{array} \right\} \rightarrow SoC(t) = 80.13\%$$

### 3.2.2.2 Objective 2: Optimization of the Valley Energy

$$f_2(SoC(t), \frac{P_{valley}}{P_{ch}}) = E_{valley} = \frac{Q \times (1 - SoC(t))}{P_{ch}} \times P_{valley} \quad (3.10)$$

The same procedure has been adopted in order to maximize the valley energy  $E_{valley}$ , where the rated battery capacity has been equally assumed at 75 Ah, and the decision variables for this objective function are  $SoC(t)$  and  $\frac{P_{valley}}{P_{ch}}$ . The genetic chromosome is set at  $[SoC(t), \frac{P_{valley}}{P_{ch}}]$ . The 12 initial chromosomes have been randomly picked in a way that SoC ranges between 10% and 90%, and the ratio  $\frac{P_{valley}}{P_{ch}}$  ranges between 0.69 and 1.3. The optimized solution's reference value for  $E_{valley}$  has been set at the maximum reachable value within the specified ranges for SoC and  $\frac{P_{valley}}{P_{ch}}$ , particularly at 87.75 kWh. Thus, the GA aims to attain the closest possible value to 87.75kWh. The constraint to satisfy regarding this objective is:  $P_{ch} > P_p + P_{aux}$ . Noting that  $(P_p + P_{aux})_{min} = 92 kW$ .

The survival population after a 50% selection rate (table 3.5):

$$\text{Chromosomes with ranks 1} \rightarrow \text{6: } \left\{ \begin{array}{l} chr_1 = [0.1, 1.29] \\ chr_2 = [0.16, 1.24] \\ chr_3 = [0.22, 1.18] \\ chr_4 = [0.27, 1.13] \\ chr_5 = [0.32, 1.09] \\ chr_6 = [0.38, 1.03] \end{array} \right.$$

**Table 3.5: Initial population of 12 chromosomes**

<b>SoC(t)</b>	<b>10% = 0.1</b>	<b>0.16</b>	<b>0.22</b>	<b>0.27</b>	<b>0.32</b>	<b>0.38</b>	0.44	0.56	0.68	0.7	0.82	0.9
$\frac{P_{valley}}{P_{ch}}$	$\frac{120}{93} = 1.29$	1.24	1.18	1.13	1.09	1.03	0.97	0.93	0.86	0.8	0.75	0.71
<b><math>E_{valley}</math> (kwh)</b>	<b>87.08</b>	<b>78.12</b>	<b>69.03</b>	<b>61.87</b>	<b>55.59</b>	<b>47.9</b>	40.74	30.69	20.64	18	10.1	5.31
<b>Rank</b>	<b>1</b>	<b>2</b>	<b>3</b>	<b>4</b>	<b>5</b>	<b>6</b>	7	8	9	10	11	12

Similarly to the calculations carried out for  $f_1$ , the offsprings generated by chromosomes matings are presented in the following table 3.6:

**Table 3.6: Matings and offsprings generation**

	<b>First mating</b> $chr_1 = [0.1, 1.29]$ & $chr_4 = [0.27, 1.13]$	<b>Second mating</b> $chr_2 = [0.16, 1.24]$ & $chr_5 = [0.32, 1.09]$	<b>Third mating</b> $chr_3 = [0.22, 1.18]$ & $chr_6 = [0.38, 1.03]$
<b>Offspring 1</b>	[0.16, 1.29]	[0.22, 1.24]	[0.28, 1.18]
<b>Offspring 2</b>	[0.21, 1.13]	[0.26, 1.09]	[0.32, 1.03]

Therefore, the fitness function and ranks related to the calculated offsprings are exhibited in table 3.7:

**Table 3.7: Six new generated offsprings as a result of the matings**

<b>SoC(t)</b>	<b>0.16</b>	<b>0.21</b>	<b>0.22</b>	0.26	<b>0.28</b>	0.32
$\frac{P_{valley}}{P_{ch}}$	<b>1.29</b>	<b>1.13</b>	<b>1.24</b>	1.09	<b>1.18</b>	1.03
<b><math>E_{valley}</math> (kwh)</b>	<b>81.27</b>	<b>66.95</b>	<b>72.54</b>	60.5	<b>63.72</b>	52.53
<b>Rank</b>	<b>1</b>	<b>3</b>	<b>2</b>	5	<b>4</b>	6

The two lowest ranks being eliminated, the survival population would be (table 3.8):

$$\text{Chromosomes with ranks } 1 \rightarrow 4: \begin{cases} chr_1 = [0.16, 1.29] \\ chr_2 = [0.22, 1.24] \\ chr_3 = [0.21, 1.13] \\ chr_4 = [0.28, 1.18] \end{cases}$$

**Table 3.8: the generation of 4 offsprings through the surviving population**

	<b>First mating</b> $chr_1 = [0.16, 1.29]$ & $chr_3 = [0.21, 1.13]$	<b>Second mating</b> $chr_2 = [0.22, 1.24]$ & $chr_4 = [0.28, 1.18]$
<b>Offspring 1</b>	[0.18, 1.29]	[0.24, 1.24]
<b>Offspring 2</b>	[0.19, 1.13]	[0.26, 1.18]

The two lowest ranks being eliminated, the survival population would be (as given in table 3.9):

$$\begin{cases} chr_1 = [0.18, 1.29] \\ chr_2 = [0.24, 1.24] \end{cases}$$

**Table 3.9: New surviving population of 4 chromosomes**

<b>SoC(t)</b>	<b>0.18</b>	0.19	<b>0.24</b>	0.26
$\frac{P_{valley}}{P_{ch}}$	<b>1.29</b>	1.13	<b>1.24</b>	1.18
$E_{valley}$ (kwh)	<b>79.3</b>	68.6	<b>70.68</b>	65.49
<b>Rank</b>	<b>1</b>	3	<b>2</b>	4

If we suppose that  $chr_1 = [0.18, 1.29]$ , and  $chr_2 = [0.24, 1.24]$  are a pair of parent chromosomes, the generated offsprings would be (table 3.10):  $\begin{cases} offspring\ 1 = [0.2, 1.29] \\ offspring\ 2 = [0.22, 1.24] \end{cases}$

**Table 3.10: The fittest two chromosomes of the population**

	<b>SoC(t)</b>	$\frac{P_{valley}}{P_{ch}}$	Fitness function: $E_{valley}$ (in kWh)
<b>1</b>	<b>0.2</b>	<b>1.29</b>	<b>77.4</b>
2	0.22	1.24	72.54

Consequently, the optimized solution reached for the  $E_{valley}$  maximization is assessed at 77.4 kWh, based on a SoC value of 20% and a  $\frac{P_{valley}}{P_{ch}}$  ratio of 1.29.

$$\text{The optimized solution for } f_2 = E_{valley}: \left. \begin{matrix} SoC(t) = 20\% \\ \frac{P_{valley}}{P_{ch}} = 1.29 \end{matrix} \right\} \rightarrow E_{valley} = 77.4\ kWh$$

### 3.2.2.3 Objective 3: Optimization of the Propulsive Energy

As previously mentioned, the vehicle's propulsive energy to be optimized is expressed in the following equation:

$$f_3((P_p, P_{aux})) = E_p = \frac{A}{v} \times (P_p + P_{aux}) \quad (3.11)$$

In order to maximize the vehicle's propulsive energy, its average velocity has been assumed at 50 km/h, and its autonomy at 100 km. In addition, the decision variables for  $f_3$  being  $P_p$  and  $P_{aux}$ , the genetic chromosome  $[P_p, P_{aux}]$  has been adopted through an initial population of 12 (table 3.11), to define the third objective's optimized solution. The parameters  $P_p$  and  $P_{aux}$  vary respectively within the following ranges:  $90 \text{ kW} \leq P_p \leq 110 \text{ kW}$  and  $2 \text{ kW} \leq P_{aux} \leq 8 \text{ kW}$ . A highest reachable value of 236 kWh has been adopted as a reference value for  $E_p$ 's optimum.

**Table 3.11: Initial population of 12 chromosomes**

$P_p$	90	92	94	96	98	100	<b>102</b>	<b>104</b>	<b>106</b>	<b>108</b>	<b>109</b>	<b>110</b>
$P_{aux}$	2.5	3	3.5	4	4.5	5	<b>5.5</b>	<b>6</b>	<b>6.5</b>	<b>7</b>	<b>7.5</b>	<b>8</b>
$E_p$	185	190	195	200	205	210	<b>215</b>	<b>220</b>	<b>225</b>	<b>230</b>	<b>233</b>	<b>236</b>
<b>Rank</b>	12	11	10	9	8	7	<b>6</b>	<b>5</b>	<b>4</b>	<b>3</b>	<b>2</b>	<b>1</b>

Survival population after 50% selection rate:

$$\text{Chromosomes with ranks } 1 \rightarrow 6: \begin{cases} chr_1 = [110, 8] \\ chr_2 = [109, 7.5] \\ chr_3 = [108, 7] \\ chr_4 = [106, 6.5] \\ chr_5 = [104, 6] \\ chr_6 = [102, 5.5] \end{cases}$$

The generation of offsprings by mating the surviving chromosomes is detailed in table 3.12.

**Table 3.12: Matings and offsprings generation**

	<b>First mating</b> $chr_1 = [110, 8]$ & $chr_4 = [106, 6.5]$	<b>Second mating</b> $chr_2 = [109, 7.5]$ & $chr_5 = [104, 6]$	<b>Third mating</b> $chr_3 = [108, 7]$ & $chr_6 = [102, 5.5]$
<b>Offspring 1</b>	[108.6, 8]	[107.25, 7.5]	[105.9, 7]
<b>Offspring 2</b>	[107.4, 6.5]	[105.75, 6]	[104.1, 5.5]

The new calculated offspring and their corresponding propulsion and ranks are presented in table 3.13.

**Table 3.13: Six new generated offsprings as a result of the matings**

$P_p$	<b>108.6</b>	<b>107.4</b>	<b>107.25</b>	105.75	<b>105.9</b>	104.1
$P_{aux}$	<b>8</b>	<b>6.5</b>	<b>7.5</b>	6	<b>7</b>	5.5
$E_p$	<b>233.2</b>	<b>227.8</b>	<b>229.5</b>	223.5	<b>225.8</b>	219.2
<b>Rank</b>	<b>1</b>	<b>3</b>	<b>2</b>	5	<b>4</b>	6

The two lowest ranks being eliminated, the survival population would be (table 3.14):

$$\text{Chromosomes with ranks } 1 \rightarrow 4: \begin{cases} chr_1 = [108.6, 8] \\ chr_2 = [107.25, 7.5] \\ chr_3 = [107.4, 6.5] \\ chr_4 = [105.9, 7] \end{cases}$$

**Table 3.14: The generation of 4 offsprings through the surviving population**

	<b>First mating</b> $chr_1 = [108.6, 8]$ & $chr_3 = [107.4, 6.5]$	<b>Second mating</b> $chr_2 = [107.25, 7.5]$ & $chr_4 = [105.9, 7]$
<b>Offspring 1</b>	[108.18, 8]	[106.78, 7.5]
<b>Offspring 2</b>	[107.82, 6.5]	[106.37, 7]

The two lowest ranks being eliminated, the survival population would be (table 3.15):

$$\begin{cases} chr_1 = [108.18, 8] \\ chr_2 = [107.82, 6.5] \end{cases}$$

**Table 3.15: New surviving population of 4 chromosomes**

$P_p$	<b>108.18</b>	<b>107.82</b>	106.78	106.37
$P_{aux}$	<b>8</b>	<b>6.5</b>	7.5	7
$E_p$	<b>232.36</b>	<b>228.64</b>	228.56	226.74
<b>Rank</b>	<b>1</b>	<b>2</b>	3	4

If we suppose that  $chr_1 = [108.18, 8]$ , and  $chr_2 = [107.82, 6.5]$  are a pair of parent chromosomes, the offsprings would be:  $\begin{cases} offspring\ 1 = [108.054, 8] \\ offspring\ 2 = [107.95, 6.5] \end{cases}$

Once the genetic algorithm's calculations have been applied, the optimized solution for  $E_p$  turned out to be of 232.108 kWh for  $P_p$  and  $P_{aux}$  with consecutive values of 108.054 kW and 8 kW (table 3.16).

**Table 3.16: The fittest 2 chromosomes of the population**

	$P_p$ (in kW)	$P_{aux}$ (in kW)	Fitness function: $E_p$ (in kWh)
<b>1</b>	<b>108.054</b>	<b>8</b>	<b>232.108</b>
2	107.95	6.5	228.9

So, the optimized solution for  $f_3 = E_p$  is given by:

$$\left. \begin{array}{l} P_p = 108.054 \text{ kW} \\ P_{aux} = 8 \text{ kW} \end{array} \right\} \rightarrow E_p = 232.108 \text{ kWh}$$

#### 3.2.2.4 Objective 4: Optimization of the losses

The fourth objective deals with the minimization of energy losses. This objective is expressed by the mathematical equation:

$$f_4(P_{ch}, P_p + P_{aux}) = l = 100 \times \frac{P_{ch} - (P_p + P_{aux})}{P_{ch}} \quad (3.12)$$

As for this objective, it involves the minimization of losses. Its decision variables are  $P_{ch}$  and  $P_p + P_{aux}$ , and the genetic algorithm approach has been applied with the genetic chromosome  $[P_{ch}, P_p + P_{aux}]$  and the following variation ranges:

- $\left. \begin{array}{l} 90kW < P_p \leq 110kW \\ 2kW < P_{aux} \leq 8kW \end{array} \right\} \rightarrow 92kW < P_p + P_{aux} \leq 118kW$
- $92kW < P_{ch} \leq 130kW$  (with  $P_{ch} > P_p + P_{aux}$  so that the vehicle could circulate)

The minimal reference value of 0.1% has been adopted for the optimized solution to converge towards.

Survival population after a 2/3<sup>rd</sup> selection rate (table 3.17):

$$\text{Chromosomes with ranks } 1 \rightarrow 8: \begin{cases} chr_1 = [92.2, 92.1] \\ chr_2 = [95.5, 95] \\ chr_3 = [98, 97.5] \\ chr_4 = [102, 100] \\ chr_5 = [104, 102.5] \\ chr_6 = [106.5, 105] \\ chr_7 = [109, 107.5] \\ chr_8 = [112, 110] \end{cases}$$

**Table 3.17: Initial population of 12 chromosomes**

<b><math>P_{ch}</math></b>	<b>92.2</b>	<b>95.5</b>	<b>98</b>	<b>102</b>	<b>104</b>	<b>106.5</b>	<b>109</b>	<b>112</b>	116	119	125	130
<b><math>P_p + P_{aux}</math></b>	<b>92.1</b>	<b>95</b>	<b>97.5</b>	<b>100</b>	<b>102.5</b>	<b>105</b>	<b>107.5</b>	<b>110</b>	112.5	115	116.5	118
<b><math>l</math></b>	<b>0.11</b>	<b>0.52</b>	<b>0.51</b>	<b>1.96</b>	<b>1.44</b>	<b>1.4</b>	<b>1.38</b>	<b>1.8</b>	3.02	3.36	6.8	9.2
<b><math>Rank</math></b>	<b>1</b>	<b>2</b>	<b>3</b>	<b>4</b>	<b>5</b>	<b>6</b>	<b>7</b>	<b>8</b>	9	10	11	12

Rank weighting:

The probability for the  $n^{\text{th}}$  place chromosome to be a parent:

$$P_n = \frac{N_{kept} - n + 1}{\sum_{i=1}^{N_{kept}} i} = \frac{8 - n + 1}{1 + 2 + 3 + 4 + 5 + 6 + 7 + 8} = \frac{9 - n}{36}$$

$$\text{Therefore, } \begin{cases} P(chr_1) = \frac{8}{36} = \frac{2}{9} \\ P(chr_2) = \frac{7}{36} \\ P(chr_3) = \frac{6}{36} = \frac{1}{6} \\ P(chr_4) = \frac{5}{36} \\ P(chr_5) = \frac{4}{36} = \frac{1}{9} \\ P(chr_6) = \frac{3}{36} = \frac{1}{12} \\ P(chr_7) = \frac{2}{36} = \frac{1}{18} \\ P(chr_8) = \frac{1}{36} \end{cases}$$

In order to produce 8 new offsprings to fill the next generation, 4 pairs of parent chromosomes / 4 matings are needed (tables 3.18 & 3.19).

**Table 3.18: Matings and offsprings generation**

	<b>First mating</b> $chr_1 = [92.2, 92.1]$ & $chr_5 = [104, 102.5]$	<b>Second mating</b> $chr_2 = [95.5, 95]$ & $chr_6 =$ $[106.5, 105]$	<b>Third mating</b> $chr_3 = [98, 97.5]$ & $chr_7 =$ $[109, 107.5]$	<b>Fourth mating</b> $chr_4 = [102, 100]$ & $chr_8 = [112, 110]$
<b>Offspring 1</b>	[96.33, 92.1]	[95.5, 95]	[98, 97.5]	[105.5, 100]
<b>Offspring 2</b>	[99.87, 102.5]	[106.5, 105]	[109, 107.5]	[108.5, 110]

**Table 3.19: Generated offsprings as a result of the matings**

$P_{ch}$	96.33	<del>99.87</del>	99.35	<del>102.65</del>	101.85	<del>105.15</del>	105.5	<del>108.5</del>	
$P_p + P_{aux}$	92.1	<del>102.5</del>	95	<del>105</del>	97.5	<del>107.5</del>	100	<del>110</del>	
$l$	4.4	<del>-2.6</del>	4.38	<del>-2.3</del>	4.3	<del>-0.02</del>	5.2	<del>-1.38</del>	
	3		2		1		4		Rank

The solutions that fail to comply with the  $P_{ch} > P_p + P_{aux}$  constraint have been stroke through in table 3.19.

So, the ranks with  $P_{ch} < P_p + P_{aux}$  being eliminated (as the vehicle wouldn't be charged enough to circulate), the survival population would be:

$$\text{Chromosomes with ranks } 1 \rightarrow 4: \begin{cases} chr_1 = [101.85, 97.5] \\ chr_2 = [99.35, 95] \\ chr_3 = [96.33, 92.1] \\ chr_4 = [105.5, 100] \end{cases}$$

New offsprings are generated using the surviving population (table 3.20):

**Table 3.20: Generation of four offsprings through the surviving population**

	<b>First mating</b> $chr_1 = [101.85, 97.5]$ & $chr_3 = [96.33, 92.1]$	<b>Second mating</b> $chr_2 = [99.35, 95]$ & $chr_4 =$ $[105.5, 100]$
<b>Offspring 1</b>	[99.9, 97.5]	[101.7, 95]
<b>Offspring 2</b>	[98.26, 92.1]	[103.8, 100]

The two lowest ranks being eliminated, the survival population would be (table 3.21):

$$\begin{cases} chr_1 = [99.9, 97.5] \\ chr_2 = [103.8, 100] \end{cases}$$



**Table 3.21: Surviving population of four chromosomes**

$P_{ch}$	<b>99.9</b>	98.26	101.7	<b>103.8</b>
$P_p + P_{aux}$	<b>97.5</b>	92.1	95	<b>100</b>
$l$	<b>2.4</b>	6.27	6.6	<b>3.67</b>
<b>Rank</b>	<b>1</b>	3	4	<b>2</b>

If we suppose that  $chr_1 = [99.9, 97.5]$ , and  $chr_2 = [103.8, 100]$  are a pair of parent chromosomes, the offsprings set would be:  $\left\{ \begin{array}{l} \text{offspring 1} = [101.27, 97.5] \\ \text{offspring 2} = [102.4, 100] \end{array} \right.$

Therefore, the optimized solution calculated for  $f_4$  is  $l = 2.34\%$  with a  $P_{ch} = 102.4 \text{ kW}$  and  $P_p + P_{aux} = 100 \text{ kW}$  (table 3.22).

**Table 3.22: The fittest two chromosomes of the population**

	$P_{ch}$	$P_p + P_{aux}$	Fitness function: $l$
<b>2</b>	101.27	97.5	3.7
<b>1</b>	<b>102.4</b>	<b>100</b>	<b>2.34</b>

Finally, the optimized solution for  $f_4 = l$  is given by:

$$\left. \begin{array}{l} P_{ch} = 102.4 \text{ kW} \\ P_p + P_{aux} = 100 \text{ kW} \end{array} \right\} \rightarrow l = 2.34\%$$

### 3.3 Optimization Scenarios

Based on the genetic algorithm's optimization calculations, as some of the objective functions defined depend on the same parameters, the obtained optimized solutions would fix conflicting values that would result in one optimized objective's solution at the expense of another objective. Indeed, noting that the optimization of our objectives is conflicting, the optimum of an objective would set a specific value for its variables that would lead to a non-optimized value of another objective. For example, a 130 kW value for  $P_{ch}$  would lead to the optimized SoC, while the same value of  $P_{ch}$  should be set to 102.4 kW for an optimized value for the losses. So, the concluded optimized solution of the four objective functions cannot be reached all at the same time. Therefore, different case studies and preference based optimization

scenarios have been carried out depending on the decision maker's priority of some objectives over the others. This issue is illustrated through various scenarios that we report in what follows.

**Scenario 1:** In this scenario, the decision maker has no specific preference for any of the objective functions, so the calculated optimized values are adopted irrespective of the conflicting parameters. Thus, the optimized solution set would be (see table 3.23):

**Table 3.23: Optimized solution for Charging Scenario 1**

$f_1 = SoC(t)$	$f_2 = E_{valley}$	$f_3 = E_p$	$f_4 = l$
80.13 %	77.4 kWh	232.108 kWh	2.34 %

**Scenario 2:** The preference is set for the objective functions  $f_1$  and  $f_3$  of the system. So, the parameters of the objective functions SoC and  $E_p$  are set and fixed, even if that affects the optimized solutions of the rest of the objective functions (table 3.24):

**Table 3.24: Optimized solution for Charging Scenario 2**

$f_1 = SoC(t)$	$f_2 = E_{valley}$	$f_3 = E_p$	$f_4 = l$
80.13 %	19.35 kWh	232.108 kWh	10.73 %

**Scenario 3:** In scenario 3, the decision maker sets a priority for the optimization of the vehicle's valley energy and losses over its battery's state of charge and propulsive energy. Therefore, in case of a priority for objectives  $f_2 = E_{valley}$  and  $f_4 = l$  over  $f_1 = SoC(t)$  and  $f_3 = E_p$ , the resulting optimization values for our objective functions would be (table 3.25):

**Table 3.25: Optimized solution for Charging Scenario 3**

$f_1 = SoC(t)$	$f_2 = E_{valley}$	$f_3 = E_p$	$f_4 = l$
20 %	77.4 kWh	200 kWh	2.34 %

**Scenario 4:** Scenario 4 involves prioritizing the optimization of the vehicle's valley and propulsive energies over its battery's SoC and its losses. Therefore, in case of a priority for objectives  $f_2 = E_{valley}$  and  $f_3 = E_p$  over  $f_1 = SoC(t)$  and  $f_4 = l$  (see table 3.26):

**Table 3.26: Optimized solution for Charging Scenario 4**

$f_1 = SoC(t)$	$f_2 = E_{valley}$	$f_3 = E_p$	$f_4 = l$
20 %	77.4 kWh	232.108 kWh	2.33 %

**Scenario 5:** In this scenario,  $f_1$  and  $f_2$  are prioritized over  $f_3$  and  $f_4$ . In this case, the prioritized objectives are conflicting, and their optimized values cannot be obtained at the same time. In fact, the optimized solution for  $f_1$  involves the values of 130kW for  $P_{ch}$  and 78.8% for  $SoC(t - 1)$  while the optimized solution for  $f_2$  embeds  $SoC(t) = 20\%$  and  $\frac{P_{valley}}{P_{ch}} = 1.29$ . Therefore, a compromise is applied in order to define quasi-optimal solutions that are the closest to the optimized solutions for both objectives. As the common variable that would affect both objectives is  $SoC(t)$ , and consequently  $SoC(t - 1)$ ,  $P_{ch}$  and  $\frac{P_{valley}}{P_{ch}}$  are fixed at the values that lead to the optimized  $SoC(t)$  and  $E_{valley}$ , respectively 130kW and 1.2, and the genetic algorithm is re-applied to sort out the Pareto-front.

The optimization would result in the following optimized solutions (see table 3.27):

**Table 3.27: Optimized solution for Charging Scenario 5**

$f_1 = SoC(t)$	$f_2 = E_{valley}$	$f_3 = E_p$	$f_4 = l$
51.58 %	48.23 kWh	232.108 kWh	10.7 %

**Scenario 6:** There's a preference for  $f_3$  and  $f_4$  over  $f_1$  and  $f_2$  in scenario 6. Noting that  $f_3$  and  $f_4$  are conflicting, the re-application of the genetic algorithm contributes to the optimized solutions exposed in table 3.28:

**Table 3.28: Optimized solution for Charging Scenario 6**

$f_1 = SoC(t)$	$f_2 = E_{valley}$	$f_3 = E_p$	$f_4 = l$
83.67 %	15.9 kWh	204 kWh	0.4 %

**Scenario 7:** In the last scenario, a priority for  $f_1$  and  $f_4$  over the other objectives is set. These two prioritized functions are also conflicting, and that contributes into the optimums that follow (table 3.29):

**Table 3.29: Optimized solution for Charging Scenario 7**

$f_1 = SoC(t)$	$f_2 = E_{valley}$	$f_3 = E_p$	$f_4 = l$
79.96 %	18 kWh	200 kWh	12.56 %

Referring to the above-mentioned scenarios, the obtained optimized solutions clearly converge towards the calculated theoretical optimums based on the preference set for each one of the objective functions. Eventually, the above stated scenarios' tables obviously show that the optimums related to the preferred functions are the closest to the hypothetical calculations.

Consequently, taking into consideration the scenarios' priorities previously set, the optimization results have been combined into a single objective function through the use of weighted sum approach further explained in the next section.

### 3.4 Weighted Sum Approach

The weighted sum approach is a priori approach as the user/decision maker assigns a chosen weight to each objective function after its normalization in order to convert the multi-objective problem into a single objective one represented by the following scalar objective function:

$$\min F(X) = w_1 \times \|f'_1(x)\| + w_2 \times \|f'_2(x)\| + w_3 \times \|f'_3(x)\| + w_4 \times \|f'_4(x)\| \quad (3.13)$$

where the sum of all assigned weights should be equal to 1,  $\sum w_i = 1$ , and  $f'_i(x)$  is the normalization of the objective functions  $f_i(x)$  as per the equation:

$$f'_i = \frac{f_i - f_{i,min}}{f_{i,max} - f_{i,min}} \quad (3.14)$$

with  $f_i$ ,  $f_{i,min}$  and  $f_{i,max}$  being respectively the objective functions and their minimal and maximal values [111], [112], [113]. The weighted sum approach, [114], will be adopted in this study.

Accordingly, the objective functions' normalization have led to the following  $f'_i$  functions:

$$\left\{ \begin{array}{l} f_1 \rightarrow SoC(t): f'_1 = \frac{f_1-10}{90-10} = \frac{SoC-10}{80} \\ f_2 \rightarrow E_{valley}: f'_2 = \frac{f_2-5.2}{82.55} = \frac{E_{valley}-5.2}{82.55} \\ f_3 \rightarrow E_p: f'_3 = \frac{f_3-184}{52} = \frac{E_p-184}{52} \\ f_4 \rightarrow l: f'_4 = \frac{f_4-0.1}{29.1} = \frac{l-0.1}{29.1} \end{array} \right. \quad (3.15)$$

And the functions  $\|f'_i(x)\|$  referred to in the weighted sum approach application are expressed as follows:

$$\left\{ \begin{array}{l} \|f'_1(x)\| = \max(f'_1(x)) = \min(-f'_1(x)) = \min(-SoC(t))' = \min[-SoC(t-1) - \eta_{ch} \frac{P_{ch}}{E_b}]' \\ \|f'_2(x)\| = \max(f'_2(x)) = \min(-f'_2(x)) = \min(-E_{valley})' = \min \left[ -\frac{Q \times (1-SoC(t))}{P_{ch}} \times P_{valley} \right]' \\ \|f'_3(x)\| = \max(f'_3(x)) = \min(-f'_3(x)) = \min(-E_p)' = \min \left[ -\frac{A}{V} \times (P_p + P_{aux}) \right]' \\ \|f'_4(x)\| = \min(f'_4(x)) = \min(l)' = \min \left[ 100 \times \frac{P_{ch} - (P_p + P_{aux})}{P_{ch}} \right]' \end{array} \right. \quad (3.16)$$

where the symbol  $\|f\|$  is adopted to represent the optima of the functions.

For coherent calculations, the elements of equation (3.16) are all brought to their maxima as follows:

$$\left\{ \begin{array}{l} \|f'_1(x)\| = \max(f'_1(x)) = \max[SoC(t-1) + \eta_{ch} \frac{P_{ch}}{E_b}]' \\ \|f'_2(x)\| = \max(f'_2(x)) = \max \left[ \frac{Q \times (1-SoC(t))}{P_{ch}} \times P_{valley} \right]' \\ \|f'_3(x)\| = \max(f'_3(x)) = \max \left[ \frac{A}{V} \times (P_p + P_{aux}) \right]' \\ \|f'_4(x)\| = \min(f'_4(x)) = \max(-l)' = \max \left[ 100 \times \left( -\frac{P_{ch} - (P_p + P_{aux})}{P_{ch}} \right) \right]' \end{array} \right. \quad (3.17)$$

Consequently, as shown in table 3.30, the weighted sum calculation has been made with randomly assigned yet preference-based weights for all 7 scenarios implemented in the previous section.

**Table 3.30: Weighted Sum Approach results for all 7 charging scenarios**

	Scen. 1	Scen. 2	Scen. 3	Scen. 4	Scen. 5	Scen. 6	Scen. 7
$w_1$	0.25	0.3	0.2	0.2	0.3	0.2	0.3
$w_2$	0.25	0.2	0.3	0.3	0.3	0.2	0.2
$w_3$	0.25	0.3	0.2	0.3	0.2	0.3	0.2
$w_4$	0.25	0.2	0.3	0.2	0.2	0.3	0.3
<b>Max F(X)</b>	<b>0.65</b>	<b>0.5</b>	<b>0.94</b>	<b>1.16</b>	<b>0.12</b>	<b>0.33</b>	<b>0.22</b>

As a recapitulation of the weighted sum approach calculations, the resulting values for the objective functions and their weighted sum in each optimization scenario are exposed in table 3.31.

**Table 3.31: MOGA/Weighted sum approach calculation results**

	Scen. 1	Scen. 2	Scen. 3	Scen. 4	Scen. 5	Scen. 6	Scen. 7	Reference Value
$f_1 = SoC$ (%)	80.13	80.13	20	20	51.58	83.67	79.96	90
$f_2 = E_{valley}$ (kWh)	77.4	19.35	77.4	77.4	48.23	15.9	18	87.75
$f_3 = E_p$ (kWh)	232.108	232.108	200	232.108	232.108	204	200	236
$f_4 = l$ (%)	2.34	10.73	2.34	2.33	10.7	0.4	12.56	0.1
Max $F(X)$	0.65	0.5	0.94	1.16	0.12	0.33	0.22	Average 0.56

In order to define a final value for  $\max F(X)$  based on the predefined weights already set for each objective function, the average of all  $\max F_i(X)$  of the discussed case studies is calculated:

- i. Average  $\max F_i(X)$  of the non-conflictual fitness functions:

Non-conflicting fitness functions:  $[SoC(t), E_p]$ ,  $[E_{valley}, l]$ ,  $[E_{valley}, E_p]$

→ case studies 1, 2, 3:

$$avg(\max F_{i,nc}(X)) = \frac{\max F_1(X) + \max F_2(X) + \max F_3(X)}{3} = \frac{0.5 + 0.94 + 1.16}{3}$$

$$\rightarrow \text{avg} (\max F_{i,nc}(X)) = 0.87$$

ii. Average  $\max F_i(X)$  of the conflictual fitness functions:

Conflicting fitness functions:  $[SoC(t), E_{valley}]$ ,  $[E_p, l]$ ,  $[SoC(t), l]$

$\rightarrow$  case studies 4, 5, 6:

$$\text{avg} (\max F_{i,c}(X)) = \frac{\max F_4(X) + \max F_5(X) + \max F_6(X)}{3} = \frac{0.12 + 0.33 + 0.22}{3}$$

$$\rightarrow \text{avg} (\max F_{i,c}(X)) = 0.22$$

iii. Average  $\max F_i(X)$  of all fitness functions combinations:

$$\text{Max } F(X) = \text{avg} (\max F_{i,nc}(X), \max F_{i,c}(X)) = \frac{\text{avg} [\max F_{i,nc}(X)] + \text{avg} [\max F_{i,c}(X)]}{2}$$

$$\text{Max } F(X) = \frac{0.87 + 0.22}{2} = 0.55$$

### 3.5 Computation and Verification

The charging multi-objective optimization has been computed and implemented in *gamultiobj* solver of Matlab software (Fig. 3.1).

The image shows a screenshot of the 'Problem Setup and Results' dialog box for the *gamultiobj* solver. The solver is set to 'gamultiobj - Multiobjective optimization using Genetic Algorithm'. The fitness function is '@fitnessFunc' and the number of variables is 5. Constraints include linear inequalities (A and b), linear equalities (Aeq and beq), and bounds (Lower: [0,90,92,90,2] and Upper: [100,120,130,110,8]). The nonlinear constraint function is '@constraintFunc'.

Figure 3.1: *gamultiobj* solver settings

Starting with an initial population of 12 chromosomes, with a Pareto-front population fraction of 1, the Pareto-front is computed as follows in table 3.32.

**Table 3.32: Weighted Sum Approach results for all 7 charging scenarios**

Index	f1=SoC	f2=Evalley	f3=Ep	f4=l	x1=t	x2=Pval	x3=Pch	x4=Pp	x5=Paux
1	88.6817	87.75	232.269	0.163273	1.948199	104.8289	116.3246	108.7535	7.381116
2	74.155	87.75	232.963	0.1	12.05094	105.3266	116.5075	109.055	7.426596
3	90	87.75	219.701	0.1	0.792465	95.1589	109.8533	104.6092	5.241439
4	70.1851	87.75	233.025	0.1	15.19053	105.8568	116.558	109.0615	7.451187
5	84.7241	87.75	232.75	0.1	4.808887	104.9737	116.3804	108.9671	7.408025
6	88.6848	87.75	231.61	0.20609	1.717537	104.5598	116.0444	108.5169	7.288336
7	88.7178	87.75	225.602	0.293766	1.47959	103.7253	113.1335	105.8537	6.947444
8	87.364	87.75	232.246	0.147049	2.51556	104.7541	116.2939	108.9089	7.213983
9	80.7596	87.75	232.931	0.1	7.351804	105.3266	116.4753	109.0525	7.412821
10	90	87.75	230.519	0.348301	0.987736	104.5001	115.6622	108.1295	7.129817
11	70.1851	87.75	233.025	0.1	15.19053	105.8568	116.558	109.0615	7.451187
12	74.155	87.75	232.963	0.1	12.05097	105.3266	116.5076	109.055	7.426665

In order to generate a unique solution (the fittest), the Pareto-front fraction is set to 1/12 with an initial population of 12 chromosomes. The solution with the first Pareto rank is then computed and given in table 3.33:

**Table 3.33: Optimized solution with an initial population of 12 chromosomes and a fraction of 1/12**

Index	f1=SoC	f2=Evalley	f3=Ep	f4=l	x1=t	x2=Pval	x3=Pch	x4=Pp	x5=Paux
1	90	87.75	186.134	0.1	0.963051	94.78714	93.08849	90.39052	2.676681

Noting that some of the fitness functions depend from the same variables, they don't seem to reach the reference values all at the same time.

Then the computation has then been expanded to start with an initial population of 50 chromosomes as given in table 3.34.

**Table 3.34: Pareto-front computed with an initial population of 50 chromosomes**



Index	f1=SoC	f2=Evalley	f3=Ep	f4=l	x1=t	x2=Pval	x3=Pch	x4=Pp	x5=Paux
1	88.729	87.75	223.82	0.20648	1.12962	102.368	112.14	105.5205	6.3884
2	88.705	87.75	228.03	0.22907	1.18833	101.223	114.277	107.5384	6.4773
3	90	87.75	216.09	0.1	0.9966	101.186	108.119	102.2288	5.8183
4	81.952	87.75	235.87	0.35745	6.06959	111.368	118.357	109.9704	7.964
5	75.272	87.75	235.99	0.12089	11.5802	111.177	118.137	109.9977	7.9965
6	88.759	87.75	218.65	0.16093	1.0395	101.675	109.502	103.5046	5.8214
7	90	87.75	226.81	0.47117	0.98509	102.011	113.944	106.3804	7.027
8	79.29	87.75	235.98	0.11347	8.39057	111.033	118.126	109.9974	7.9945
9	88.664	87.75	235	0.30549	1.22293	103.921	117.862	109.6314	7.8709
10	76.468	87.75	236	1.17138	10.9455	111.01	119.397	109.9996	7.9987
11	81.927	87.75	235.99	0.61531	6.90673	110.81	118.727	109.9992	7.9974
12	87.439	87.75	225.42	0.22691	2.02783	103.526	112.965	106.818	5.8911
13	90	87.75	235.1	2.20872	0.5467	106.405	120.204	109.6054	7.9441
14	83.274	87.75	235.99	0.58116	5.9589	111.11	118.685	109.9985	7.9973
15	76.573	87.75	236	0.40375	10.5533	111.01	118.477	109.9995	7.9986
16	90	87.75	235.74	2.2809	0.7212	111.483	120.621	109.8754	7.9941
17	85.933	87.75	235.99	1.35524	3.36446	110.165	119.616	109.998	7.9974
18	87.296	87.75	235.98	1.10698	2.88578	109.344	119.312	109.9953	7.9964
19	88.694	87.75	229.39	0.49878	1.74823	104.633	115.27	108.2524	6.4426
20	77.948	87.75	235.99	0.13325	9.10691	111.132	118.153	109.9982	7.9977
21	73.759	87.75	236	1.18932	12.3718	110.989	119.419	109.9996	7.9987
22	88.694	87.75	228.99	0.65475	1.03767	107.609	115.25	108.1493	6.3462
23	77.814	87.75	236	1.23194	9.71884	111.244	119.47	109.9996	7.9987
24	90	87.75	233.5	0.73127	0.72293	103.921	117.612	109.1314	7.6209
25	85.937	87.75	235.99	1.25599	3.25165	109.807	119.494	109.9972	7.9959
26	81.89	87.75	236	1.06326	6.98633	111.002	119.266	109.9994	7.9987
27	84.579	87.75	235.99	1.32402	4.94289	110.456	119.58	109.9991	7.998
28	76.439	87.75	236	1.38481	10.4655	111.028	119.655	109.9997	7.9987
29	80.446	87.75	236	2.02144	7.42232	110.978	120.433	109.9997	7.9987
30	85.974	87.75	235.98	0.36731	3.32237	109.651	118.424	109.9937	7.995
31	88.744	87.75	221.52	0.1	1.04784	101.461	110.822	104.679	6.0795
32	88.639	87.75	235.91	1.74654	1.69522	110.605	120.05	109.9562	7.9974
33	81.827	87.75	236	1.81964	6.94694	110.955	120.185	109.9996	7.9987
34	88.639	87.75	235.91	1.74654	1.69522	110.605	120.05	109.9562	7.9974
35	88.729	87.75	223.82	0.20648	1.12962	102.368	112.14	105.5205	6.3884
36	87.326	87.75	235.49	0.18268	2.01123	107.083	117.961	109.963	7.783
37	79.137	87.75	236	1.51808	8.81932	111.187	119.817	109.9997	7.9987
38	84.619	87.75	235.99	0.58833	4.1991	110.467	118.693	109.9992	7.9955
39	81.914	87.75	236	0.76881	6.51423	111.076	118.912	109.9994	7.9982
40	83.202	87.75	236	1.64663	5.63171	111.159	119.973	109.9993	7.9986
41	77.784	87.75	236	1.47849	9.22591	111.323	119.769	109.9997	7.9987
42	87.306	87.75	235.98	0.71588	2.90329	109.644	118.841	109.9945	7.9959
43	90	87.75	216.09	0.1	0.9966	101.186	108.119	102.2288	5.8183
44	88.646	87.75	235.51	1.46269	1.94438	110.533	119.503	109.8433	7.9117
45	80.468	87.75	236	1.79675	7.73977	111.158	120.157	109.9996	7.9987
46	83.23	87.75	235.99	1.23943	5.86515	110.943	119.478	109.9992	7.9983
47	81.895	87.75	236	1.00174	6.218	111.005	119.192	109.9993	7.9986
48	79.071	87.75	236	2.11205	8.56247	111.033	120.544	109.9997	7.9987
49	88.664	87.75	235.18	0.23588	1.22684	103.921	117.866	109.6939	7.8944
50	73.859	87.75	236	0.5783	12.3244	111.024	118.685	109.9996	7.9986

It is to be reminded that the constraint  $P_{ch} > P_p + P_{aux}$  is crucial for the vehicle to circulate, and the optimization would not be possible in case the charging power does not exceed the sum of the propulsive and auxiliary powers. Consequently, the computation through gamultiobj solver has been programmed in a way to return the imposed value “-1” whenever this constraint is not applicable.

Therefore, in some cases, depending on the initial population adopted by the solver, the value  $f_4 = l = -1$  is returned whenever  $P_{ch} < P_p + P_{aux}$ . The corresponding rows would be then deleted as the vehicle would not be able to circulate if its propulsive and auxiliary powers surpass its charging power.

For example, for a random population of 25 combinations of chromosomes resulting in -1 values for  $f_4$  (see table 3.35).

**Table 3.35: Pareto-front computed with an initial population of 25 chromosomes**

Index	f1=SoC	f2=Evalley	f3=Ep	f4=l	x1=t	x2=Pval	x3=Pch	x4=Pp	x5=Paux
1	88.676	87.75	233.64	-1	1.33868	97.4429	116.82	108.896	7.92556
2	90	87.75	227.27	-1	0.97733	96.1756	113.635	106.374	7.26165
3	88.665	87.75	235.64	0.1	1.73725	98.1467	117.829	109.869	7.95049
4	88.676	87.75	233.65	-1	1.33087	97.4498	116.827	108.902	7.92556
5	88.662	87.75	235.98	0.1	1.99347	98.5792	118.052	109.993	7.99864
6	88.666	87.75	235.46	0.1	1.87348	98.5331	117.738	109.757	7.97498
7	88.671	87.75	234.52	0.1	1.56012	97.8905	117.263	109.315	7.94233
8	85.987	87.75	236	0.1	3.00539	98.596	118.039	110	7.99991
9	88.67	87.75	234.7	0.1	1.6989	97.9275	117.36	109.416	7.93494
10	90	87.75	234.12	0.1	0.974	97.6771	117.061	109.112	7.94769
11	88.672	87.75	234.34	0.1	1.63243	97.9044	117.199	109.235	7.9368
12	87.327	87.75	235.9	-1	2.75722	98.3867	117.948	109.981	7.96811
13	88.676	87.75	233.64	-1	1.33868	97.4429	116.82	108.896	7.92556
14	88.667	87.75	235.14	0.1	1.84769	98.0235	117.598	109.594	7.97443
15	88.664	87.75	235.8	0.1	1.8264	98.3273	117.912	109.936	7.96206
16	88.666	87.75	235.49	0.1	1.76053	98.1648	117.747	109.795	7.95116
17	85.987	87.75	236	0.1	3.00539	98.596	118.039	110	7.99991
18	87.324	87.75	236	0.1	2.98539	98.6173	118.04	110	7.99985
19	88.668	87.75	235	0.1	1.74648	97.9594	117.548	109.534	7.96754
20	88.673	87.75	234.19	0.1	1.73435	97.923	117.111	109.16	7.93579
21	88.671	87.75	234.54	0.1	1.65578	97.8932	117.303	109.332	7.93835
22	90	87.75	227.27	-1	0.97733	96.1756	113.635	106.374	7.26165
23	87.327	87.75	235.9	-1	2.75722	98.3867	117.948	109.981	7.96811
24	88.666	87.75	235.33	0.1	1.86738	98.2509	117.728	109.708	7.95525
25	88.669	87.75	234.88	0.1	1.73982	97.9673	117.45	109.484	7.95431

Noting that in this specific example, the ranks 1, 2, 4, 12, 13, 22 and 23 result in a value  $f4 = -1$ , the values for these ranks would be deleted, and the remaining ranks would be:  $25 - 7 = 18$ .

Consequently, once the ranks where  $P_{ch} < P_p + P_{aux}$  are deleted, the resulting Pareto-front computed by Matlab is exposed in table 3.36:

**Table 3.36: Pareto-front with the ranks where  $P_{ch} < P_p + P_{aux}$  deleted**

Index	f1=SoC	f2=Evalley	f3=Ep	f4=l	x1=t	x2=Pval	x3=Pch	x4=Pp	x5=Paux
1	88.665	87.75	235.64	0.1	1.7373	98.1467	117.829	109.869	7.950489
2	88.662	87.75	235.98	0.1	1.9935	98.5792	118.052	109.993	7.99864
3	88.666	87.75	235.46	0.1	1.8735	98.5331	117.738	109.757	7.974978
4	88.671	87.75	234.52	0.1	1.5601	97.8905	117.263	109.315	7.94233
5	85.987	87.75	236	0.1	3.0054	98.596	118.039	110	7.999912
6	88.67	87.75	234.7	0.1	1.6989	97.9275	117.36	109.416	7.934942
7	90	87.75	234.12	0.1	0.974	97.6771	117.061	109.112	7.947691
8	88.672	87.75	234.34	0.1	1.6324	97.9044	117.199	109.235	7.936802
9	88.667	87.75	235.14	0.1	1.8477	98.0235	117.598	109.594	7.974428
10	88.664	87.75	235.8	0.1	1.8264	98.3273	117.912	109.936	7.962059
11	88.666	87.75	235.49	0.1	1.7605	98.1648	117.747	109.795	7.951159
12	85.987	87.75	236	0.1	3.0054	98.596	118.039	110	7.999912
13	87.324	87.75	236	0.1	2.9854	98.6173	118.04	110	7.999846
14	88.668	87.75	235	0.1	1.7465	97.9594	117.548	109.534	7.967542
15	88.673	87.75	234.19	0.1	1.7344	97.923	117.111	109.16	7.935793
16	88.671	87.75	234.54	0.1	1.6558	97.8932	117.303	109.332	7.938351
17	88.666	87.75	235.33	0.1	1.8674	98.2509	117.728	109.708	7.955254
18	88.669	87.75	234.88	0.1	1.7398	97.9673	117.45	109.484	7.954313

After running the MATLAB gamultiobj solver with an initial population of 50 chromosomes, but with a Pareto front population fraction of 1/50, the solution with the first Pareto rank is computed, and a unique (the fittest) solution would be generated in table 3.37:

**Table 3.37: Optimized solution with an initial population of 50 chromosomes and a fraction of 1/50**

Index	f1=SoC	f2=Evalley	f3=Ep	f4=l	x1=t	x2=Pval	x3=Pch	x4=Pp	x5=Paux
1	88.9573333	87.75	184	0.1	1.4416425	90	92	90	2

After running the MATLAB gamultiobj solver with an initial population of 250 combinations of chromosomes, the fittest solution would be (table 3.38).

**Table 3.38: Optimized solution with an initial population of 250 chromosomes and a fraction of 1/250**

Index	f1=SoC	f2=E <sub>valley</sub>	f3=E <sub>p</sub>	f4=l	x1=t	x2=P <sub>val</sub>	x3=P <sub>ch</sub>	x4=P <sub>p</sub>	x5=P <sub>aux</sub>
1	88.6625	87.75	236	0.1	1.96817	103.957	118.01	110	8

It is to be noted that no matter how large the initial population would be, the fittest solution is very close to the reference values for each of the objective functions, and the more iterations are performed, the closer solutions to the reference values are reached.

Referring to the simulation results of the studied multi-objective optimization, the optimized Pareto-front tends to converge towards the defined reference values that are the maximal values for SoC,  $E_{valley}$  and  $E_p$ , and the minimal value for the losses. However, as some of the objective functions seem to be conflicting and dependent from the same variables, they might not reach their optimized values at the same time since the optimized common variable for an objective function might not be the fittest value for another. Noting that the optimization of our objectives is conflicting, the optimum of an objective would set a specific value for its parameters that would lead to a non-optimized value of another objective.

### 3.6 Conclusion

A multi-objective optimization for the energy flows G2V, H2V and B2V between the grid, home or building and electric vehicles based on the supply and demand of electricity has been performed. The multi-objective genetic algorithm has been developed in order to acquire the Pareto-optimal solutions for the developed system aiming to find the maximal state of charge, valley energy, propulsive energy and minimal losses that could be reached by EVs during their charging phase. As some of the obtained optimized solutions are conflicting, a compromise is applied in order to define quasi-optimal solutions that are the closest to the optimal ones. Thus, it is crucial to define the decision maker's priority for specific conflicting fitness functions over the others and this is why it has been referred to the weighted sum approach.

So, once the Pareto-front of the defined fitness functions has been set, the weighted sum approach has been applied in order to define the optimized solutions based on the decision maker's preference as some of the fitness functions seemed to be conflicting.

The calculated optimized solutions contributed by the application of the multi-objective genetic approach seem to converge towards the theoretical optimum of each of the defined fitness functions.

The results have been computed and the simulation of the optimization through the gamultiobj solver of Matlab showed a convergence towards the defined optimal reference values. In fact, the bigger the population, the closer the convergence towards the theoretical optimums would be. Besides, as the battery's state-of-charge and losses both depend on the same variable, their optimization imposes the interference of the prioritization of one objective over the other as they could not reach their optimized values at the same time. Thus, the weighted sum approach was implemented according to random weights based on the decision maker's priorities. The Pareto-front obtained by simulation obviously verifies the genetic algorithm calculation proving that the obtained solutions are very close to the theoretical values theoretically optimized.

## **Chapter 4 - Energy retrieval multi-objective optimization**

4.1	Introduction.....	119
4.2	Multi-Objective Optimization for discharging.....	119
4.2.1	Objectives definition and modeling .....	120
4.2.2	Multi-objective optimization – Genetic Algorithm.....	123
4.2.2.1	Objective 1: Optimization of the state-of-charge .....	123
4.2.2.2	Objective 2: Optimization of the discharging time .....	127
4.2.2.3	Objective 3: Optimization of the battery life .....	130
4.2.2.4	Objective 4: Optimization of the losses .....	132
4.3	Optimization Scenarios .....	134
4.4	Weighted Sum Approach .....	136
4.5	Computation and Verification.....	138
4.6	Conclusion .....	140

## **4.1 Introduction**

As previously stated, the electric vehicles' batteries can be referred to as means of energy storage and retrieval. The energy storage and charging process of the vehicles have been extensively discussed in chapter 3. Actually, the charging and discharging of vehicles can both be scheduled depending on the electricity demand and supply. Thus, whenever there's a lack of supply compared to the electricity demand, the discharging of vehicles would be launched, and then, the exceeding energy stored in the batteries could be, besides the vehicles' personal use, retrieved back to the grid or to supply houses. The restitution generally occurs whenever the demand exceeds the electricity supply. In this case, the energy retrieval process takes into account the sufficient amount of energy that would be kept in the battery for the vehicles' personal needs and planned trips. To do so, the energy retrieval is proposed through a multi-objective optimization of the flow of energy leaving the vehicles during their discharging process.

For this end, following the same procedure as the energy storage of chapter 3, this chapter first defines the restitution's multi-objective discharging optimization model while expressing the objective functions and various constraints. Similarly to the charging process, the optimization approach adopted to calculate the fitness functions' optimized solutions is the genetic algorithm. Successively, combining the obtained solutions into a final optimized one necessitates the normalization of the studied fitness functions, and the adoption of the weighted sum approach with weights assigned randomly based on the decision maker's priorities. Lastly, the optimization is verified and validated through a Matlab simulation using the gamultiobj solver.

## **4.2 Multi-Objective Optimization for discharging**

At the phase when the energy production falls short of its consumption, the regulation algorithm takes in charge triggering the retrieval of energy from the vehicles' batteries in order to compensate the lack of production, thus discharging the fleets. It would be interesting then to optimize the energy flows related to this retrieval. Consequently, a multi-objective optimization is operated in the discharging mode, with a heuristic identification of the optimized solution for



specific discharging objectives. The optimization model for discharging is defined by equation (3.1).

The optimization is performed using the genetic algorithm approach where each function's Pareto-front is indicated. For this energy retrieval process, we follow the same steps as in the storage process.

#### 4.2.1 Objectives definition and modeling

In order to optimize the energy retrieval process, several objectives have been defined and modeled during the vehicle's discharging stage. The study mainly seeks the following objectives:

i. Minimization of the vehicle's SoC in order to harness the largest possible amount of the batteries' energy, taking into account the amount of energy that should be retained from restitution for the vehicle's personal trips and needs. Hence, the vehicle's state-of-charge must not decrease beyond the energy needed for the next planned trip of the vehicle. Thus, the energetic requirements related to the vehicle's personal trips are defined by the decision maker and/or the vehicle's owner during discharging phase. Then, the remaining energy available in the vehicle's battery would be discharged and driven back to supply the grid or houses. The discharging batteries' SoC is depicted by the following model:

$$f_1 = SoC(t) = SoC(t - 1) - \eta_d \frac{P_d}{E_b} \quad (4.1)$$

whereas  $E_b$ ,  $\eta_d$  and  $P_d$  consecutively represent the batteries' nominal capacity, discharging efficiency and discharging power [96], [115], [116].

ii. Minimization of the vehicle's discharging time, so that the available energy gets restituted as soon as the consumption exceeds the production. To this end, the charging process would mostly happen during night time. Yet, once the electric demand surpasses the supply, the vehicle's owner would benefit the most from the financial incentives set if the discharging process does not take too long to fulfill the restitution requirements of the grid. The vehicle's discharging time  $t_d$  is modeled as follows:

$$f_2 = t_d = \frac{E_b}{I_d} \quad (4.2)$$

whereas  $I_d$  is the discharging current of the battery [117].

iii. Maximization of the battery life of the vehicle and battery cycles' control.

Actually, the battery life can be expressed using the formula:

$$f_3 = L_b = n_c \times DoD \times E_b \quad (4.3)$$

whereas  $n_c$  and DoD represent the battery's number of cycles and Depth of Discharge respectively. It is to be mentioned that the batteries' lifespan progressively decreases as its number of cycles increases and would significantly vary based on the temperature and charging/discharging usage conditions.

Based on the NiMH batteries adopted in this study (defined in chapter 2) and their technical specifications:  $n_c$  approximately equals to 2000 cycles under recommended charge/discharge conditions for NiMH Panasonic BK1100HFU batteries.

As the DoD for NiMH batteries ranges between 80 % and 100 % (table 1.3), and the lower and upper boundaries for the SoC being set at 10 % and 90 %. The maximal DoD referred to in this study will be of 80 %.

Therefore, the life of our unused vehicle's battery would be:

$$L_b = n_c \times DoD \times E_b = 2000 \times 0.8 \times 75 = 120000 \text{ Ah.}$$

$L_b = n_c \times DoD \times E_b$  Thus, the battery's life cycle ends when its nominal capacity decreases to 80% of its original value. Nevertheless, the owner might not immediately notice this capacity drop as his vehicle might acquire less than 80 % of the nominal capacity at times. Consequently, as the nominal capacity decreases, the discharging time  $t_d$  also decreases. Hence, the vehicle's battery discharges faster as the number of cycles is closer to the end [118].

However, it is to be mentioned that the discharging time should be minimized at optimized conditions without affecting the battery's life cycle or performance.

iv. Minimization of the vehicle's losses involving the instantaneous power going in to the vehicle and departing out of it. These losses can be calculated using the formula:

$$f_4 = l = 100 \times \frac{|(P_p + P_{aux}) - P_d|}{P_p + P_{aux}} \quad (4.4)$$

whereas  $P_p$  and  $P_{aux}$  respectively identify the propulsive power of the vehicle and its auxiliary power resulting from the usage of on-board auxiliary electric accessories (such as air conditioning, heating, windshield wipers, radio, headlights, seat heaters, etc.) [105], [103], [104].

Eventually, the losses are embodied by the ratio of the difference between the power incoming to the vehicle  $P_p+P_{aux}$  and the power leaving it  $P_d$ , over the incoming power  $P_p+P_{aux}$ . Yet, as the outgoing power might exceed the incoming depending on the functional accessories, the speed and the energy available within the vehicle, the losses equation's numerator has been set in absolute value so that the value for the losses would be positive anyway [119], [120].

Ultimately, the electric vehicle's efficiency and performance do not get affected by the different state-of-charge levels, but another perspective of losses reduction to be taken into consideration during the vehicle's charging process would be the power converter's losses that might significantly decrease the charger's efficiency [121].

It is to be noted that the calculations related to the vehicle's energy consumption are made, based on the average values related to the variation of weather conditions, road loads, and acceleration-deceleration profiles.

Consequently, the optimization system's model can be summarized as follows:

- $f_i$  (for  $i = 1, 2, 3, 4$ ) are objective functions:

$$\begin{cases} f_1(SoC(t-1), P_d) = SoC(t) = SoC(t-1) - \eta_d \frac{P_d}{E_b} \\ f_2(I_d) = t_d = \frac{E_b}{I_d} \\ f_3(n_c, DoD) = L_b = n_c \times DoD \times E_b \\ f_4(P_p + P_{aux}, P_d) = l = 100 \times \frac{|(P_p+P_{aux})-P_d|}{P_p+P_{aux}} \end{cases} \quad (4.5)$$

The constraint related to the discharging optimization particularly involves the SoC's lower limit  $SoC_{min}$  where the SoC should get minimized considering both its own trips' usage and its technical specifications boundaries beyond which the battery would get damaged [101].

- $g_1$  is the constraint function:

$$\{g_1 \rightarrow SoC \geq SoC_{min} + y \quad (4.6)$$

with  $SoC_{min}$  and  $y$  representing the minimal allowable value for SoC that would not deteriorate the batteries' specifications, and the amount of energy related to the vehicle's personal trips respectively.

#### 4.2.2 *Multi-objective optimization – Genetic Algorithm*

The energy flows optimization has been performed using the multi-objective genetic algorithm GA approach in order to define the optimized solution for each of the pre-defined objectives, therefore ensuring an optimized restitution of energy from the vehicle towards the houses (or grid) [96].

As explained in chapter 3, the genetic algorithm approach is an evolutionary procedure based on extracting the fittest and most optimized generation out of a wide population of chromosomes. Eventually, starting with a randomly selected population of chromosomes, several successor population generations of child chromosomes are extracted through an iterative recombination and fitness improvement evolving into an optimized solution [106]. So, this algorithm has been used in order to find the fittest solution to each one of the instigated objective functions [120].

Following the same procedure adopted for the charging mode, the optimization of each one of the predefined objectives has been made using the genetic algorithm approach. It involves the extraction of the fittest Pareto-front out of a large chromosomes population that gets reduced iteratively through the recombination of generations and their fitness improvement [96], [106], [120].

##### 4.2.2.1 *Objective 1: Optimization of the state-of-charge*

The first objective that should be optimized is the vehicle's state-of-charge, expressed by the following equation:

$$f_1(SoC(t-1), P_d) = SoC(t) = SoC(t-1) - \eta_d \frac{P_d}{E_b} \quad (4.7)$$

In order to optimize the first objective related to the vehicle's SoC (represented in equation (4.1)) using the genetic algorithm method, the battery capacity  $E_b$  has been fixed at 75 Ah based on the vehicle's datasheet. Besides, the vehicle's depth of discharge DoD has also been fixed at

80 %. The constraint on this objective function would be setting boundaries for the SoC not to surpass, particularly, a lower limit that would respect the battery's DoD also keeping a predefined amount of energy within the vehicle's battery for the electric vehicle's personal needs.

Therefore, the DoD is assumed to be 80 % in this study; hence, SoC would range between 10 % and 90 %, and  $SoC_{min}$  being set at 10 %. The constraint to respect is given by, for each  $t > 0$ :

$$SoC(t) \geq SoC_{min} + y \quad (4.8)$$

$SoC \geq SoC_{min} + y$  whereas  $y$  identifies the amount of energy to be kept in the vehicle's battery for its personal needs, and  $SoC_{min}$  represents the minimum allowable state-of-charge that could be reached without affecting the batteries specifications and performance that would lead into its deterioration.

As the optimization aims to minimize the value of  $f_1 = SoC(t)$ , and noting that the applied multi-objective genetic algorithm GA is heuristic providing approximate values that are the closest possible to the optimal solution,  $SoC(t) = 10\%$  is adopted as the minimal reference value that the optimization aims to reach. Therefore, the GA aims to get the closest possible value to 10 %.

The battery's charging and discharging efficiency for different types of batteries is specified in the below table 4.1 [122], [123], [124], [125]:

**Table 4.1: Batteries' charging and discharging efficiency**

Batteries' efficiency	
Li-ion	80 % - 90 %
Lead-Acid	50 % - 92 %
NiMH	66 % - 92 %
Ni-Cd	70 % - 90 %

As NiMH batteries' efficiency is set between 66 % and 92 %, the value adopted in this study is 85 % for  $\eta_d$ . The ranges for SoC and  $P_d$  are assumed as follows  $10\% \leq SoC(t) \leq 90\%$  and  $0 kW \leq P_d \leq 130 kW$ .

The decision variables for this objective being  $SoC(t - 1)$  and  $P_d$ , the genetic chromosome defined for this first optimization has been set at  $[SoC(t - 1), P_d]$ , and the genetic algorithm has been initialized with a population of 12 chromosomes presented in table 4.2.

**Table 4.2: Initial population of 12 chromosomes**

<b><math>SoC(t - 1)</math> (%)</b>	<b>11.5</b>	<b>12.9</b>	<b>15</b>	<b>19</b>	<b>24</b>	<b>32</b>	49	64	78	81	87	90
<b><math>P_d</math> (kW)</b>	<b>130</b>	<b>128</b>	<b>123</b>	<b>119</b>	<b>110</b>	<b>106</b>	94	76	64	37	21	2
<b><math>SoC(t)</math> (%)</b>	<b>10.03</b>	<b>11.45</b>	<b>13.6</b>	<b>17.65</b>	<b>22.75</b>	<b>30.8</b>	47.93	63.1	77.2	80.6	86.8	89.9
<b>Rank</b>	<b>1</b>	<b>2</b>	<b>3</b>	<b>4</b>	<b>5</b>	<b>6</b>	7	8	9	10	11	12

The population of 12 is reduced to 6 chromosomes through a selection of the fittest values at a rate of 50 %. The survival population after a 50 % selection rate involves the chromosomes

$$\text{with ranks } 1 \rightarrow 6: \begin{cases} chr_1 = [11.5, 130] \\ chr_2 = [12.9, 128] \\ chr_3 = [15, 123] \\ chr_4 = [19, 119] \\ chr_5 = [24, 110] \\ chr_6 = [32, 106] \end{cases}$$

As previously proceeded in section 3.2.2, Haupt's method is referred to, so that the 6 chromosomes are replaced with 6 new offsprings generated by 3 parent matings [126].

So, 6 child chromosomes are generated by the mating of each 2 of the survival population's chromosomes based on Haupt's method [6] where each parent chromosome  $[m, f]$  would create

$$2 \text{ offsprings } os_1 \text{ and } os_2 \text{ as follows: } \begin{cases} os_1 = [(1 - M) \times x_m + M \times x_f, y_m] \\ os_2 = [(1 - M) \times x_f + M \times x_m, y_f] \end{cases} \quad (4.9)$$

whereas  $M$  is the mutation rate assumed as 0.35.

The offsprings generated by chromosomes matings are presented in the table 4.3, and the fitness function and ranks related to the calculated offsprings are exhibited in table 4.4:

**Table 4.3: Matings and offsprings generation**

	<b>First mating</b> $chr_1 = [11.5, 130]$ & $chr_4 = [19, 119]$	<b>Second mating</b> $chr_2 = [12.9, 128]$ & $chr_5 = [24, 110]$	<b>Third mating</b> $chr_3 = [15, 123]$ & $chr_6 = [32, 106]$
<b>Offspring 1</b>	[14.3, 130]	[16.79, 128]	[20.95, 123]
<b>Offspring 2</b>	[16.38, 119]	[20.12, 110]	[26.05, 106]

**Table 4.4: Six new generated offsprings as a result of chromosomes matings**

<i>SoC</i> ( <i>t</i> - 1) (%)	14.13	16.38	16.79	20.12	20.95	26.05
<i>P<sub>d</sub></i> (kW)	130	119	128	110	123	106
<i>SoC</i> ( <i>t</i> ) (%)	12.66	15.03	15.34	18.87	19.56	24.85
<i>Rank</i>	1	2	3	4	5	6

By omitting the two least fit chromosomes, the population gets then reduced to 4 chromosomes instead of 6. Crossing again the chromosomes into 2 new matings, and omitting the lowest ranks (table 4.5):

**Table 4.5: Generation of 4 offsprings through the surviving population**

	<b>First mating</b> <i>chr</i> <sub>1</sub> = [14.3, 130] & <i>chr</i> <sub>3</sub> = [16.79, 128]	<b>Second mating</b> <i>chr</i> <sub>2</sub> = [16.38, 119] & <i>chr</i> <sub>4</sub> = [20.12, 110]
<b>Offspring 1</b>	[15.06, 130]	[17.69, 119]
<b>Offspring 2</b>	[15.86, 128]	[18.81, 110]

The two lowest ranks being eliminated, the survival population would be (table 4.6):

$$\begin{cases} chr_1 = [15.06, 130] \\ chr_2 = [15.86, 128] \end{cases}$$

**Table 4.6: New surviving population of 4 chromosomes**

<i>SoC</i> ( <i>t</i> - 1) (%)	15.06	15.86	17.69	18.81
<i>P<sub>d</sub></i> (kW)	130	128	119	110
<i>SoC</i> ( <i>t</i> ) (%)	13.59	14.4	16.34	17.56
<i>Rank</i>	1	2	3	4

If we suppose that *chr*<sub>1</sub> = [15.06, 130], and *chr*<sub>2</sub> = [15.86, 128] are a pair of parent chromosomes, the generated offsprings would be (table 4.7):  $\begin{cases} offspring\ 1 = [15.47, 130] \\ offspring\ 2 = [15.58, 128] \end{cases}$

**Table 4.7: The fittest two chromosomes of the population**

	<i>SoC</i> ( <i>t</i> - 1)	<i>P<sub>d</sub></i>	<i>SoC</i> ( <i>t</i> )
<b>1</b>	15.47	130	13.99
2	15.58	128	14.13

Consequently, the optimized solution reached for the  $SoC$  minimization is:

$$\left. \begin{array}{l} P_d = 130 \text{ kW} \\ SoC(t - 1) = 15.47 \% \end{array} \right\} \rightarrow SoC(t) = 13.99 \% \quad (4.10)$$

The optimized value of  $SoC(t)$  calculated using the GA approach consists of  $SoC_{min}$  that is the lower boundary of the state-of-charge. Yet, the optimized value of  $SoC_{min}$  being defined, the constraint function would require summing up the optimized  $SoC_{min}$  to the amount of energy  $y$  linked with the vehicle's planned trips that the owners must define. Hence,  $y$  is to be implemented by the vehicle's owner/user in order to assess the percentage of  $SoC$  to be kept in the vehicle's battery during the discharging process. Particularly, the owner defines the distance (in kilometers) that his vehicle still needs to travel, and  $y$  would then be concluded referring to the vehicle's autonomy and battery's depth of discharge. Knowing the distance related to the vehicle's personal needs, and assuming that the vehicle's average velocity would be constant,  $y$  could be calculated. For instance, if a vehicle with 100 km autonomy and a depth of discharge of 80 % needs to travel a round-trip distance of 20 km, the value of  $y$  would be 16 % of the battery's  $SoC$ . A margin of 7 % is added to the optimized value in order to take into consideration different types of roads (roughness and slopes) and any acceleration or deceleration in the trip. The optimized solution for  $f_1 = SoC(t)f_1$  would then be:

$$SoC_{opt}(t) + y + 7 = 13.99 + 16 + 7 = 36.99 \% . SoC_{opt}(t) + y + 7\% = 13.99 + 16 + 7 = 36.99\%$$

#### 4.2.2.2 Objective 2: Optimization of the discharging time

The second objective to be optimized during the discharging process is the discharging time, embodied by the following expression:

$$f_2(I_d) = t_d = \frac{E_b}{I_d} \quad (4.11)$$

In order to minimize the vehicle's discharging time  $t_d$  represented in equation 4.11, the same GA procedure has been carried out with  $E_b$  fixed at 75 Ah and the GA chromosome defined as  $[I_d, E_b]$  (as this objective's decision variables are  $I_d$  and  $E_b$ ) while  $0 < I_d < 125 A$ , and an initial population of 12 randomly picked chromosomes (table 4.8).



**Table 4.8: Initial population of 12 chromosomes**

$I_d$ (A)	5	10	16	25	32	44	<b>63</b>	<b>75</b>	<b>100</b>	<b>112</b>	<b>121</b>	<b>125</b>
$E_b$ (Ah)	75	75	75	75	75	75	<b>75</b>	<b>75</b>	<b>75</b>	<b>75</b>	<b>75</b>	<b>75</b>
$t_d$ (hr)	15	7.5	4.69	3	2.34	1.7	<b>1.2</b>	<b>1</b>	<b>0.75</b>	<b>0.67</b>	<b>0.62</b>	<b>0.6</b>
<b>Rank</b>	12	11	10	9	8	7	<b>6</b>	<b>5</b>	<b>4</b>	<b>3</b>	<b>2</b>	<b>1</b>

The 50 % rate surviving population would then be composed of the fittest chromosomes ranking from 1 till 6:

$$\text{Chromosomes with ranks } 1 \rightarrow 6: \begin{cases} chr_1 = [125, 75] \\ chr_2 = [121, 75] \\ chr_3 = [112, 75] \\ chr_4 = [100, 75] \\ chr_5 = [75, 75] \\ chr_6 = [63, 75] \end{cases}$$

Referring to Haupt's method previously explained where several offsprings are generated out of the chromosomes' matings (table 4.9):

**Table 4.9: Matings and offsprings generation**

	<b>First mating</b> $chr_1 = [125, 75]$ & $chr_4 = [100, 75]$	<b>Second mating</b> $chr_2 = [121, 75]$ & $chr_5 = [75, 75]$	<b>Third mating</b> $chr_3 = [112, 75]$ & $chr_6 = [63, 75]$
<b>Offspring 1</b>	[116.25, 75]	[104.9, 75]	[94.85, 75]
<b>Offspring 2</b>	[108.75, 75]	[91.1, 75]	[80.15, 75]

The two lowest ranks being eliminated, the survival population would be (table 4.10):

$$\text{Chromosomes with ranks } 1 \rightarrow 4: \begin{cases} chr_1 = [116.25, 75] \\ chr_2 = [108.75, 75] \\ chr_3 = [104.9, 75] \\ chr_4 = [91.1, 75] \end{cases}$$

**Table 4.10: Six new generated offsprings as a result of the matings**

$I_d$ (A)	<b>116.25</b>	<b>108.75</b>	<b>104.9</b>	<b>91.1</b>	94.85	80.15
$E_b$ (Ah)	75	75	75	75	75	75
$t_d$ (hr)	<b>0.64</b>	<b>0.69</b>	<b>0.71</b>	<b>0.82</b>	0.79	0.94
<b>Rank</b>	<b>1</b>	<b>3</b>	<b>2</b>	<b>4</b>	5	6

The matings created using the surviving population would contribute into four new offsprings (table 4.11).

**Table 4.11: Generation of four offsprings through the surviving population**

	<b>First mating</b> $chr_1 = [116.25, 75]$ & $chr_3 = [104.9, 75]$	<b>Second mating</b> $chr_2 = [108.75, 75]$ & $chr_4 = [94.85, 75]$
<b>Offspring 1</b>	[112.28, 75]	[103.89, 75]
<b>Offspring 2</b>	[108.87, 75]	[99.7, 75]

**Table 4.12: New surviving population of 4 chromosomes**

$I_d$ (A)	<b>112.28</b>	<b>108.87</b>	103.89	99.7
$E_b$ (Ah)	<b>75</b>	<b>75</b>	75	75
$t_d$ (hr)	<b>0.67</b>	<b>0.69</b>	0.72	0.75
<b>Rank</b>	<b>1</b>	<b>2</b>	3	4

The two lowest ranks being eliminated, the survival population would be (table 4.12):

$$\begin{cases} chr_1 = [112.28, 75] \\ chr_2 = [108.87, 75] \end{cases}$$

If we suppose that  $chr_1 = [112.28, 75]$ , and  $chr_2 = [108.87, 75]$  are a pair of parent chromosomes, the generated offsprings would be (table 4.13):  $\begin{cases} offspring\ 1 = [111.09, 75] \\ offspring\ 2 = [110.06, 75] \end{cases}$

**Table 4.13: The fittest two chromosomes of the population**

	$I_d$	$E_b$	Fitness function: $t_d$ (h)
<b>1</b>	<b>111.09</b>	<b>75</b>	<b>0.675h = 40 min 30 sec</b>
2	110.06	75	0.68h = 40 min 48 sec

The elimination of the two lowest ranks for two consecutive generations would contribute to the optimized solution for the vehicle's discharging time  $f_2 = t_d$  (for a complete discharge cycle of 80 %):

$$\left. \begin{matrix} I_d = 111.09\ A \\ E_b = 75\ Ah \end{matrix} \right\} \rightarrow t_d = 0.675\ h = 40\ min\ 30\ sec$$

#### 4.2.2.3 Objective 3: Optimization of the battery life

The third objective of the study concerns the maximization of the battery life. In order to do so, the genetic algorithm is executed on the fitness function shown in equation (4.12).

$$f_3(n_c, DoD) = L_b = n_c \times DoD \times E_b \quad (4.12)$$

The decision variables for  $f_3$  are  $n_c$  and DoD and the defined chromosome for the battery life is  $[n_c, DoD]$  ranging as per  $0 \leq n_c \leq 2000$  and  $0\% \leq DoD \leq 80\%$ . Noting that the discharging optimization seeks to maximize the battery life value, and as the adopted GA approach is heuristic and would provide approximate solutions to the most optimized  $L_{b_{ref}}$ , the theoretical maximal value of  $L_b$ , is considered as the reference that the optimization aims to reach:

$$L_{b_{ref}} = (n_c \times DoD \times E_b)_{max} = 2000 \times \frac{80}{100} \times 75 = 120000 \text{ Ah.}$$

Similarly to the previous calculations, the GA initial population of 12 chromosomes is randomly chosen, then reduced to the 6 fittest chromosomes with the best rankings (table 4.14):

**Table 4.14: Initial population of 12 chromosomes**

$n_c$	2000	1970	1940	1900	1810	1730	1420	1030	660	350	114	63
$DoD$	80	78	74	70	67	61	53	42	24	12	7	1
$L_b$ (Ah)	1200	1152	1076	9975	9095	7914	5644	3244	118	315	614.	47.25
	00	45	70	0	2.5	7.5	5	5	80	0	25	
<b>Ran</b> <b>k</b>	1	2	3	4	5	6	7	8	9	10	11	12

The 50 % selection rate surviving population would then be (tables 4.15 & 4.16):

$$\text{Chromosomes with ranks } 1 \rightarrow 6: \begin{cases} chr_1 = [2000, 80] \\ chr_2 = [1970, 78] \\ chr_3 = [1940, 74] \\ chr_4 = [1900, 70] \\ chr_5 = [1810, 67] \\ chr_6 = [1730, 61] \end{cases}$$

**Table 4.15: Matings and offsprings generation**

	<b>First mating</b> $chr_1 = [2000, 80]$ & $chr_4 = [1900, 70]$	<b>Second mating</b> $chr_2 = [1970, 78]$ & $chr_5 = [1810, 67]$	<b>Third mating</b> $chr_3 = [1940, 74]$ & $chr_6 = [1730, 61]$
<b>Offspring 1</b>	[1965, 80]	[1914, 78]	[1866.5, 74]
<b>Offspring 2</b>	[1935, 70]	[1866, 67]	[1803.5, 61]

**Table 4.16: Six generated offsprings as a result of chromosomes matings**

$n_c$	1965	1935	1914	1866	1866.5	1803.5
<b>DoD (%)</b>	80	70	78	67	74	61
<b><math>L_b</math> (Ah)</b>	117900	101587.5	111969	93766.5	103590.75	82510
<b>Rank</b>	1	4	2	5	3	6

The two lowest ranks being eliminated, the survival population would be (table 4.17):

$$\text{Chromosomes with ranks } 1 \rightarrow 4: \begin{cases} chr_1 = [1965, 80] \\ chr_2 = [1914, 78] \\ chr_3 = [1866.5, 74] \\ chr_4 = [1935, 70] \end{cases}$$

**Table 4.17: Generation of four offsprings through the surviving population**

	<b>First mating</b> $chr_1 = [1965, 80]$ & $chr_3 = [1866.5, 74]$	<b>Second mating</b> $chr_2 = [1914, 78]$ & $chr_4 = [1935, 70]$
<b>Offspring 1</b>	[1930.35, 80]	[1921.35, 78]
<b>Offspring 2</b>	[1900.975, 74]	[1927.65, 70]

The two lowest ranks being eliminated, the survival population would be (table 4.18):

$$\begin{cases} chr_1 = [1930.35, 80] \\ chr_2 = [1921.35, 78] \end{cases}$$

**Table 4.18: New surviving population of four chromosomes**

$n_c$	1930.35	1900.975	1921.35	1927.65
<b>DoD (%)</b>	80	74	78	70
<b><math>L_b</math> (Ah)</b>	115821	105504	112399	101201.6
<b>Rank</b>	1	2	3	4

If we suppose that  $chr_1 = [1930.35, 80]$ , and  $chr_2 = [1921.35, 78]$  are a pair of parent chromosomes, the generated chromosomes would be (table 4.19):  $\left. \begin{array}{l} \text{offspring 1} = [1927.2, 80] \\ \text{offspring 2} = [1924.5, 78] \end{array} \right\}$

**Table 4.19: The fittest two chromosomes of the population**

	$n_c$	$DoD$	Fitness function: $L_b$
<b>1</b>	<b>1927.2</b>	<b>80</b>	<b>115632</b>
2	1924.5	78	112583.25

Hence, the optimized solution for  $f_3(n_c, DoD) = L_b$  is:  $\left. \begin{array}{l} n_c = 1927.2 \text{ cycles} \\ DoD = 80 \% \end{array} \right\} \rightarrow L_b = 115632 \text{ Ah}$

#### 4.2.2.4 Objective 4: Optimization of the losses

The vehicle's losses are the fourth objective function to be minimized. They are expressed in the following equation:

$$f_4(P_p + P_{aux}, P_d) = l = 100 \times \frac{|(P_p + P_{aux}) - P_d|}{P_p + P_{aux}} \quad (4.13)$$

As for the fourth objective function concerning the vehicle's losses to be minimized that is exposed in equation 4.13, the GA method is then applied with chromosomes set at  $[P_p + P_{aux}, P_d]$  ( $P_p + P_{aux}$  and  $P_d$  being the decision variables) with a random population initially defined with 12 chromosomes (table 4.20). The variables ranges are defined as per the following:

$$\left. \begin{array}{l} 90 \text{ kW} < P_p \leq 110 \text{ kW} \\ 2 \text{ kW} < P_{aux} \leq 8 \text{ kW} \end{array} \right\} \rightarrow 92 \text{ kW} < P_p + P_{aux} \leq 118 \text{ kW} \text{ and } 0 \text{ kW} < P_d \leq 130 \text{ kW}.$$

The calculation of the theoretical minimum for  $l$  would lead to the value 0.1% that will be considered as the reference value for the optimization.

**Table 4.20: Initial population of 12 chromosomes**

$P_p + P_{aux}$	92	92.2	92.7	94	96	98	102	107	111	113	116	118
$P_d$	91.9	92	92.8	93.3	95.4	98.8	10	50	107	114	119	128
$l$	0.1	0.22	0.1	0.74	0.63	0.82	90	53	3.6	0.88	2.6	8.47
<b>Rank</b>	<b>1</b>	<b>3</b>	<b>1</b>	<b>5</b>	<b>4</b>	<b>6</b>	7	8	9	10	11	12

Survival population after a 50% selection rate (tables 4.21 & 4.22):

$$\text{Chromosomes with ranks } 1 \rightarrow 6: \begin{cases} chr_1 = [92, 91.9] \\ chr_2 = [92.7, 92.8] \\ chr_3 = [92.2, 92] \\ chr_4 = [96, 95.4] \\ chr_5 = [94, 93.3] \\ chr_6 = [98, 98.8] \end{cases}$$

**Table 4.21: Matings and offsprings generation**

	<b>First mating</b> $chr_1 = [92, 91.9]$ & $chr_4 = [96, 95.4]$	<b>Second mating</b> $chr_2 = [92.7, 92.8]$ & $chr_5 = [94, 93.3]$	<b>Third mating</b> $chr_3 = [92.2, 92]$ & $chr_6 = [98, 98.8]$
<b>Offspring 1</b>	[93.4, 91.9]	[93.16, 92.8]	[94.23, 92]
<b>Offspring 2</b>	[94.6, 95.4]	[93.55, 93.3]	[95.97, 98.8]

**Table 4.22: Six generated offsprings as a result of chromosomes matings**

<b><math>P_p + P_{aux}</math></b>	93.4	94.6	93.16	93.55	94.23	95.97
<b><math>P_d</math></b>	91.9	95.4	92.8	93.3	92	98.8
<b><math>l</math></b>	1.6	0.85	0.39	0.27	2.37	2.9
<b>Rank</b>	4	3	2	1	5	6

The two lowest ranks being eliminated, the survival population would be (table 4.23):

$$\text{Chromosomes with ranks } 1 \rightarrow 4: \begin{cases} chr_1 = [93.55, 93.3] \\ chr_2 = [93.16, 92.8] \\ chr_3 = [94.6, 95.4] \\ chr_4 = [93.4, 91.9] \end{cases}$$

**Table 4.23: Generation of four offsprings through the surviving population**

	<b>First mating</b> $chr_1 = [93.55, 93.3]$ & $chr_3 = [94.6, 95.4]$	<b>Second mating</b> $chr_2 = [93.16, 92.8]$ & $chr_4 = [93.4, 91.9]$
<b>Offspring 1</b>	[93.92, 93.3]	[93.24, 92.8]
<b>Offspring 2</b>	[94.23, 95.4]	[93.32, 91.9]

The two lowest ranks being eliminated, the survival population would be (table 4.24):

$$\begin{cases} chr_1 = [93.24, 92.8] \\ chr_2 = [93.92, 93.3] \end{cases}$$

**Table 4.24: New surviving population of four chromosomes**

$P_p + P_{aux}$	<b>93.92</b>	94.23	<b>93.24</b>	93.32
$P_d$	<b>93.3</b>	95.4	<b>92.8</b>	91.9
$l$	<b>0.66</b>	1.2	<b>0.47</b>	1.52
<b>Rank</b>	<b>2</b>	3	<b>1</b>	4

If we suppose that  $chr_1 = [93.24, 92.8]$ , and  $chr_2 = [93.92, 93.3]$  are a pair of parent chromosomes (table 4.25):

$$\begin{cases} offspring\ 1 = [93.48, 92.8] \\ offspring\ 2 = [93.68, 93.3] \end{cases}$$

**Table 4.25: The fittest two chromosomes of the population**

	$P_p + P_{aux}$	$P_d$	Fitness function: $l$
	93.48	92.8	0.72
	<b>93.68</b>	<b>93.3</b>	<b>0.4</b>

The resulting optimized solution after 2 generations where the lowest ranks would be omitted and a mating of the 2 remaining chromosomes:  $\left. \begin{matrix} P_p + P_{aux} = 93.68\ kW \\ P_d = 93.3\ kW \end{matrix} \right\} \rightarrow l = 0.4\ \%$ .

### 4.3 Optimization Scenarios

Similarly to the charging optimization's conflicting optimized solutions, as some objectives' models have the same parameters as other objective functions, the optimized solutions of the objectives cannot all be obtained at one time. Thus, in order to compromise the objective functions for an optimized solution of all four functions, the decision maker's preference has been taken into consideration through prioritizing some objectives over the others. As the objective functions  $f_1$  and  $f_4$  both depend from the same variable  $P_d$  that has different values for the optimized solutions of each of these functions, the most optimized solution would rely on the decision maker's prioritizing of one specific fitness function.

Consequently, several scenarios have been studied in order to highlight the optimized solution of all the objective functions taking into account the decision maker's priorities. The presented optimized solution involves the optimized State-of-Charge calculated for an amount of energy that is equivalent to consecutive round trip distances of 0 and 20 kilometers. It also includes the optimized values for the discharging time, battery life and losses.

Scenario 1: In this scenario, the optimized solutions are implemented irrespective from any conflictive parameters, as the decision maker does not have any preferences set for specific objective functions. The solution set would then be (table 4.26):

**Table 4.26: Optimized solution for Discharging Scenario 1**

$f_1 = SoC(t)$		$f_2 = t_d$	$f_3 = L_b$	$f_4 = l$
$y \rightarrow 0$ km	$y \rightarrow 20$ km			
13.99 %	36.99 %	0.675 h = 40 min 30 sec	115632 Ah	0.4 %

Scenario 2: In this scenario, the decision maker sets a priority for the optimization of the EV batteries' state-of-charge over the losses. The optimized solution in this case is as follows (table 4.27):

**Table 4.27: Optimized solution for Discharging Scenario 2**

$f_1 = SoC(t)$		$f_2 = t_d$	$f_3 = L_b$	$f_4 = l$
$y \rightarrow 0$ km	$y \rightarrow 20$ km			
13.99 %	36.99 %	0.675 h = 40 min 30 sec	115632 Ah	11.18 %

Scenario 3: Unlike the previous scenario, in this case, the decision maker prioritizes the losses over the SoC. Hence, the heuristic solution for the optimization would be (table 4.28):



**Table 4.28: Optimized solution for Discharging Scenario 3**

$f_1 = SoC(t)$		$f_2 = t_d$	$f_3 = L_b$	$f_4 = l$
$y \rightarrow 0$ km	$y \rightarrow 20$ km			
14.28 %	37.28 %	0.675 h = 40 min 30 sec	115632 Ah	0.4 %

Similarly to the storage process, and based on the set preference for specific objectives, the scenario's results shown in tables 4.27 and 4.28 allow a closer convergence of the prioritized objective functions towards the calculated values of their Pareto-front than in the case of table 4.26 where decision maker's preference is disregarded.

#### 4.4 Weighted Sum Approach

Having applied the genetic algorithm in all three studied scenarios, all fitness functions have been normalized and the weighted sum approach has been performed through the following equation according the randomly assigned weights in each optimization scenario:

$$\min F(X) = w_1 \times \|f'_1(x)\| + w_2 \times \|f'_2(x)\| + w_3 \times \|f'_3(x)\| + w_4 \times \|f'_4(x)\| \quad (4.14)$$

Besides, the normalization of the fitness functions would lead to the following equations:

$$\begin{cases} f'_1 = \frac{SoC-10}{80} \\ f'_2 = \frac{t_d-0.6}{749.4} \\ f'_3 = \frac{L_b}{120000} \\ f'_4 = \frac{l-0.1}{99.8} \end{cases} \quad (4.15)$$

$$\begin{cases} \|f'_1\| = \min(f'_1) = \min(SoC(t)') = \min\left(\frac{SoC-10}{80}\right) \\ \|f'_2\| = \min(f'_2) = \min(t_d)' = \min\left(\frac{t_d-0.6}{749.4}\right) \\ \|f'_3\| = \max(f'_3) = \min(-f'_3) = \min(-L_b)' = \min\left(-\frac{L_b}{120000}\right) \\ \|f'_4\| = \min(f'_4) = \min(l)' = \min\left(\frac{l-0.1}{99.8}\right) \end{cases} \quad (4.16)$$

where the symbol  $\|f\|$  represents the functions' optima.

For coherent calculations, equation (4.16) is brought to the functions' maxima:

$$\begin{cases} \|f'_1\| = \max(-f'_1) = \max\left(-\frac{SoC-10}{80}\right) \\ \|f'_2\| = \max(-f'_2) = \max\left(-\frac{t_d-0.6}{749.4}\right) \\ \|f'_3\| = \max(f'_3) = \max\left(\frac{L_b}{120000}\right) \\ \|f'_4\| = \max(-f'_4) = \max\left(-\frac{l-0.1}{99.8}\right) \end{cases} \quad (4.17)$$

Therefore, the weighted sum approach is executed and weights  $w_1, w_2, w_3, w_4$ , the sum of which is exactly equal to 1, are randomly assigned based on the decision maker's preference as in the studied optimization scenarios 1, 2, 3.

Thus, the weighted sum execution of all three scenarios has led to the following results (table 4.29):

**Table 4.29: Optimized Solution - initial population of 12 chromosomes**

	Scen. 1	Scen. 2	Scen. 3
$w_1$	0.25	0.3	0.2
$w_2$	0.25	0.25	0.25
$w_3$	0.25	0.25	0.25
$w_4$	0.25	0.2	0.3
<b>Max F(X)</b>	<b>0.15</b>	<b>0.12</b>	<b>0.17</b>

In order to define a final value for  $\max F(X)$  based on the predefined weights already set for each objective function, the average of  $\max F_i(X)$  of the discussed case studies is calculated (table 4.30):

$$\text{Max } F(X) = \text{avg}(\max F_i(X)) = \frac{\max F_1(X) + \max F_2(X) + \max F_3(X)}{3} = 0.15$$

As table 4.30 shows, the weighted sum approach of all three discussed scenarios results in relatively close values of the calculated single objective function using random weights chosen based on the previously defined scenarios preference.

**Table 4.30: MOGA/Weighted sum approach calculation results**

	Scen. 1	Scen. 2	Scen. 3	Reference Value
$f_1 = SoC_{/y=0 km}$ (%)	13.99	13.99	14.28	10
$f_1 = SoC_{/y=20 km}$ (%)	36.99	36.99	37.28	33
$f_2 = t_d$ (h)	0.675	0.675	0.675	0 <sup>+</sup>
$f_3 = L_b$ (Ah)	115632	115632	115632	120000
$f_4 = l$ (%)	0.4	11.18	0.4	0.1
Max $F(X)$	0.15	0.12	0.17	Average 0.15

#### 4.5 Computation and Verification

In order to verify the calculation results, the fitness functions related to the vehicle's discharging and retrieval of energy have been computed through the *gamultiobj* solver of Matlab (Fig. 3.1). The simulation of the genetic algorithm has been launched for several initial populations of different sizes. Particularly, the computation has been run starting with an initial population of 12 as calculated (table 4.32), and then the same process has been restarted with a population of 200 chromosomes (table 4.33).

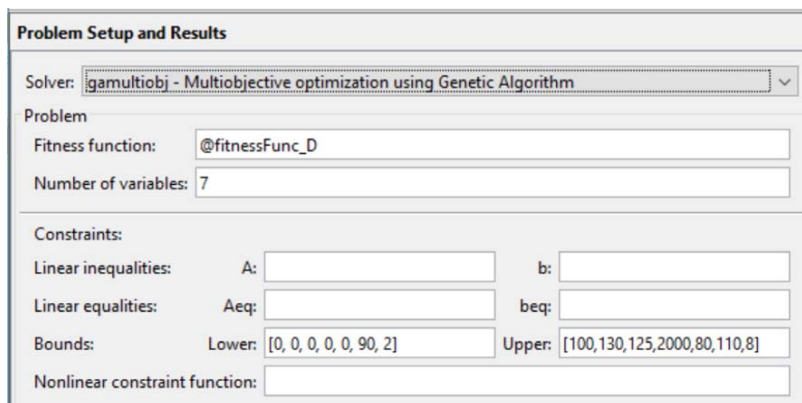


**Figure 4.1: gamultiobj solver discharging setting**

Using the settings shown in Fig. 4.1, the computation of the system's Pareto-front has led to the following optimized solution that is completely compliant to the calculations exhibited in section 4.2 (table 4.31):

**Table 4.31: Multi-objective optimization Pareto-front computation result**

Pareto front - function values and decision variables											
In...	f1	f2	f3	f4	x1	x2	x3	x4	x5	x6	x7
1	10	0.6	-120,0...	0.1	72.082	111.335	125	707.35	30.753	103.645	7.602

The computed optimized solution of table 4.31 is further clarified in table 4.32 where the signification of every variable and fitness function is exhibited with its exact computed value.

**Table 4.32: Optimized Solution - initial population of 12 chromosomes**

Optimized Solution	
f1 = SoC(t) (%)	10
f2 = Evalley (kWh)	0.600000000001047
f3 = Ep (kWh)	-120000
f4 = l (%)	0.1000000000000000
x1 = t (sec)	72.0824896780670
x2 = Pd (kW)	111.335337884925
x3 = Id (A)	124.999999999782
x4 = nc (cycles)	707.350012327776
x5 = DoD (%)	30.7533658615563
x6 = Pp (kW)	103.644711807971
x7 = Paux (kW)	7.60221201125857

**Table 4.33: Optimized Solution - initial population with 200 chromosomes**

Optimized Solution	
f1 = SoC(t) (%)	10
f2 = Evalley (kWh)	3.50676957642366
f3 = Ep (kWh)	-120000
f4 = l (%)	0.323708305908542
x1 = t (sec)	55.037783588448356
x2 = Pd (kW)	103.261495942000
x3 = Id (A)	21.3872050516898
x4 = nc (cycles)	873.529873478065
x5 = DoD (%)	54.3758630601104
x6 = Pp (kW)	100.134468559499
x7 = Paux (kW)	3.46237898265463

It is to be notified that the variable  $x_1$  represents the time  $t$  in seconds, which indirectly defines the fitness function  $f_1 = \text{SoC}(t)$ .

Besides, the computation of the fitness function  $L_b$  representing the battery life has been performed through the function's opposite  $-L_b$  as the genetic algorithm approach operates on the minimization of functions. Thus, as the maximization of  $L_b$  is aimed, the GA operation would be executed through the minimization of its opposite. Noting that the maximum of a function equals the exact opposite of the minimum of its opposite function:  $\max F(x) = \min (-F(x))$ .

Referring to the obtained Pareto-fronts of both populations, the wider initial population would generate a closer solution to the theoretical reference values.

#### 4.6 Conclusion

In this chapter, the energy retrieval from electric vehicles in order to supply the grid or homes whenever the electric demand exceeds the supply has been investigated. This energy retrieval process has been carried out using a multi-objective optimization algorithm. This aims

at minimizing the battery's state of charge, the vehicle's discharging time and losses, and to maximize the battery's lifetime. The optimization has been carried out using the genetic algorithm approach, and has then been verified with Matlab simulation through the gamultiobj solver. Consequently, the optimization has contributed into an effective optimized solution for all four fitness functions that would converge into the calculated theoretical optimum, while taking into account the vehicle's needs in energy that should not be retrieved from its battery.

Having followed the same procedure for both the charging and discharging processes, despite the difference in the objectives of each mode, it has been proven through calculations and simulation that the obtained optimized solutions converge towards their theoretical reference. However, as some objectives depend from the same parameters, the intervention of compromises and priorities has been proven crucial for a final combination of optimums.

The originality of the work done in chapters 3 and 4 lays in the use of GA approach for vehicles' charging and discharging optimizations and the validation of its results with a Matlab simulation.

Moreover, having assessed both the charging and discharging optimizations, it is now possible to create an energetic strategy linked to the behavior of a fleet of vehicles during their charging and discharging processes depending on the demand and supply of electricity. To do so, a control algorithm will be developed in chapter 5 to ensure a balanced regulation of the energy flow between EVs and infrastructures (homes and grid) according to the electricity supply and demand.

## **Chapter 5 - Control and regulation of energy flows based on electricity supply and demand**

5.1	Introduction.....	144
5.2	Control and regulation algorithm.....	144
5.2.1	Energy Storage – Production exceeding consumption.....	148
5.2.2	Energy retrieval – Consumption exceeding production.....	150
5.2.3	Equilibrium state of the system.....	151
5.3	Validation and Simulation of the control algorithm .....	152
5.3.1	Assigned input data.....	152
5.3.2	Output and Results.....	153
5.3.3	Discussion.....	156
5.4	Improved regulation through the optimization of number of vehicles.....	156
5.4.1	Assigned input data.....	157
5.4.2	Output and Results.....	159
5.4.3	Discussion.....	161
5.5	Conclusion .....	165



## **5.1 Introduction**

The difference margin between energy consumption and production would contribute into a huge energy waste. Indeed, the excessive production would be discarded at times while the deficient production results in expensive compensations of the consumption, whence the need for an energy regulation. In order to control the flows of energy circulating between a renewable energy supplied domestic residence, electric vehicles and the grid, and aiming to attain a balanced system, an optimization and regulation algorithm has been developed. Particularly, this algorithm manipulates the vehicles' charging and discharging processes depending on the energy production and consumption, thus the electricity demand and supply. Mostly, as mentioned in chapter 2 of this study, the considered system consists of a domestic household with an average consumption of 31.1 kWh daily, which would be either partially or entirely compensated by the energy produced by a HAWT horizontal axis wind turbine of a 2.8 kW power and 33 mono-crystalline photovoltaic modules of 280 W<sub>p</sub> of rated power under standard conditions. Another component of the studied system would be a fleet of electric vehicles (EV) used not only for its personal energetic needs, but also as energy storage and retrieval means. Each EV is equipped with Nickel Metal Hydride on-board batteries (NiMH) of a depth of discharge of 80 % and a 75 Ah capacity, thus a substantial storage capacity. The electric grid also interferes in the system to fulfil the energetic needs or recover the excess of energy when the rest of the system's components are not enough for the balance inquiry between the energy production and consumption.

## **5.2 Control and regulation algorithm**

The developed heuristic algorithm aims to define whether there is an excess or lack of energy through weighing and comparing the production and consumption.

Accordingly the algorithm proceeds the launching of the vehicle's charging or discharging processes so that the system's energetic needs are fulfilled and its equilibrium is reached. Once the system gets balanced, the margin of difference between the electricity demand and its supply would then be tightened. In order to tighten the margin of difference between the supply and demand of electricity, the heuristic algorithm for control and



For more clarification, the pseudo-code of this regulation algorithm is stated as follows:

```
-----  
global production consumption SoCMax vehicles SoCOnePercent SoCMin y  
chargingUnits dischargingUnits done  
  
if production == consumption  
    disp('System in balance');  
    done = true;  
    return  
elseif production > consumption  
    if differenceBetweenSoCMaxAndSoC >= 5*SoCOnePercent  
        vehicles(x) = vehicles(x) + 5*SoCOnePercent;  
        production = production - 5*SoCOnePercent;  
        consumption = consumption + 5*SoCOnePercent;  
        chargingUnits = chargingUnits + 5*SoCOnePercent;  
    elseif differenceBetweenSoCMaxAndSoC > 0  
        vehicles(x) = vehicles(x) + differenceBetweenSoCMaxAndSoC;  
        production = production - differenceBetweenSoCMaxAndSoC;  
        consumption = consumption + differenceBetweenSoCMaxAndSoC;  
        chargingUnits = chargingUnits + differenceBetweenSoCMaxAndSoC;  
    else  
        x = x + 1;  
        break;  
    end  
    disp('Charging...');  
    if vehicles(x) == SoCMax  
        x = x + 1;  
        break;  
    end  
    disp('Charged fleet - Supply the grid');  
    done = true;  
    return  
elseif production < consumption  
    while x <= numberOfVehicles
```

```

if differenceBetweenSoCMinAndSoC >= 5*SoCOnePercent
    vehicles(x) = vehicles(x);
    production = production + 5*SoCOnePercent;
    discharginUnits = discharginUnits + 5*SoCOnePercent;
elseif differenceBetweenSoCMinAndSoC > 0
    vehicles(x) = vehicles(x) - differenceBetweenSoCMinAndSoC;
    production = production + differenceBetweenSoCMinAndSoC;
    discharginUnits = discharginUnits +
differenceBetweenSoCMinAndSoC;
else
    x = x + 1;
    break;
end
disp('Discharging...');
if vehicles(x) == SoCMin + y
    x = x + 1;
    break;
end
end
disp('Discharged fleet - Retrieve energy from the grid');
return
end

```

-----

The regulation process operates as follows. As a first step, the algorithm collects the data input related to the energy production and consumption, as well as the vehicles' State-of-Charge SoC and the percentage of energy to be kept in the batteries during discharge for the fleet's personal needs. Then it operates a comparison between the production and consumption values. The variable  $x$  ( $x > 0$ ) embodied in the algorithm's organizational chart represents the vehicles to be charged and/or discharged, consecutively, one by one. Mostly, the energy production results from the supply of the installed renewable energy sources, and the consumption is that of the household appliances, and the vehicles' personal needs. Generally, this algorithm evolves into 3 cases corresponding to the 3 blocks of the organizational chart (Fig. 5.1):

### 5.2.1 Energy Storage – Production exceeding consumption

If the production exceeds the consumption, the algorithm launches the vehicles' charging process. In this case, as the charging process starts, the excess of energy is stored within the vehicles' batteries. Thus, as soon as there's an excess of production, the charging process of the electric vehicles intended for energy storage is launched progressively. In this case, the system is embodied by the following equation:

$$E_p(PV + WT) > E_c(H + EV) \quad (5.1)$$

Whereas  $E_p(PV + WT)$  characterizes the energy produced by the photovoltaic panels and the wind turbine, and  $E_c(H + EV)$  represents the energy consumed by the home and vehicle.

Referring to the global energetic model of the system exposed in chapter 2- section 2.4, the equation (5.1) can be illustrated as follows:

$$N_{H_j,PV} \times P_{f,PV} \times k + \frac{0.01328 \times D^2 \times v^3}{365.25} > \sum_{home\ appliances} N_{H_j} \times P_f + \frac{A}{V} [F_p V + P_{aux}] \quad (5.2)$$

whereas  $N_{H_j,PV}$  and  $P_{f,PV}$  represent the daily number of hours of use of the photovoltaic panels, and their operating power,  $k$  is a correction factor ( $k = 1.3$ ),  $D$  is the wind turbine's rotor diameter and  $v$  is the annual average wind speed. On the other hand,  $N_{H_j}$  is the daily number of hours of use of the functional home appliances, and  $P_f$  is their operating power.

It is to be mentioned that the home appliances refer to any functional household appliances such as those related to heating, ventilation, cooking, lighting, washing, drying, refrigerator, audiovisual and electronics.

Once the State-of-Charge SoC of the charging vehicle reaches its allowed maximum (above which the nominal characteristics of the battery might get deteriorated or damaged and its life cycle gets shortened), the charging switches to the next vehicle of the fleet.

So, as long as the vehicles are charging, a new production/consumption comparison is assessed every 5 % SoC increase in order to make a decision concerning whether to proceed in the vehicles' charging or to switch to another cycle where the consumption would beat the production.

Actually when the charging vehicle needs more than 5% of SoC to reach its maximum value  $SoC_{max}$ , the state-of-charge increases of 5%, while the production decreases of the amount of energy equivalent to 5 % of SoC and the consumption increases of the same amount.

The equations of SoC, P and C would be in this case:

$$\begin{cases} SoC = SoC + 5 \% \\ P = P + \Delta P - 5 * P_{1\%} \\ C = C + \Delta C + 5 * C_{1\%} \end{cases} \quad (5.3)$$

whereas P, C,  $\Delta P$ ,  $\Delta C$ ,  $P_{1\%}$  and  $C_{1\%}$  respectively represent the energy production and consumption, their consecutive variations and the amount of energy of the production and consumption equivalent to 1 % of SoC.

A new comparison between the production and consumption is operated after each 5 % variation.

Similarly, when the  $SoC_{max}$  exceeds the charging vehicle's SoC of less than 5 %, the equations (5.3) would become:

$$\begin{cases} SoC = SoC_{max} \\ P = P + \Delta P - P_{SoC_{max}-SoC} \\ C = C + \Delta C + C_{SoC_{max}-SoC} \end{cases} \quad (5.4)$$

whereas  $P_{SoC_{max}-SoC}$  and  $C_{SoC_{max}-SoC}$  represent the energy of the production and the consumption that is equivalent to the percentage of  $SoC_{max} - SoC$ .

However, once all the fleet's vehicles are charged, and in case the production still tops the consumption, the excessive energy would then be injected into the grid for beneficial incentives, economic regulations and financial purposes.

The charging process would stop anytime the consumption value reaches the production or tops it to switch to another cycle.

### 5.2.2 Energy retrieval – Consumption exceeding production

If the energy consumption surpasses its production, the discharging process starts. In fact, when the supply of photovoltaic panels and the wind turbine are not being able to fulfill all the household's needs, the lack of energy would then be covered by the energy already stored within the fleet's batteries. Consequently, the discharging of the vehicles specifically intended for storage and retrieval is launched. The model of the discharging phase would then be presented as follows:

$$E_p(PV + WT + EV) < E_c(H) \quad (5.5)$$

whereas  $E_p(PV + WT + EV)$  embodies the energy produced by the photovoltaic panels, the wind turbine and the electric vehicle; and  $E_c(H)$  exhibits the energy consumed by the house.

The global energetic model assessment shows that equation (5.5) can be detailed as follows:

$$N_{Hj,PV} \times P_{f,PV} \times k + \frac{0.01328 \times D^2 \times v^3}{365.25} + E_0 \times d < \sum_{home\ appliances} N_{Hj} \times P_f \quad (5.6)$$

During this phase, the vehicles would be discharging progressively, one by one, until reaching their minimal SoC, where a certain amount of energy, represented by the variable  $y$ , remains in their batteries for their personal planned trips.

Moreover, during discharging process, the algorithm keeps repeating the production and consumption comparison with intervals of 5 % SoC drop, in order to stop the discharging or switch again to the first case when needed.

Eventually, when the discharging vehicle's SoC exceeds the sum of the minimal State-of-Charge  $SoC_{min}$  and the amount of energy  $y$  to be kept for personal trips by more than 5 %, the algorithm decreases the actual SoC of 5 %.

The production also increases of the equivalent of 5 % in energy while the consumption value remains the same. The equations of SoC, P and C would be characterized by the following:

$$\begin{cases} SoC = SoC - 5\% \\ P = P + \Delta P + 5 * P_{1\%} \\ C = C + \Delta C \end{cases} \quad (5.7)$$

Yet, when the discharging vehicle's SoC exceeds  $(SoC_{min} + y)$  by less than 5 %, equations (5.7) would become:

$$\begin{cases} SoC = SoC_{min} + y \\ P = P + \Delta P + P_{SoC-(SoC_{min}+y)} \\ C = C + \Delta C \end{cases} \quad (5.8)$$

whereas  $P_{SoC-(SoC_{min}+y)}$  represents the amount of energy in kWh equivalent to the percentage value of  $SoC - (SoC_{min} + y)$  %.

Once all the fleet of vehicles is discharged and in case the stored energy would still not be enough to cover the lack of production, the insufficiency would then be insured by the electric grid.

### 5.2.3 *Equilibrium state of the system*

When the production and consumption values are equal, the system would be in a balance situation, and the algorithm does not take any action until a difference margin between both values occurs again.

Particularly, once the comparison between the production and consumption values is made, in case the energy production and consumption are equivalent, the balanced system is attained. On these terms, the system is in equilibrium and it functions normally without involving any energy storage or retrieval processes.

So, the energy produced by the photovoltaic panels and wind turbine would be congruent with the house consumption of appliances and electric vehicle's needs. The system equilibrium state is expressed by the following equation:

$$E_p(PV + WT) = E_c(H) \quad (5.9)$$

This energetic model would then be depicted as per the following equation:

$$N_{H_j,PV} \times P_{f,PV} \times k + \frac{0.01328 \times D^2 \times v^3}{365.25} = \sum_{\text{home appliances}} N_{H_j} \times P_f + E_0 \times d \quad (5.10)$$

whereas  $E_0$  is the energy linked to the on-board electric outlet, and  $d$  is the distance travelled by the vehicle.



Thus, generally, the regulation algorithm sets the adequate charging and discharging processes of the vehicles' fleet, and is responsible for triggering the convenient energy storage or retrieval mode.

### **5.3 Validation and Simulation of the control algorithm**

In order to confirm the relevancy of the proposed regulation algorithm, and consequently to tighten the margin of difference between the energy production and consumption, the algorithm has been implemented and verified through a simulation over Matlab software.

#### **5.3.1 Assigned input data**

Average data inputs of production, consumption and fleets' SoC have been set for a sample period of 31 days.

In order to define precise input values, and referring to the technical specification of the system's components, the energy production and consumption have been calculated based on realistic energy values defined by the photovoltaic panels and wind turbine, and exact household appliances' consumption. For instance, the first week (from 1<sup>st</sup> day to 7<sup>th</sup> day) has been set to be very sunny, yet very windy.

Therefore, as the number of sun exposure hours has been set between 9 and 12 hours, and the annual average wind speed ranging between 38.6 and 49.9 kilometers per hour, the corresponding production of photovoltaic panels and wind turbine have been summed up to calculate the energy production during this week. Similarly, having fixed the exact functional household appliances and the electric vehicle's consumption each day, the total energy consumption has been calculated. Successively, the second week (including days 8 through 14), has been set as very sunny, and hardly windy. As for the third week (days 15 to 21), it is windy but hardly sunny. The last 10 days (day 22 to 31) were hardly sunny or windy. The fleets' states-of-charge were randomly defined with a daily sample set of 3 to 6 vehicles per fleet. So, the defined data input are summarized in the table 5.1, where SoC, P, and C progressively represent the fleets' state-of-charge, the energy production and its consumption. As for  $\Delta P$  and  $\Delta C$ , they represent the consecutive daily variations of production and consumption (table 5.1). In this table, the color codes refer to:

Blue: Production > Consumption (charging process).

Green: Production < Consumption (discharging process).

Gray: Production = Consumption (equilibrium state).

**Table 5.1: Control and Regulation Algorithm's Input Data**

Day	SoC	Input Data			
		P	$\Delta P$	C	$\Delta C$
1	[11 28 46 53]	145.75	0	40.36	0
2	[19 23 27 74 33]	135.48	-10.27	38.7	3.95
3	[26 12 12 14 87]	122.2	-13.28	34.2	-4.5
4	[26 56 42 29]	122.39	0.19	9.8	-24.4
5	[16 26 16]	122.72	0.33	1.9	-7.9
6	[43 39 64]	134.39	11.67	30.51	28.61
7	[26 38 16 29 36 25]	136.69	2.3	40.1	9.59
8	[72 88 35 43 29]	81.64	-55.05	36.8	-3.3
9	[26 71 18 29 32 19]	64.77	-16.87	32.1	-4.7
10	[65 42 22 28 33 20]	61.37	-3.4	26.36	-5.74
11	[39 78 28 54 22]	82.22	20.85	21.9	-4.46
12	[81 23 17 12 69]	71.78	-10.44	5.2	-16.7
13	[17 76 83]	85.03	13.25	3.17	-2.03
14	[70 64 38 29 14]	77.8	-7.23	24.3	21.13
15	[17 32 43 14 82]	8.12	-69.68	18.7	-5.6
16	[73 52 21 38]	24.16	16.04	34.2	15.5
17	[47 32 16 79]	10.6	-13.56	23.3	-10.9
18	[90 89 29]	15.92	5.32	14.17	-9.13
19	[66 74 58 21]	20.79	4.87	11.5	-2.67
20	[90 63 87 32]	5.78	-15.01	7.3	-4.2
21	[81 19 36 45 66]	14.72	8.94	4.9	-2.4
22	[77 66 86 30]	1.87	-12.85	36.5	31.6
23	[44 35 14 23 68 88]	18.56	16.69	33.27	-3.23
24	[19 32 23 90 89]	4.69	-13.87	27.4	-5.87
25	[29 41 81 61]	11.54	6.85	21.6	-5.8
26	[88 36 61]	15.2	3.66	14	-7.6
27	[76 80 25 42]	21.5	6.3	12.1	-1.9
28	[26 43 90]	8.59	-12.91	8.9	-3.2
29	[90 67 30 25]	5.23	-3.36	5.2	-3.7
30	[65 89 86 78 49]	24.93	19.7	4.8	-0.4
31	[28 60 43]	13.72	-11.21	13.72	8.92

The daily calculation step involves the phase where there would be no significant variation in the production/consumption difference. Thus, in the defined input data sample, the assumption of just one variation a day is made as a schematic example to highlight, on a large scale, this variation and its impact on the production, the consumption and the vehicles' states-of-charge. Yet, practically, several variations may occur within each day.

### 5.3.2 *Output and Results*

Once the simulation has been performed and the regulation has been applied for the set input data, the output values of the corresponding production and consumption, as well as the charged and discharged energy quantities have been assessed as shown in the below table 5.2:

**Table 5.2: Control and Regulation Algorithm's Output Data**

Day	Output Data			
	P	C	Charging units	Discharging units
1	103.57	82.54	42.18	0
2	89.89	89.89	45.59	0
3	78.2	78.2	44	0
4	83.06	49.13	39.33	0
5	82.44	42.18	40.28	0
6	110.83	54.07	23.56	0
7	88.39	88.39	48.3	0
8	59.22	59.22	22.42	0
9	48.44	48.44	16.34	0
10	43.87	43.87	17.5	0
11	52.06	52.06	30.16	0
12	38.49	38.49	33.29	0
13	67.17	21.03	17.86	0
14	51.05	51.05	26.75	0
15	18.7	18.7	0	10.58
16	34.2	34.2	0	10.04
17	23.33	23.3	0	12.7
18	15.05	15.05	0.88	0
19	16.15	16.15	4.64	0
20	7.3	7.3	0	1.52
21	9.81	9.81	4.91	0
22	28.47	36.5	0	26.6
23	33.27	33.27	0	14.71
24	27.4	27.4	0	22.71
25	21.6	21.6	0	10.06
26	14.6	14.6	0.6	0
27	16.8	16.8	4.7	0
28	8.9	8.9	0	0.31
29	5.21	5.21	0.01	0
30	14.87	14.87	10.07	0
31	13.72	13.72	0	0

Furthermore, the plotted curves of the production and consumption inputs and outputs as well as the vehicles' SoC are displayed in the following figures and graphs (Fig. 5.2, 5.3).

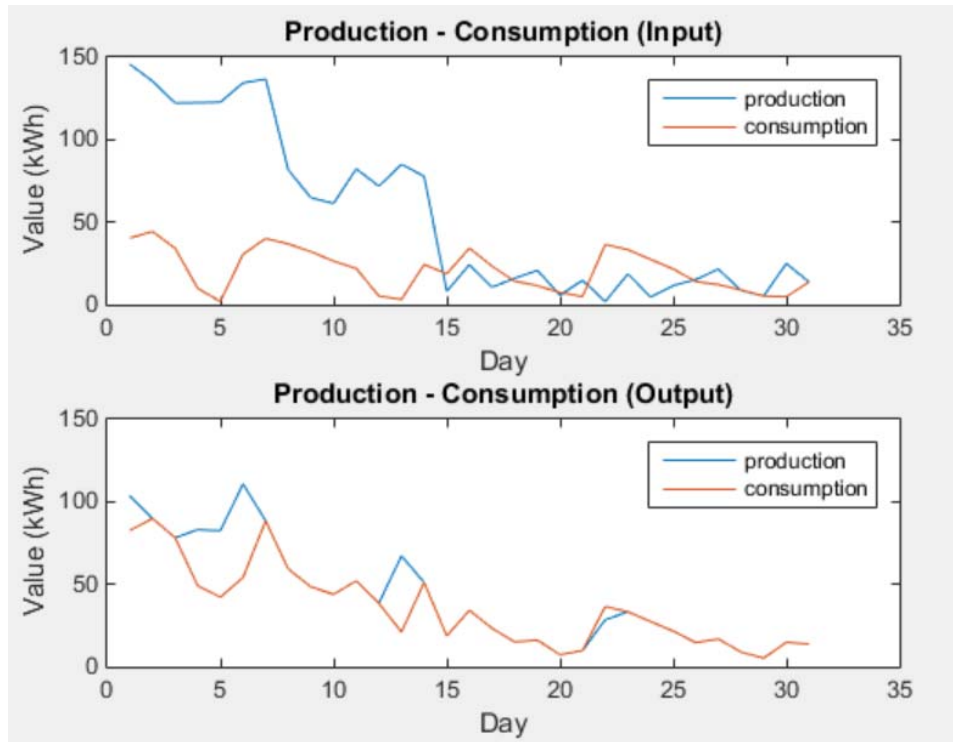


Figure 5.2: Input and Output Production and Consumption curves

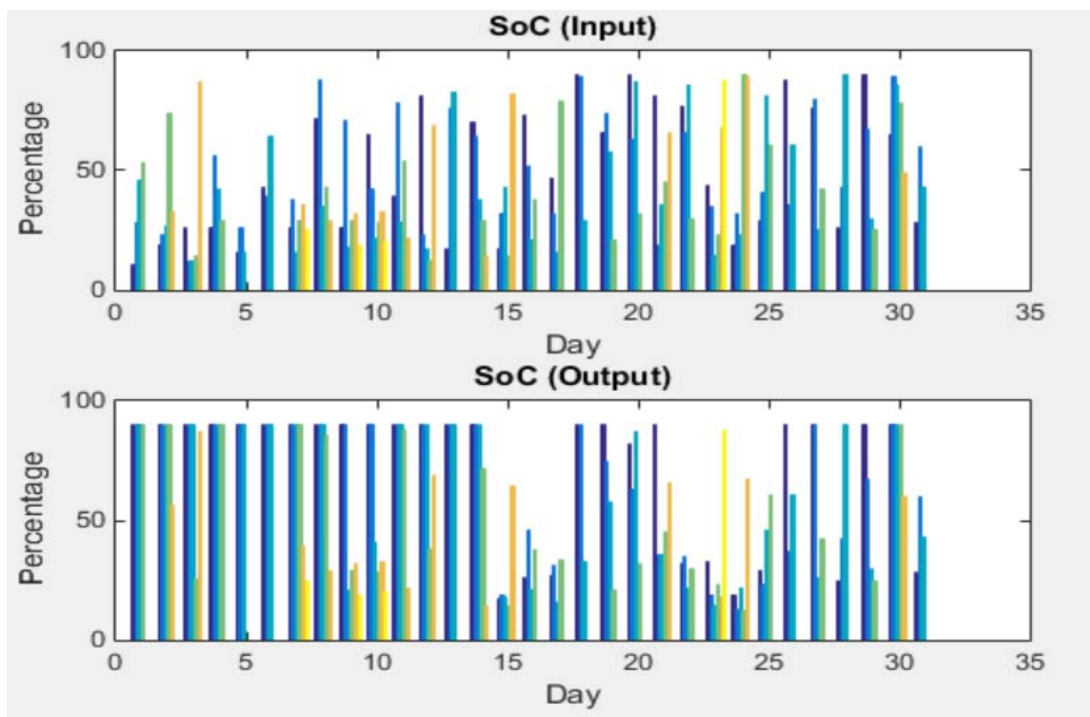


Figure 5.3: Input and Output SoC bar graphs

It is to be mentioned that the colorful bars of Fig. 5.3 vary on each day depending on the number of vehicles in which consists the fleet intended for charging and/or discharging, which explains the different bar colors. For instance, as days 1 and 25 consist of fleets of 4 vehicles represented each by 4 bars three of which having different shades of blue and the fourth being green. Also, days 10 and 23 consist of fleets of 6 vehicles represented by bars of three shades of blue, green, orange and yellow.

### **5.3.3 Discussion**

Based on the plotted curves of the input production and consumption compared with the output curves after regulation (Fig. 5.2), it is clearly shown that the margin between both curves is tighter, and in some cases, the regulation allows for a balanced system where P is equal to C. Besides, the state-of-charge of the electric vehicles is affected by the regulation process, and referring to the excess or lack of energy, the vehicles get charged or discharged. Particularly, in the regulation example set, the vehicles' depth of discharge is of 80 %, thus the maximal value for the batteries' SoC is of 90 %, and its minimal value is of 10 %. However, taking into consideration a fixed percentage of 15 % of all the batteries' SoC to be kept in the vehicles for their personal needs, the discharging process does not allow a SoC drop beyond 25 %. Thus, as it is shown on the presented bar graphs of Fig. 5.3, some of the fleets get partially or fully charged, and the excess of energy would then be used for grid supply if available. And some other fleets get fully or partially discharged.

Consequently, based on the available input and output values for the production and consumption of the studied 31 days example set, the regulation's percentage of equilibrium has been calculated. Therefore, this percentage has been found to be of 80.26 % for the first week, consecutively 82.89 % and 91.54 for weeks 2 and 3, and 96.67 % for the last 10 days. Hence, these calculations have led to a total average equilibrium percentage of 88.43 % for the 31 days example set.

## **5.4 Improved regulation through the optimization of number of vehicles**

As the study allows an endless number of vehicles to be integrated as a storage system, an optimization of the number of vehicle to charge/discharge would allow a convenient energy

transfer and a reduced consumption of batteries. Consequently, it would be interesting to improve the results obtained in section 5.3 through optimizing the number of vehicles and order of charging/discharging based on their available SoC as well as their battery lives. This optimization is further developed in this section.

#### **5.4.1**      *Assigned input data*

In order to minimize the number of vehicles to be charged or discharged, all vehicles available for storage or retrieval first need to be classified based on their storage capability and battery lives.

To this end, we use a combinatorial optimization based problem. More precisely, we apply the knapsack algorithm, with a set of vehicles each with a SoC and battery life, aiming to determine the vehicles to include in processes for charging/discharging so that the total SoC is arranged between both values Min and Max and the battery lives are as large as possible for charging process, and as less as possible for discharging process. The number of vehicles in a fleet should not be exceeded. The problem often arises in resource allocation where the decision makers have to choose from a set of vehicles under a fixed set of constraints. The algorithm is firstly based on the classification ratio  $r = \frac{L_b}{SoC}$  where  $L_b$  represents the vehicles' battery life and SoC represents their state-of-charge. For the storage process where the vehicles get charged, the vehicles are classified based on the decreasing order of the ratio  $r$ .

In fact, the charging starts with the vehicle corresponding to the highest value of  $r$ . More specifically this corresponds to vehicles with the highest battery lives and the lowest SoC. Thus, in other words, before charging, the vehicles are classified in a way to start with highest battery lives and highest storage capability.

As for the discharging, the classification is based on the increasing order of the vehicles' ratios  $r$  and the restitution starts with the vehicles with the highest SoC and the lowest battery lives.

Therefore, referring to the same sample data of 31 days, in order to calculate the value of  $r$  related to each fleet of vehicles, battery lives  $L_b$  are calculated as per equation (4.12) of chapter 4 where batteries' number of cycles is randomly defined as follows (table 5.3):

**Table 5.3: Vehicles' batteries number of cycles and SoC percentage to be kept in the vehicle**

Day	Cycles	Y
1	[1200 1300 1000 1000]	[10 12 14 11]
2	[1200 1000 1300 1000 1400]	[14 16 9 13 9]
3	[1200 1000 1300 1000 1400]	[34 7 7 12 21]
4	[1200 1300 1000 700]	[11 11 11 11]
5	[1200 1300 1000]	[17 11 8]
6	[1200 1300 1000]	[22 22 15]
7	[850 1200 1300 900 1000 1450]	[10 14 24 17 11 21]
8	[1200 1300 650 930 1125]	[12 19 17 9 7]
9	[1200 1200 850 1100 1300 1000]	[14 11 17 10 9 11]
10	[1200 1300 1000 1350 1100 550]	[10 9 8 7 8 9]
11	[1200 1300 1000 750 1430]	[11 13 11 12 21]
12	[1200 1300 1000 1112 933]	[32 12 41]
13	[1200 1300 1000]	[5 10 0 ]
14	[1200 1300 672 1000 832]	[14 13 14 12]
15	[1200 457 1300 1000 1123]	[15 9 8 8 9]
16	[1200 1012 1300 1000]	[16 10 16 12]
17	[1200 1300 947 1000]	[17 21 17 19]
18	[1200 1300 1000]	[14 20 10 ]
19	[1200 1300 1000 950]	[19 13 17 12]
20	[1200 690 1300 1000]	[20 62 20 22]
21	[1200 1300 1000 1043 1387]	[21 9 18 8 17]
22	[1200 1300 1020 1000]	[22 25 12 23]
23	[1200 1300 1000 876 1489 1312]	[23 9 18 20 8 10]
24	[1200 1300 1000 770 1240]	[24 3 12 2 33]
25	[1200 1300 1000 1125]	[25 13 18 9]
26	[1200 1300 1000]	[4 10 10 ]
27	[1200 1300 783 1000]	[26 13 17 10]
28	[1200 1300 1000]	[15 15 19]
29	[1200 499 1300 1000]	[29 23 19 10]
30	[1200 760 1430 1300 1000]	[5 15 10 19 7 ]
31	[1200 1300 1000]	[31 31 12]

In addition to the number of cycles chosen for the fleets' batteries, table 5.3 shows the SoC percentage y neither to be charged nor discharged, but to be kept in the vehicles' batteries for their personal use.

### 5.4.2 Output and Results

Accordingly, the control and regulation algorithm is launched and the output values for SoC before and after the classification are listed in the below table 5.4.

**Table 5.4: Input and Output SoC values before and after vehicles' classification**

Day	Unclassified Fleet		Classified Fleet	
	Input SoC	Output SoC	Input SoC	Output SoC
1	[11 28 46 53]	[90 90 90 90]	[11 28 46 53]	[90 90 90 90]
2	[19 23 27 74 33]	[90 90 90 90 55.9211]	[19 27 23 33 74]	[90 90 90 71.9211 74]
3	[26 12 12 14 87]	[90 90 90 25.5789 87]	[12 12 14 26 87]	[90 90 89.5789 26 87]
4	[26 56 42 29]	[90 90 90 90]	[26 29 42 56]	[90 90 90 90]
5	[16 26 16]	[90 90 90]	[16 16 26]	[90 90 90]
6	[43 39 64]	[90 90 90]	[39 43 64]	[90 90 90]
7	[26 38 16 29 36]	[90 90 90 90 39.1842]	[16 25 26 38 29]	[90 90 90 89.1842 29 36]
8	[72 88 35 43 29]	[90 90 90 86 29]	[29 43 35 72 88]	[90 90 45 72 88]
9	[26 71 18 29 32]	[90 90 20.9737 29 32 19]	[19 18 26 32 29]	[90 32.9737 26 32 29 71]
10	[65 42 22 28 33]	[90 90 41.1316 28 33]	[28 22 33 42 20]	[90 52.1316 33 42 20 65]
11	[39 78 28 54 22]	[90 90 90 87.7368 22]	[22 28 39 78 54]	[90 90 67.7368 78 54]
12	[81 23 17 12 69]	[90 90 90 38.2105 69]	[12 17 23 81 69]	[90 90 47.2105 81 69]
13	[17 76 83]	[90 90 90]	[17 76 83]	[90 90 90]
14	[70 64 38 29 14]	[90 90 90 71.7895 14]	[14 29 64 38 70]	[90 90 67.7895 38 70]
15	[17 32 43 14 82]	[17 19 18 14 64.3158]	[82 32 43 17 14]	[26.3158 32 43 17 14]
16	[73 52 21 38]	[26 46.1579 21 38]	[73 52 38 21]	[26 46.1579 38 21]
17	[47 32 16 79]	[27 31 16 33.1579]	[79 47 32 16]	[29 30.1579 32 16]
18	[90 89 29]	[90 90 32.6053]	[29 89 90]	[33.6053 89 90]
19	[66 74 58 21]	[90 74.4474 58 21]	[21 66 74 58]	[45.4474 66 74 58]
20	[90 63 87 32]	[82 63 87 32]	[63 90 87 32]	[63 82 87 32]
21	[81 19 36 45 66]	[90 35.8421 36 45 66]	[19 36 45 66 81]	[44.8421 36 45 66 81]
22	[77 66 86 30]	[32 35 22 30]	[86 77 66 30]	[22 32 35 30]
23	[44 35 14 23 68]	[33 19 14 23 18]	[88 68 44 35 23]	[20 58.5789 44 35 23 14]
24	[19 32 23 90 89]	[19 13 22 12 67.4737]	[90 89 32 23 19]	[12 47.4737 32 23 19]
25	[29 41 81 61]	[29 23 46.0526 61]	[81 61 41 29]	[28.0526 61 41 29]
26	[88 36 61]	[90 37.1579 61]	[36 61 88]	[39.1579 61 88]
27	[76 80 25 42]	[90 90 25.7368 42]	[25 42 80 76]	[49.7368 42 80 76]
28	[26 43 90]	[25 42.3684 90]	[90 43 26]	[88.3684 43 26]
29	[90 67 30 25]	[90 67.0789 30 25]	[30 25 90 67]	[30.0789 25 90 67]
30	[65 89 86 78 49]	[90 90 90 90 59.9737]	[49 65 78 86 89]	[90 76.9737 78 86 89]
31	[28 60 43]	[28 60 43]	[28 60 43]	[28 60 43]



The number of vehicles that have been charged or discharged before and after classification is defined as follows:  $\text{Min } Z = \sum X_i$  where  $X_i = \begin{cases} 1 & \text{if the vehicles is charged or discharged} \\ 0 & \text{if not} \end{cases}$

The calculation of  $\sum X_i$  through the algorithm's simulation results in the following table 5.5 and Fig.5.4 where the result of minimization of  $Z$  after classification is clear:

**Table 5.5: Number of vehicles charged/discharged before and after classification**

Day	$Z = \sum X_i$ before	$Z = \sum X_i$ after
1	4	4
2	5	4
3	4	3
4	4	4
5	3	3
6	3	3
7	5	4
8	4	3
9	3	2
10	3	2
11	4	3
12	4	3
13	3	3
14	4	3
15	3	1
16	2	2
17	3	2
18	2	1
19	2	1
20	1	1
21	2	1
22	3	3
23	4	2
24	4	2
25	2	1
26	2	1
27	3	1
28	2	1
29	1	1
30	5	2
31	0	0
<b>Total</b>	<b>94</b>	<b>67</b>

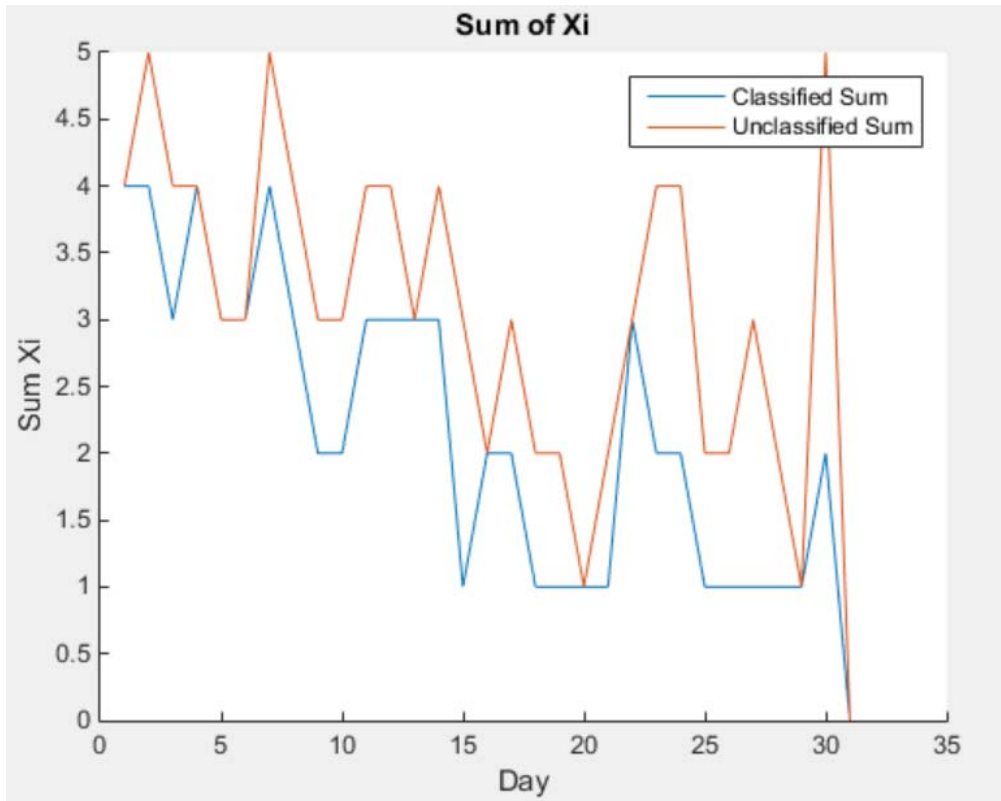


**Figure 5.4: Number of vehicles charged/discharged before and after classification**

### 5.4.3 Discussion

As shown in table 5.5 and Fig. 5.4 where the number of vehicles charged or discharged is calculated and plotted, after classification, the number of vehicles used for storage and restitution is clearly less (or equal) than the random charging/discharging without classification.

In order to compare the SoC input and output values in some of the cases where the vehicles were charged or discharged with or without classification, days 13, 15, 22 and 30 of our study were further investigated and discussed.

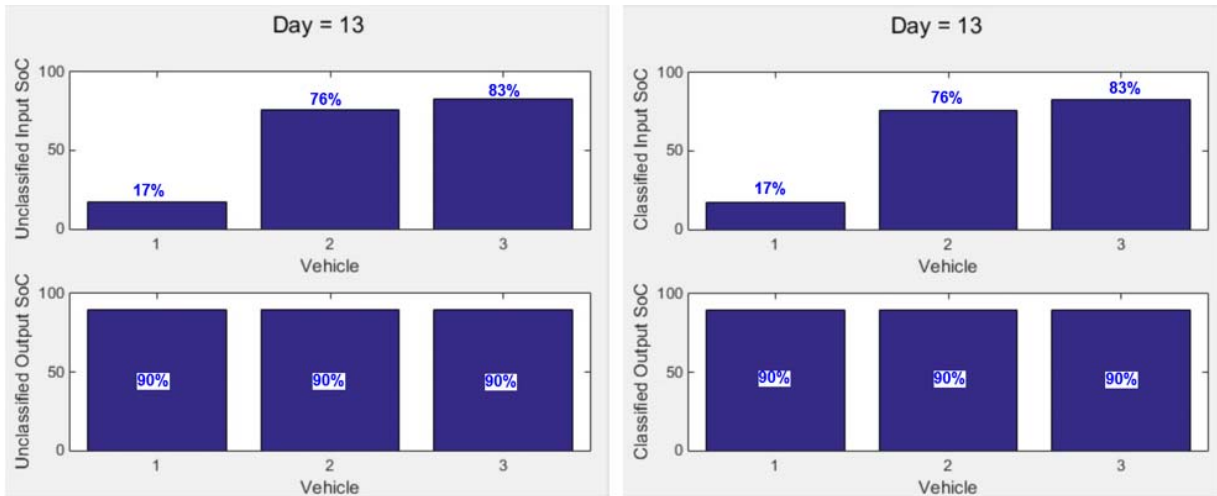


**Figure 5.5: Day 13 - Input & Output SoC - without & with classification**

On day 13 (a charging day), illustrated in Fig. 5.5, the input SoC of the fleet of three vehicles is progressively of 17 %, 76 % and 83 %. As  $P = 85.03 \text{ kWh} > C = 3.17 \text{ kWh}$  in this case, the charging process of the vehicles gets launched until fully charging the fleet with a 90 % SoC for all 3 vehicles. The vehicles classification results in the same order of charging in this case, and the output after charging would end up with a fully charged fleet as well.

At the end of the process,  $P = 67.17 \text{ kWh}$  would still be higher than  $C = 21.03 \text{ kWh}$ , and the excess of production can be used to supply the electric grid.

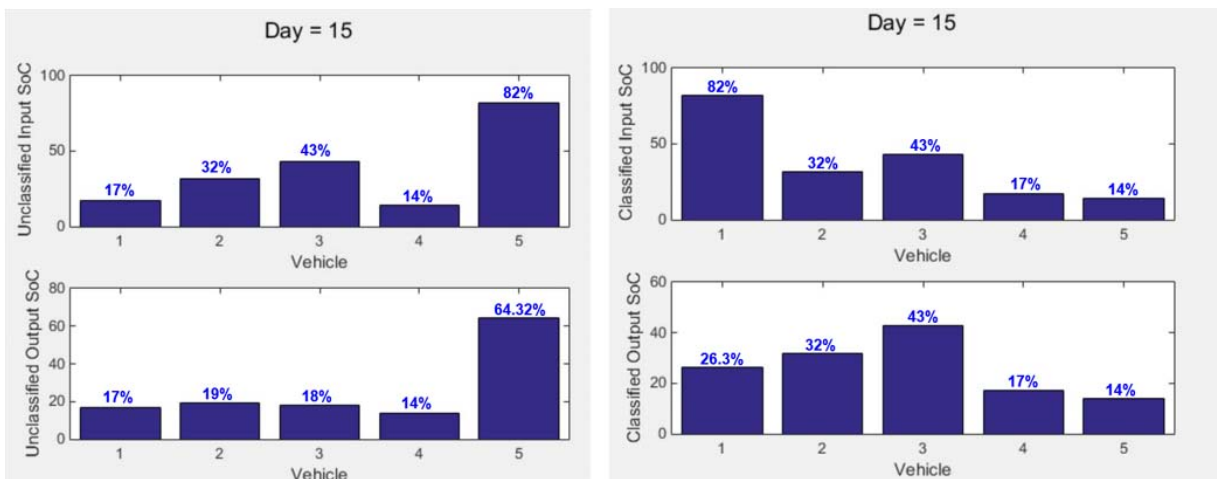


**Figure 5.6: Day 15 - Input & Output SoC - without & with classification**

On day 15, illustrated in Fig. 5.6,  $P = 8.12 \text{ kWh} < C = 18.7 \text{ kWh}$ ; therefore the algorithm launches the discharging process. The initial input SoCs of the fleet of five vehicles are respectively of 17 %, 32 %, 43 %, 14 % and 82 %. However, the progressive values of  $y$  that must be kept in the vehicles' batteries for their personal use are of 15 %, 9 %, 8 %, 8 % and 9 %. Therefore, the vehicles' SoCs must not fall short of the progressive values  $\text{SoC}_{\min}+y$  for the five vehicles that are respectively 25 %, 19 %, 18 %, 18 % and 19 %. In this case, as the SoCs of the 1<sup>st</sup> and 4<sup>th</sup> vehicle are already below their lower limit  $\text{SoC}_{\min}+y$ , the discharging process is launched for the three remaining vehicles and the output SoC would then be of 17 %, 19 %, 18 %, 14 % and 64.3158 %. The discharging of the 2<sup>nd</sup>, 3<sup>rd</sup>, and 5<sup>th</sup> vehicles allows the balanced system to be reached with  $P = C = 18.7 \text{ kWh}$ .

However, in the case when the vehicles are classified at the input based on their cycles/ battery lives and SoCs, the classification allows the discharging process to start with the vehicle with a SoC of 82 % and the balanced system would then be reached before discharging any other vehicle and extending their usage thus shortening their battery lives. So, the discharging of the classified vehicles results in output SoCs of 26.3 %, 32 %, 43 %, 17 %, and 14 %; with the 1<sup>st</sup> vehicle being the only one affected by the discharging process.

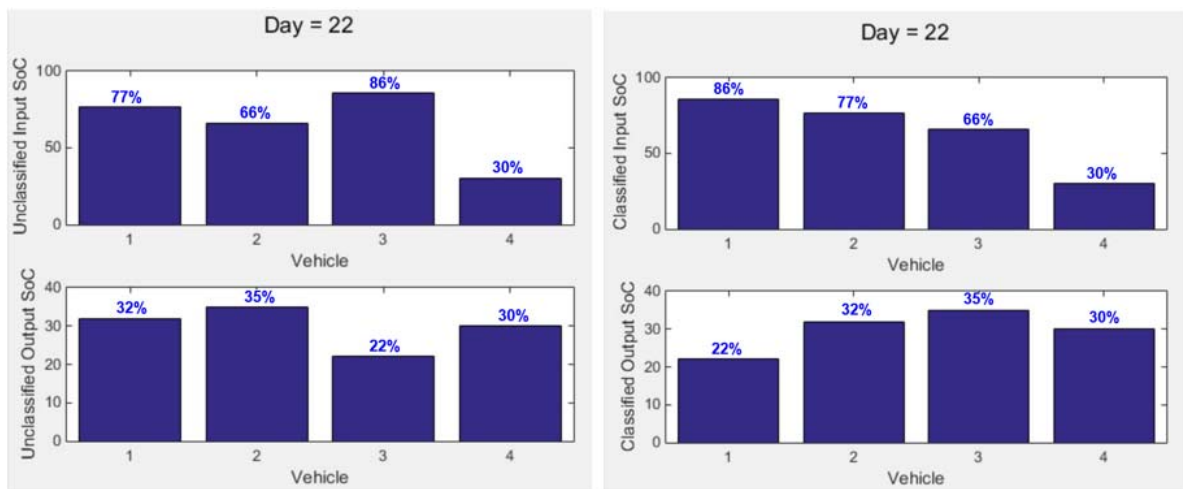


**Figure 5.7: Day 22 - Input & Output SoC - without & with classification**

Similarly, the day 22 involves  $P = 1.87 \text{ kWh} < C = 36.5 \text{ kWh}$ , hence a launching of the discharging mode (Fig. 5.7).

The initial input SoCs of a four vehicles' fleet are of 77 %, 66 %, 86 % and 30 %, and their minimum allowable values  $SoC_{min+y}$  are of 32 %, 35 %, 22 % and 33 %. Once classified, the input SoCs would be of 86 %, 77 %, 66 % and 30 % respectively. Whether classified or not, the discharging process operates until the fleet is fully discharged, and as  $P = 28.47$  kWh would still be lower than  $C = 36.5$  kWh, the lack of production can be compensated from the electric grid restitution.

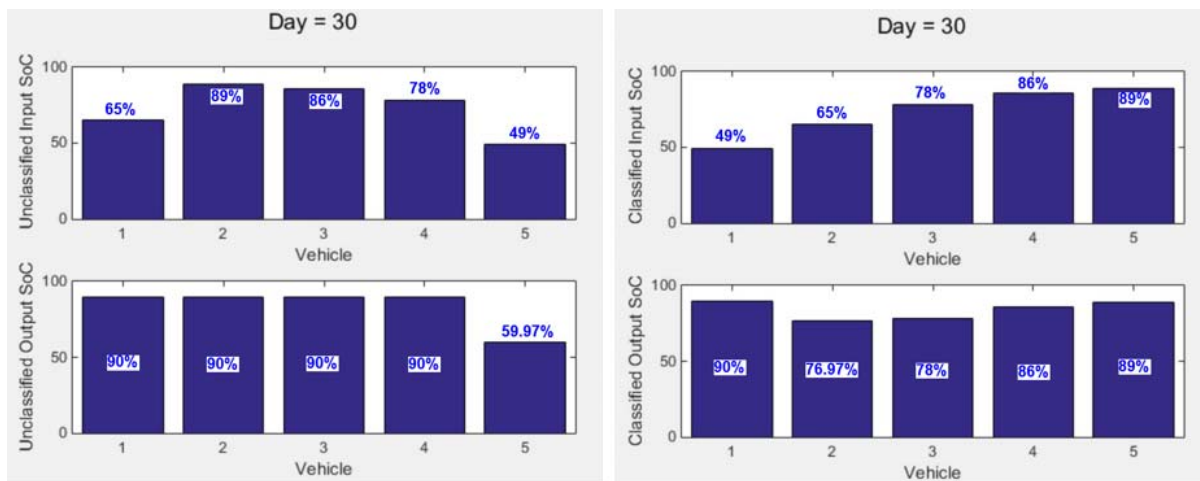


**Figure 5.8: Day 30 - Input & Output SoC - without & with classification**

On day 30, illustrated in Fig. 5.8,  $P = 24.93$  kWh and  $C = 4.8$  kWh, the charging process would then be launched. The initial input SoCs of the fleet of vehicles are respectively 65 %, 89 %, 86 %, 78 % and 49 %. All five vehicles are affected by the charging process with 4 fully charged vehicles out of 5 with respective output SoCs of 90 %, 90 %, 90 %, 90 % and 59.97 %. The balance of the system is then reached with  $P = C = 14.87$  kWh.

If the classification is made before launching the charging process, the initial input SoCs would be of 49 %, 65 %, 78 %, 86 % and 89 %. And the same amount of energy used to reach the balanced system would be injected in this case in only 2 vehicles instead of 5 with final output SoCs of 90 %, 76.97 %, 78 %, 86 % and 89 %. In this case, the remaining vehicles are not integrated into the charging process, which preserves (thus extends) their batteries lifetime while consuming fewer charging and discharging cycles.

As for day 31, at the first comparison operated by the regulation algorithm, as the production and consumption have equivalent values, the system is already in balance situation

and the vehicles can neither charge nor discharge their batteries. In this case, the input values of the fleet's SoC are the same as their output values. The algorithm takes no action then and waits until a margin between the production and consumption occurs again.

## **5.5 Conclusion**

In this chapter, a control and regulation algorithm for the energy flowing between a domestic household, electric vehicles and the grid has been assessed. The regulation is mostly performed based on the electricity supply and demand, and seeking a balanced production/consumption system. The regulation algorithm has been simulated through a sample input set of 31 days with different input values for the production and consumption as well as the fleet of 3 to 6 electric vehicles. The output results showed a total convergence of 88.43% towards the equilibrium state. Consequently, the production and consumption regulation proposed seem to be an extremely effective solution for the energy waste caused by the misuse of the excess and lack of energy.

However, as the study allows an endless number of vehicles to be integrated as a storage system, a combinatorial optimization of the number of vehicle to charge/discharge would allow a convenient energy transfer and a reduced consumption of batteries. This optimization study is based on knapsack algorithm. Therefore, an improved management solution has been implemented allowing a classification of the available vehicles before injecting or retrieving their energy based on their states-of charge and battery life. Therefore, the energy storage and retrieval processes have been further optimized through the minimization of the number of vehicles that would be charged or discharged.

As a future work of this part, it would also be intriguing to generate a realistic prototype that would further verify the theoretical studies and obtained results.

## General Conclusion

Electric vehicles have recently been brought into attention for their major contribution in the polluting greenhouse gases reduction subsequent from the transportation sector. Consequently, this research work has shed the light on electric vehicles and energy systems. So first, the investigations implied a literature review related to the electric vehicles and systems' components. Then, the multi-objective optimization approach, as well as the energy management strategies comprising the scheduling of vehicular charging and discharging have been studied based on the available literature.

To do so, a specific energy system including a domestic household connected to photovoltaic panels and a wind turbine, a fleet of electric vehicles and the electric grid has been conceived. The system's detailed configuration as well as the modeling and sizing of its components have been described. A main focus of the study implies in the control of energy flows entering and leaving the fleet of vehicles and their regulation based on the electricity supply and demand. Moreover, the global energetic model of the system has been depicted through a discussion of three case studies with different production and consumption difference margin variations.

Furthermore, the vehicular charging and discharging processes have been optimized using the multi-objective genetic algorithm as an optimization approach. As a result, the Pareto-front of predefined objective functions is identified culminating in the fulfillment of the system's energetic needs. Particularly, the optimization of the charging process thrives towards finding the maximal state of charge, valley energy, propulsive energy and the minimal losses that the fleet could attain. As for the discharging process, the acquired optimization embeds the minimization of the battery's state of charge, the vehicles' discharging time and losses, and the maximization of the battery's lifetime. In some cases, the conflicting solutions imposed the application of the weighted sum approach based on the decision maker's priorities defined through several scenarios. Consequently, quasi-optimal solutions that are the closest possible to the optimal ones have been obtained, and the calculated optimized solutions basically converged towards the theoretical objective functions' theoretical optima. This convergence obtained by the genetic algorithm calculations has also been verified by simulation using the gamultiobj solver of Matlab for both the storage and retrieval optimizations.

Additionally, the fleet's behavior has been evaluated through an energetic strategy based on the

electricity production and consumption, thus its demand and supply. So, a control algorithm has been developed to ensure a balanced regulation of the energy flows between the vehicles and the infrastructure (home and the grid eventually). The regulation algorithm's simulation has shown a significant convergence towards the equilibrium state and a tightened difference margin between energy production and consumption. Consecutively, an improved management solution has been proposed through a classification of the available vehicles before the energy injection or retrieval in order to minimize the number of vehicles that would be charged or discharged. Thus, an improved version of the regulation algorithm has been projected and the energy storage and retrieval have been further optimized.

Briefly, in this research work, a control and regulation algorithm for the energy flowing between a domestic household, electric vehicles and the grid has been assessed. The major findings and conclusions of this research work are:

- The energy flows regulation is mostly performed based on the electricity supply and demand, seeking a balanced production/consumption system.
- Once triggered by the regulation algorithm, vehicular charging and discharging modes are optimized through the multi-objective genetic algorithm.
- The regulation algorithm was simulated through a sample input set of 31 days and the output results showed a total convergence of 88.43% towards the equilibrium state.
- The number of vehicles to charge/discharge has been optimized allowing a convenient energy transfer and a reduced consumption of batteries' cycles and longevity.

Consequently, the production and consumption regulation proposed by this study and the assessed optimization of both the vehicular charging and discharging modes seem to be an extremely effective solution for the energy waste caused by the misuse of the excess and lack of energy.

For future studies and implications, it would be interesting to expand the energy system to a larger scale involving the assessment of a whole city with numerous habitats and more sophisticated renewable sources. It would also be intriguing to generate a realistic prototype that would exemplify the theoretical studies.



Moreover, even though it is always recommended to flatten the demand profile and avoid charging electric vehicles during peak hours (for which the electricity tariffs become more substantial), an economic study of such a problem remains to be addressed in future research projects.

## References

- [1] A. Dargahi, "Gestion des flux multi-énergie pour les systèmes V2H," Thèse de Doctorat, Energie Electrique, Université de Grenoble, France, 2014.
- [2] R. Zgheib, K. Al-Haddad and I. Kamwa, "V2G, G2V and Active Filter Operation of a Bidirectional Battery Charger for Electric Vehicles," in *IEEE International Conference on Industrial Technology (ICIT)*, Taipei, 2016.
- [3] A. Kriukov and M. Gavrilas, "Smart Energy Management in Distribution Networks with Increasing Number of Electric Vehicle," in *International Conference and Exposition on Electrical and Power Engineering*, Iasi, Romania, 2014.
- [4] J. Kiriakos and N. Moubayed, "Electric Vehicles Supply from Renewable Resources," Lebanese University/Saint Joseph University Faculty of Engineering Masters Division, 2016.
- [5] P. Jain and T. Jain, "Impacts of G2V and V2G Power on Electricity Demand Profile," in *IEEE International Electric Vehicle Conference (IEVC)*, Florence, 2014.
- [6] J. D. Ftzsimmons, S. J. Kritzer, V. A. Muthiah, J. J. Parmer, T. J. Rykal, M. T. Stone, M. C. Brannon, J. P. Wheeler, D. L. Slutzky and J. H. Lambert, "Simulation of an Electric Vehicle Fleet to Forecast Availability of Grid Balancing Resources," in *IEEE Systems and Information Engineering Design Conference (SIEDS, 16)*, Charlottesville, 2016.
- [7] V. L. Nguyen, "Couplage des systèmes photovoltaïques et des véhicules électriques au réseau Problèmes et solutions," Université de Grenoble, France, 2014.
- [8] IEA, "Global EV Outlook," [www.iea.org/publications/reports/globalevoutlook2019/](http://www.iea.org/publications/reports/globalevoutlook2019/), IEA Paris, 2019.
- [9] D. Guo and C. Zhou, "Potential performance analysis and future trend prediction of electric vehicle with V2G/ V2H/ V2B capability," *AIMS Energy*, vol. 4, no. 2, pp. 331-346, 2016.
- [10] E. Saberbari, H. Saboori and S. Saboori, "Utilizing PREYs for Peak-Shaving, Loss Reduction and Voltage Profile Improvement via V2B Mode," in *The 19th Electrical Power Distribution Conference (EPDC)*, Niroo Research Institute, Tehran, 2014.
- [11] C. Pang, P. Dutta, S. Kim, M. Kezunovic and I. Damnjanovic, "PHEVs as Dynamically Configurable Dispersed Energy Storage for V2B Uses in Smart Grid," in *7th Mediterranean Conference and Exhibition on Power Generation, Transmission, Distribution and Energy Conversion*, Ayia Napa, Cyprus, 2010.

- [12] L. Hua, J. Wang and C. Zhou, "Adaptive Electric Vehicle Charging Coordination on Distribution Network," *IEEE Transactions on Smart Grid*, vol. 5, no. 6, pp. 2666-2675, 2014.
- [13] J. Donoghue and A. Cruden, "Whole System Modelling of V2G Power Network Control, Communications and Management," in *EVS27 Symposium*, Barcelona, Spain, 2013.
- [14] N. Xu and C. Chung, "Reliability Evaluation of Distribution Systems Including Vehicle-to-Home and Vehicle-to-Grid," *IEEE Transactions on Power Systems*, vol. 31, no. 1, pp. 759-768, 2016.
- [15] Z. Zhou, J. Bai and S. Zhou, "A Stackelberg Game Approach for Energy Management in Smart Distribution Systems with Multiple Microgrids," in *IEEE twelfth International Symposium on Autonomous Decentralized Systems (ISADS)*, 2015.
- [16] M. Kintner-Meyer, K. Schneider and R. Pratt, "Impacts Assessment of Plug-in Hybrid Vehicles on Electric Utilities and Regional US Power Grids Part 1: Technical Analysis Pacific Northwest," National Laboratory, 2007.
- [17] W. Kempton and J. Tomic, "Vehicle to grid power implementation: From stabilizing the grid to support large-scale renewable energy," *Journal of Power Sources*, no. 144, pp. 280-294, 2004.
- [18] W. Kempton and J. Tomic, "Vehicle-to-grid Power Fundamentals: Calculating Capacity and Net Revenue," *Journal of Power Sources*, no. 144, pp. 268-279, 2005.
- [19] W. Yen-Ching, W. Yen-Chun and I. Tzung-Lin, "Design and implementation of a bidirectional isolated dual-active-bridge-based DC/DC converter with dual-phase-shift control for electric vehicle battery," in *Energy Conversion Congress and Exposition ECCE*, 2013.
- [20] S. Zeljkovic, R. Vuletic, A. Miller and A. Denais, "Control of SiC-based dual active bridge in high power three phase on-board charger of EVs," in *International Conference on Electrical Systems for Aircraft, Railway, Ship Propulsion and Road Vehicles (ESARS)*, Aachen, Germany, 2015.
- [21] Y. Liu, R. Deng and H. Liang, "Game-theoretic control of PHEV charging with power flow analysis," *AIMS Energy*, vol. 4, no. 2, pp. 379-396, 2016.
- [22] J. Jan and L. Wang, "Real-time charging navigation of electric vehicles to fast charging stations: a hierarchical game approach," *IEEE T Smart Grid*, 2015.
- [23] S. Yoon, Y. Choi, S. Bahk and J. Park, "Stackelberg game based demand response for at-home electric vehicle charging," *IEEE T Veh Technol*, 2015.
- [24] Z. Lei and Y. Li, "A game theoretic approach to optimal scheduling of parking-lot electric vehicle charging," *IEEE T Veh Technol*, 2015.

- [25] S. Bolognani and S. Zampieri, "On the existence and linear approximation of the power flow solution in power distribution networks," *IEEE Transaction on Power Systems*, vol. 31, no. 1, pp. 163-172, 2016.
- [26] S. Nojavan, B. Mohammadi-Ivatloo and a. K. Zare, "Optimal bidding strategy of electricity retailers using robust optimisation approach considering time-of-use rate demand response programs under market price uncertainties," *IET Generation, Transmission & Distribution*, vol. 9, pp. 328-338, 2015.
- [27] M. Scott, M. Kintner-Meyer, D. Elliot and W. Warwick, "Impacts assessment of plug-in hybrid electric vehicles on the electric utilities and regional U.S. power grids: part 1: technical assessment," 2007.
- [28] R. C. Green, L. Wang and M. Alam, "The impact of plug-in hybrid electric vehicles on distribution networks: a review and outlook," *IEEE PES General Meeting, Providence, RI*, pp. 1-8, 2010.
- [29] B. Sovacoola and R. Hirshb, "Beyond batteries: an examination of the benefits and barriers to plug in hybrid electric vehicles (PHEVs) and a vehicle-to-grid (V2G) transition," *Energy Policy*, no. 37, pp. 1095-1103, 2009.
- [30] A. Kriukov, B. Vicol, M. Gavrilas and O. Ivanov, "A stochastic method for calculating energy losses in low voltage distribution networks using genetic algorithm," *Buletinul AGIR*, no. 3/2012, 2012.
- [31] J. F. Orjuela, "Integration des vehicules Electriques dans le reseau electrique residentiel : impact sur le desequilibre et strategies V2G innovantes," Universite de Grenoble, France, 2014.
- [32] A. Sharma, S. Shih and D. Srinivasan, "A Smart Scheduling Strategy for Charging and Discharging of Electric Vehicles," *IEEE Innovative Smart Grid Technologies*, 2015.
- [33] W. Michel, "Véhicules électriques et hybrides," Dossier technique crée avec la collaboration du Groupement National pour la Formation Automobile ANFA, France, Edition 2011.
- [34] A. B. Pedersen, B. Andersen, S. J. J, R. D, R. J and L. J, "Electric Vehicle Integration into Modern Power Networks," in *The Impact of EV charging on the System Demand*, Springer Science + Business Media, 2012, pp. 107-154.
- [35] B. Chauchat, "Chargeur de batteries integres pour vehicule electrique," these de doctorat, INPG, 1997.
- [36] R. Mkahl, "Contribution a la modelisation, au dimensionnement eta la gestion des flux energetiques d'un systeme de recharge de vehicules electriques : etude de l'interconnexion avec le reseau electrique," Universite de technologie de Belfort-Montbeliard, 2015.

- [37] B. P. Jelle, C. Breivik and H. D. Rokenes, "Building intergrated photovoltaic products: A state-of-the art review and uture research opportunities," *Solar Energy Materials and Solar Cells*, vol. 100, pp. 69-96, May 2012.
- [38] S.-H. Yoo, "Simulation for an optimal application through parameter variation," *Solar Energy*, vol. 85, no. 7, pp. 1291-1301, July 2011.
- [39] A. Hamidi, D. Nazarpour and S. Golshannavaz, "Multi-Objective Scheduling of Microgrids to Harvest Higher Photovoltaic Energy," *IEEE Transactions on Industrial Informatics*, vol. 14, no. 1, pp. 45-57, 2017.
- [40] J. McCall, "Genetic algorithms for modelling and optimization," *Journal of computational and applied mathematics*, vol. 184, no. 1, pp. 205-222, 2005.
- [41] G. Merhy, A. Nait-Sidi-Moh and N. Moubayed, "Control of electric vehicles energy flows through a multi-objective and multi-criteria optimization algorithm," in *12th International conference on multiple objective programming and goal programming MOPGP*, Metz, France, 2017.
- [42] L. Fang, S. Qin, G. Xu, T. ti and K. Zhu, "Simultaneous Optimization for Hybrid Electric Vehicle Parameters Based on Multi-Objective Genetic Algorithms," *Energies*, no. 4, pp. 532-544, 2011.
- [43] R. Bessa and M. Matos, "Optimization Models for EV Aggregator Participation in a Manual Reserve Market," *Power Systems, IEEE Transactions*, no. 28, pp. 3085-3095, 2013.
- [44] G. Venter, "Review of Optimization Techniques," *Encyclopedia of Aerospace Engineering*, 2010.
- [45] P. Depincé, B. Guédas and J. Picard, "Multidisciplinary and multiobjective optimization: Comparison of several methods," in *7th World Congress on Structural and Multidisciplinary Optimization*, Seoul, Korea, 2007.
- [46] G. Chiandussi, M. Codegone, S. Ferrero and F. Varesio, "Comparison of multi-objective optimization methodologies for engineering applications," *Computers and Mathematics with Applications*, no. 63, pp. 912-942, 2012.
- [47] V. Sedenka and Z. Raida, "Critical Comparison of Multi-objective Optimization Methods: Genetic Algorithms versus Swarm Intelligence," *Radioengineering*, vol. 19, no. 3, pp. 369-377, 2010.
- [48] R. Marler and J. Arora, "Survey of multi-objective optimization methods for engineering," *Struct Multidisc Optim*, no. 26, pp. 369-395, 2004.
- [49] E. Zitzler, "Evolutionary Algorithms fo.r Multiobjective Optimization: Methods and Applications," Swiss Federal Institute of Technology, Zurich, 1999.

- [50] R. Bessa and M. Matos, "The role of an aggregator agent for EV in the electricity market, in Power Generation, Transmission, Distribution and Energy Conversion," in *7th Mediterranean Conference and Exhibition on MedPower*, 2010.
- [51] S. Bahrami and M. Parnian, "Game Theoretic Based Charging Strategy for Plug-in Hybrid Electric Vehicles," *IEEE Transactions on Smart Grid*, vol. 5, pp. 2368-2375, 2014.
- [52] J. Figueiredo and J. Martins, "Energy Production System Management- Renewable energy power supply," *Energy Conversion and Management*, vol. 51, pp. 1120-1126, 2010.
- [53] P. Thomas and F. Chacko, "Electric Vehicle Integration to Distribution Grid Ensuring Quality Power Exchange," in *International Conference on Power, Signals, Controls and Computation (EPSC/CON)*, 2014.
- [54] M. Duvall, "Transportation Electrification- A Technology Overview, Power Delivery & Utilization," *Electric Power Research Institute Palo Alto, California*, no. 1021334, pp. 3.1-3.2, 2011.
- [55] Z. Darabi and M. Ferdowsi, "Aggregated Impact of Plug-in Hybrid Electric Vehicles on Electricity Demand Profile," *IEEE Trans. On Sustainable Energy*, vol. 2, no. 4, pp. 501-508, 2011.
- [56] F. Kalhamme, H. Kamath, M. Duvall, M. Alexander and B. Jungers, "Plug-In Hybrid Electric Vehicles: Promises, Issues and Prospects," in *Proc. EVS24 Int. Battery, Hybrid and Fuel Cell Electric Vehicle Symp.*, Stavanger, Norway, 2009.
- [57] M. Shahidehpour, H. Yamin and Z. Li, " Example Systems Data, in Market Operations in Electric Power Systems: Forecasting, Scheduling, and Risk Management," *New York, IEEE, John Wiley & Sons, appx. D, sec. D.4, p. 477, 2002.*
- [58] R. Haque, T. Jamal, N. Maruf, S. Ferdous, S. Farhana and H. Priya, "Smart Management of PHEV and Renewable Energy Sources for Grid Peak Demand Energy Supply," in *2nd Int'l Conf. on Electrical Engineering and Information & Communication Technology (ICEEICT)*, 2015.
- [59] S. Hadley and A. Tsvetkova, "Potential impacts of plug-in hybrid electric vehicles on regional power generation," Oak Ridge National Laboratory, 2008.
- [60] A. Saber and G. Venayagamoorthy, "Optimization of vehicle-to-grid scheduling in constrained parking-lots," *Power & Energy Society General Meeting PES '09. IEEE*, vol. 1, no. 8, 2009.
- [61] B. Band and R. Hirsh, "Beyond batteries: An examination of the benefits and barriers to plug-in hybrid electric vehicles (PHEVs) and a vehicle-to-grid (V2G) transition," *Energy Policy*, no. 03/2009, 2009.
- [62] W. Kempton and S. Letendre, "Electric vehicles as a new power source for electric utilities,"

*Transportation Research*, vol. 2, no. 3, pp. 157-175, 1997.

- [63] I. Zongfeng, G. Chunlin, C. Zhongjun, C. Jun and I. Xiaojuan, "Design and Development of the Platform for Electric Vehicle to Grid," *IEEE*, 2015.
- [64] A. Kriukov and M. Gavrilas, "Managing a multi-purpose parking lot for Electric Vehicles," *Buletinul AGIR*, no. 3/2013, pp. 307-312, 2013.
- [65] R. Rezanian and W. Pruggler, "Business models for the integration of electric vehicles into the Austrian energy system," in *9th International Conference on the European Energy Market*, Florence, Italy, 2012.
- [66] W. Zhong, R. Yu, Y. Zhang, J. Kang, H. Zhang and S. Xie, "Dynamic Demand Balance in Vehicle-to-Grid Mobile Energy Networks," *IEEE ICC*, 2015.
- [67] H. Liang, B. Choi, W. Zhuang and X. Shen, "Optimizing the energy delivery via v2g systems based on stochastic inventory theory," *IEEE Trans. Smart Grid*, 2013.
- [68] C. Jin, J. Tang and A. P. Ghosh, "Optimizing electric vehicle charging: a customer's perspective," *IEEE Trans. Vehicular Technology*, vol. 62, no. 7, pp. 2919-2927, 2013.
- [69] R. Mehta, D. Srinivasan, A. Khambadkone, J. Yang and A. Trivedi, "Smart Charging Strategies for Optimal Integration of Plug-in Electric Vehicles within Existing Distribution System Infrastructure," *IEEE Transactions on Smart Grid*, vol. 9, no. 1, pp. 299-312, 2018.
- [70] R. Mkahl, A. Nait-Sidi-Moh, J. Gaber and M. Wack, "An optimal solution for charging management of electric vehicles fleets," *Electric Power Systems Research*, no. 146, pp. 177-188, 2017.
- [71] R. Hagura, S. Kitayama and Y. Yasui, "Development of energy management of hybrid electric vehicle for improving fuel consumption via sequential approximate optimization," *IFAC proceedings*, vol. 46, no. 21, pp. 800-805, 2013.
- [72] M. Ahmad, I. Saba, S. Azuma and T. Sugie, "Model free tuning of variable state of charge targets of hybrid electric vehicles," *IFAC Proceedings*, vol. 46, no. 21, pp. 789-793, 2013.
- [73] H. Qin and W. Zhang, "Charging scheduling with minimal waiting in a network of electric vehicles and charging stations," in *Proceedings of the Eighth ACM international workshop on Vehicular inter-networking*, ACM, 51-60., 2011.
- [74] A. Ruzmetov, A. Nait-Sidi-Moh and J. Gaber, "A (max - plus)-based approach for charging management of electric vehicles," in *The 2nd World Conference on Complex Systems (WCCS14)*, Agadir, Morocco, 2014.

- [75] J. Kang, S. Duncan and D. Mavris, "Real-time scheduling techniques for electric vehicle charging in support of frequency regulation," *Procedia Computer Science, Elsevier*, vol. 16, pp. 767-775, 2013.
- [76] O. Sundström and C. Binding, "Planning electric-drive vehicle charging under constrained grid conditions," in *International Conference on Power System Technology.*, 2010.
- [77] A. Ruzmetov, A. Nait-Sidi-Moh, M. Bakhouya and J. Gaber, "Towards an optimal assignment and scheduling for charging electric vehicles," in *IEEE International Renewable and Sustainable Energy Conference (IRSEC), Ouarzazate, Morocco*, 2013.
- [78] Y. He, B. Venkatesh and L. Guan, "Optimal scheduling for charging and discharging of electric vehicles," *IEEE transactions on smart grid*, vol. 3, 2012.
- [79] A. Nait-Sidi-Moh, A. Ruzmetov, M. Bakhouya, Y. Naitmalek and J. Gaber, "A Prediction Model of Electric Vehicle Charging Requests," in *The 9th International Conference on Emerging Ubiquitous Systems and Pervasive Networks (EUSPN). Procedia Computer Science*, 2018.
- [80] M. Aiad and P. Lee, "Energy disaggregation of overlapping home appliances consumptions using a cluster splitting approach," *Sustainable Cities And Society*, vol. 43, pp. 487-494, 2018.
- [81] Z. Yu, F. Haghghat and B. Fung, "Advances and challenges in building engineering and data mining applications for energy-efficient communities," *Sustainable Cities and Society*, vol. 25, pp. 33-38, 2016.
- [82] J. Brady and M. O. Mahony, "Modelling charging profiles of electric vehicles based on real-world electric vehicle charging data," *Sustainable Cities and Society*, vol. 26, pp. 203-216, 2016.
- [83] B. Amirhosseini and S. Hosseini, "Scheduling charging of hybrid-electric vehicles according to supply and demand based on particle swarm optimization, imperialist competitive and teaching-learning algorithms," *Sustainable Cities And Society*, vol. 43, pp. 339-349, 2018.
- [84] K. Karmaker, R. Ahmed, A. Hossain and M. Sikder, "Feasibility Assessment & Design of Hybrid Renewable Energy Based Electric Vehicle Charging Station in Bangladesh," *Sustainable Cities and Society*, vol. 39, pp. 189-202, 2018.
- [85] R. Garcia-Valle and J. P. L. (eds.), "Electric Vehicle Integration into Modern Power Networks," *Power Electronics and Power Systems, Springer Science+Business Media*, pp. DOI 10.1007/978-1-4614-0134-6\_2, New York 2013.
- [86] A. Li, "Analyse expérimentale et modélisation d'éléments de batteries et de leurs assemblages : application aux véhicules électriques et hybrides," Université Claude Bernard-Lyon I, 2013.
- [87] Panasonic, *Nickel Metal Hydride Battery Catalog*, 2018.



- [88] M. P. Co., *Sealed Lead-Acid Batteries Catalog*.
- [89] E. Kinab, T. Salem and G. Merhy, "BIPV Building Integrated Photovoltaic Systems in Mediterranean Climate," in *2nd Renewable Energy for Developing Countries REDEC*, Lebanon, 2014.
- [90] DualSun, *DualSun Spring solar panels catalog*, [www.dualsun.com](http://www.dualsun.com), 2017.
- [91] E. R. & E. 4.0, *AN3000 Horizontal wind turbine detailed specifications*.
- [92] S. T. Inc., *Three phase inverters catalog*, [www.solaredge.us](http://www.solaredge.us), 2017.
- [93] R. Marler and J. Arora, "Survey of multi-objective optimization methods for engineering," *Struct Multidisc Optim*, no. 26, pp. 369-395, 2004.
- [94] K. Amouzgar, "Multi-Objective Optimization using Genetic Algorithms," Thesis work 2012 product development and materials engineering, 30-05-2012.
- [95] L. Guzzella and A. Sciarretta, "Vehicle propulsion systems," *Springer-Verlag Berlin Heidelberg*, vol. 1, 2007.
- [96] A. Hamidi, D. Nazarpour and S. Golshannavaz, "Multi-Objective Scheduling of Microgrids to Harvest Higher Photovoltaic Energy," *IEEE Transactions on Industrial Informatics*, vol. 14, no. 1, pp. 47-57, 2017.
- [97] M. Kisacikoglu, F. Erden and N. Erdogan, "Distributed Control of PEV Charging based on Energy Demand Forecast," *IEEE Transactions on Industrial Informatics*, pp. 99, 1-1., 2017.
- [98] R. Mkahl, "Contribution à la modélisation, au dimensionnement et à la gestion des flux énergétiques d'un système de recharge de véhicules électriques : étude de l'interconnexion avec le réseau électrique," Université de technologie de Belfort-Montbéliard, 2015.
- [99] T. Gaonac'H, "Contribution à l'analyse de l'impact des véhicules électrifiés sur le réseau de distribution d'électricité," Supélec, 2015.
- [100] R. Mkahl, A. Nait-Sidi-Moh, J. Gaber and M. W. M, "An optimal solution for charging management of electric vehicles fleets," *Electric Power Systems Research*, no. 146, pp. 177-188, 2017.
- [101] R. P. Joshi and A. P. Deshmukh, "Hybrid electric vehicles: The next generation automobile revolution," *IEEE Electric and Hybrid Vehicles*, p. 1-6, 2006.
- [102] C. G. C, M. Krotova and L. Guerlais, "Distribution network applications and recommendations for 2020 EV infrastructure charge development in France," in *CIREN 21st International conference on electricity distribution*, 2011.

- [103] D. Guo and C. Zhou, "Potential performance analysis and future trend prediction of electric vehicle with V2G/V2H/V2B capability," *AIMS Energy*, vol. 4, no. 2, pp. 331-346, 2016.
- [104] N. Xu and C. Chung, "Reliability Evaluation of Distribution Systems Including Vehicle-to-Home and Vehicle-to-Grid," *IEEE T Power Syst* 31, pp. 759-768, 2015.
- [105] E. Apostolaki-Iosifidou, P. Codani and W. Kempton, " Measurement of power loss during electric vehicle charging and discharging," *Energy*, vol. 127, pp. 730-742, 2017.
- [106] M. J, "Genetic algorithms for modelling and optimization," *Journal of computational and applied mathematics*, vol. 184, no. 1, pp. 205-222, 2005.
- [107] J. Shi, Z. Liu, L. Tang and J. Xiong, "Multi-objective optimization for a closed-loop network design problem using an improved genetic algorithm," *Applied Mathematical Modelling*, vol. 45, pp. 14-30, 2017.
- [108] F. Altiparmak, M. Gen, L. Lin and T. Paksoy, " A genetic algorithm approach for multi-objective optimization of supply chain networks," *Computers & Industrial Engineering*, vol. 51, pp. 196-215, 2006.
- [109] R. Malhotra, N. Singh and Y. Singh, "Genetic Algorithms: Concepts, Design for Optimization of Process Controllers," *Computer and Information Science*, vol. 4, no. 2, 2011.
- [110] I. Y. Kim and O. L. D. Weck, "Adaptive Weighted Sum Method for Multiobjective Optimization: a new method for pareto front generation," *Structural and Multidisciplinary Optimization*, vol. 31, no. DOI 10.1007/s00158-005-0557-6., pp. 105-116, 2006.
- [111] J. Carr, *An Introduction to Genetic Algorithms*, 2014.
- [112] R. Rojas, " Genetic Algorithms," *Neural Networks Springer-Verlag, Berlin*, 1996.
- [113] R. T. Marler, " A Study of MultiObjective Optimization Methods for Engineering Applications," PhD thesis, The University of Iowa..
- [114] I. Stanimirovic', M. L. Zlatanovic' and M. Petkovic', "on the linear weighted sum method for multi-objective optimization," *facta universitatis (ni's) ser. math. Inform.*, vol. 26, pp. 49-63, 2011.
- [115] K. Clement-Nyns, E. Haesen and J. Driesen, "The Impact of Charging Plug-In Hybrid Electric Vehicles on a Residential Distribution Grid," *IEEE Transactions on Power Systems*, vol. 25, no. 1, pp. 371-380, 2010.
- [116] S. Deilami, A. S. Masoum, P. S. Moses and M. A. S. Masoum, "Real-time coordination of plug-in electric vehicle charging in smart grids to minimize power losses and improve voltage profile," *IEEE*

*Transactions on Smart Grid*, vol. 2, no. 3, p. 456, 2011.

- [117] B. Vulturescu, S. Butterbach, C. Forgez, G. Coquery and G. Friedrich, "Ageing study of a supercapacitor-battery storage system," *XIX International Conference on Electrical Machines*, pp. 1364-1369, 2010.
- [118] L. Serrao, Z. Chehab, Y. Guezennec and G. Rizzoni, "An aging model of Ni-MH models for hybrid electric vehicles," *IEEE Vehicle power and propulsion conference*, pp. 78-85, 2005.
- [119] G. Merhy, A. Nait-Sidi-Moh and N. Moubayed, "Control of electric vehicles energy flows through a multi-objective and multi-criteria optimization algorithm," in *12th International conference on multiple objective programming and goal programming MOPGP*, Metz, France, 2017.
- [120] G. Merhy, N. Moubayed and A. Nait-Sidi-Moh, "Energy Flows Management: Notes on implementation of the charging and discharging of Electric Vehicles technologies," *International Journal of E-Learning and Educational Technologies in the Digital Media (IJEETDM)*, vol. 4, no. 2, pp. 53-60, 2017.
- [121] A. Kieldsen, A. Thingvad, S. Martinenas and T. Sorensen, "Efficiency test method for electric vehicle chargers," in *Proceedings of EVS29 - International Battery, Hybrid and Fuel Cell Electric Vehicle Symposium*, 2016.
- [122] W. H. Zhu, Y. Zhu, Z. Davis and B. J. Tatarchuk, "Energy Efficiency and Capacity Retention of Ni-MH Batteries for Storage Applications," *Applied Energy, Elsevier*, vol. 106(C), pp. 307-313, June 2013.
- [123] M. F. Colishaw, "The Characteristics and Use of Lead-Acid Cap Lamps," *Trans. British Cave Research Association*, vol. 1, no. 199, 1974.
- [124] Y. Idota, T. Kubota, A. Matsufuji, Y. Maekawa and T. Miyasaka, "Tin Based Amorphous Oxide : A High-Capacity Lithium-Ion-Storage Material," *Science*, vol. 276, pp. 1395-1397, 1997.
- [125] M. A. Fetcenko, S. R. Ovshinsky, B. Reichman, K. Young, C. Fierro, J. Koch, A. Zallen, W. Mays and T. Ouchi, "Recent Advances in NiMH Battery Technology," *Journal of Power Sources*, vol. 165, pp. 544-551, 2007.
- [126] A. Ruzmetov, A. Nait-Sidi-Moh, M. Bakhouya and J. Gaber, "Towards an optimal assignment and scheduling for charging electric vehicles," in *IEEE International Renewable and Sustainable Energy Conference (IRSEC)*, Ouarzazate, Morocco, 7-9 March 2013.

## Appendices

### Appendix A – Technical Specifications

- A.1. On-board batteries:

Panasonic

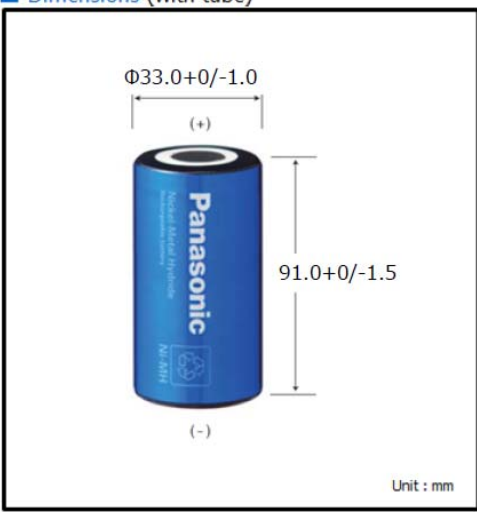
New

# BK1100FHU

High temperature & long life type

H type

**■ Dimensions (with tube)**



Unit : mm

Battery performance and cycle life are strongly affected by how they are used. In order to maximize battery safety, please consult Panasonic when determining charge/discharge specs, warning label contents and unit design.

**■ Specifications**

Diameter		33.0 +0 / -1.0 mm	
Height		91.0 +0 / -1.5 mm	
Approximate Weight		300g	
Nominal Voltage		1.2V	
Discharge*1	Average*2	11300 mAh	
	Capacity Rated (min.)	11000 mAh	
Approx. Internal Impedance at 1000Hz at charged state.		5 mΩ	
Charge	Standard	1100 mA X 16 hrs.	
	Rapid*3	5500 mAh X 2.4 hrs.	
	Low rate	550 mA X 32 hrs. 367 mA X 48 hrs.	
Ambient Temperature	Charge	Low rate	-30 °C to 75 °C
		Standard	
	Rapid	-30 °C to 60 °C	
Discharge		-40 °C to 85 °C	
Storage	<1 year	-20 °C to 35 °C	
	<6 months	-20 °C to 45 °C	
	<1 month	-20 °C to 55 °C	
	<1 week	-20 °C to 65 °C	

\*1 After charging at 0.1 It for 16 hours, discharging at 0.2 It  
\*2 For reference only.  
\*3 Need specially designed control system. Please contact Panasonic for details.

\*The data in this document are for descriptive purposes only and are not intended to make or imply any guarantee or warranty.

### Nickel Metal Hydride Battery

2016/08

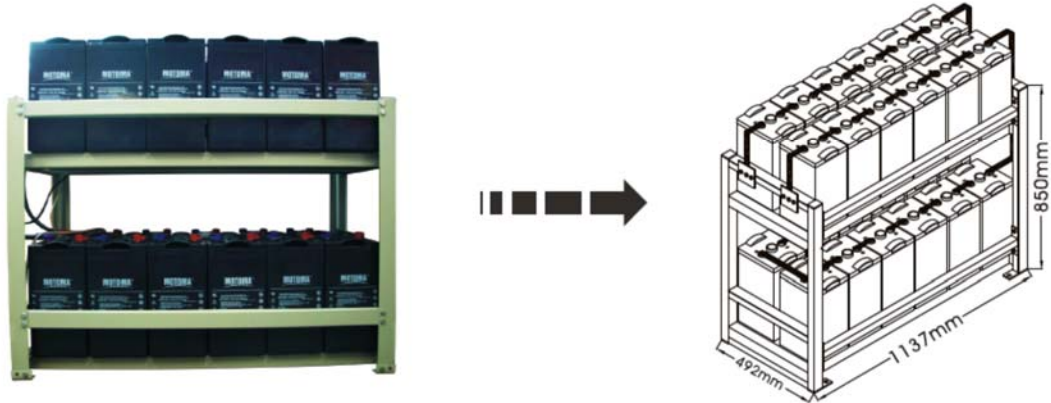
- A.2. Stationary Lead-Acid Batteries:

#### 48V System

Battery Type	Voltage (V)	Capacity (AH)	HORIZONTAL	VERTICAL
			LengthxWidthxHeight(mm)	LengthxWidthxHeight(mm)
MS48V3000		3000	4816x776x850	—————

## 48V Group

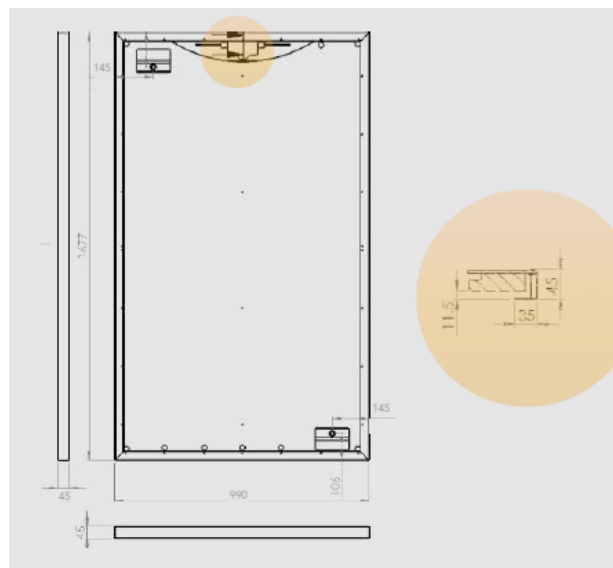
### HORIZONTAL



- A.3. Photovoltaic panels:**

GENERAL DATA	
Length	1677 mm
Width	990 mm
Frame width	45 mm
Weight empty / filled	28 kg / 33 kg
Frame color / backsheet	Black / Black

ELECTRICAL DATA	
Number of cells per module	60
Cell type (dimensions)	Monocrystalline (156 mm * 156 mm, 6 inches)
Nominal power ( $P_{mpp}$ )	280 Wp
Module efficiency	17,20 %
Power tolerance	0/+3 %
Rated voltage ( $V_{mpp}$ )	31,95 V
Rated current ( $I_{mpp}$ )	8,77 A
Open circuit voltage ( $V_{oc}$ )	38,88 V
Short circuit current ( $I_{sc}$ )	9,30 A
Maximum system voltage	1000 V DC
Reverse current load	15 A
NOCT	46,9 °C
Connectors	Genuine MC4
Application class	Class A
Voltage ( $\mu Voc$ )	-0,345 %/°C
Current ( $\mu Isc$ )	0,047 %/°C
Efficiency loss	0,467 %/°C



- **A.4. Horizontal wind turbine:**

Number of blades	5
Blades material	composite FE 1630PW
Generator	3phase PMG
<b>Nominal power</b>	<b>2,8kW</b>
Voltage	48V / 220V
Wind Class	CLASS III IEC 61400-2
Swept area	3m <sup>2</sup>
Weight	42Kg
Cut-in wind speed	2,6m/s
Nominal wind speed	12,5m/s
Cut-out wind speed	14,5m/s
Transmission	Direct Drive
Power control	MPPT curve of the generator
Brake and protection	Dump-load and short-circuit brake
Controller	48V for Lithium battery charge
Inverter	ABB type efficiency 97%
Noise	Max. 50dBa
Pole type	for flat or inclined roofs

- A.5. DC/AC inverter:



### Three Phase Inverters for the 208V Grid<sup>(1)</sup> for North America

SE9KUS / SE14.4KUS

	SE9KUS	SE14.4KUS	
<b>OUTPUT</b>			
Rated AC Power Output	9000	14400	VA
Maximum AC Power Output	9000	14400	VA
AC Output Line Connections	4-wire WYE (L1-L2-L3-N) plus PE or 3 wire Delta		
AC Output Voltage Minimum-Nominal-Maximum <sup>(2)</sup> (L-N)	105-120-132.5		Vac
AC Output Voltage Minimum-Nominal-Maximum <sup>(2)</sup> (L-L)	183-208-229		Vac
AC Frequency Min-Nom-Max <sup>(3)</sup>	59.3 - 60 - 60.5		Hz
Max. Continuous Output Current (per Phase)	25	40	A
GFDI Threshold	1		A
Utility Monitoring, Islanding Protection, Country Configurable Set Points	Yes		
<b>INPUT</b>			
Maximum DC Power (Module STC)	12150	19400	W
Transformer-less, Ungrounded	Yes		
Maximum Input Voltage DC to Gnd	250	300	Vdc
Maximum Input Voltage DC+ to DC-	500	600	Vdc
Nominal Input Voltage DC to Gnd	200		Vdc
Nominal Input Voltage DC+ to DC-	400		Vdc
Maximum Input Current	26.5	38	Adc
Maximum Input Short Circuit Current	45		Adc
Reverse-Polarity Protection	Yes		
Ground-Fault Isolation Detection	1MΩ Sensitivity	350kΩ Sensitivity <sup>(3)</sup>	
CEC Weighted Efficiency	96.5	97	%
Night-time Power Consumption	< 3	< 4	W
<b>ADDITIONAL FEATURES</b>			
Supported Communication Interfaces	RS485, Ethernet, ZigBee (optional)		
Rapid Shutdown – NEC 2014 and 2017 690.12	Automatic Rapid Shutdown upon AC Grid Disconnect <sup>(4)</sup>		
RS485 Surge Protection	Supplied with the inverter		
<b>STANDARD COMPLIANCE</b>			
Safety	UL1741, UL1741 SA, UL1699B, CSA C22.2, Canadian AFCI according to T.I.L. M-07		
Grid Connection Standards	IEEE1547, Rule 21, Rule 14 (HI)		
Emissions	FCC part15 class B		
<b>INSTALLATION SPECIFICATIONS</b>			
AC output conduit size / AWG range	3/4" minimum / 12-6 AWG	3/4" minimum / 8-4 AWG	
DC input conduit size / AWG range	3/4" minimum / 12-6 AWG		
Number of DC inputs	2 pairs	3 pairs <sup>(5)</sup>	
Dimensions (H x W x D)	21 x 12.5 x 10.5 / 540 x 315 x 260		in / mm
Dimensions with Safety Switch (H x W x D)	30.5 x 12.5 x 10.5 / 775 x 315 x 260		in / mm
Weight	73.2 / 33.2	99.5 / 45	lb / kg
Weight with Safety Switch	79.7 / 36.2	106 / 48	lb / kg
Cooling	Fans (user replaceable)		
Noise	< 50	< 55	dBA
Operating Temperature Range	-40 to +140 / -40 to +60 <sup>(6)</sup>		F / °C
Protection Rating	NEMA 3R		